

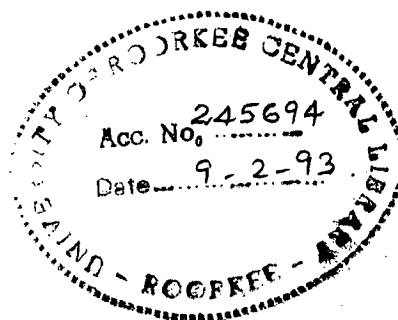
**CRYSTALLIZATION KINETICS AND ANNEALING STUDIES ON
ELECTROLESS AMORPHOUS TRANSITION METAL-METALLOID
SYSTEM : Ni-Co-P**

A THESIS

submitted in fulfilment of the
requirements for the award of the degree
of
DOCTOR OF PHILOSOPHY
in
PHYSICS

By

KAMYAR AJDARI



**DEPARTMENT OF PHYSICS
UNIVERSITY OF ROORKEE
ROORKEE-247 667 (INDIA)**

November, 1990

Dedicated

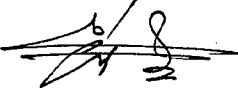
To my beloved

Simin

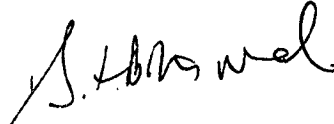
CANDIDATE'S DECLARATION


I hereby certify that the work which is being presented in the thesis entitled **"CRYSTALLIZATION KINETICS AND ANNEALING STUDIES ON ELECTROLESS AMORPHOUS TRANSITION METAL-METALLOID SYSTEM : Ni-Co-P"** in fulfilment of the requirement for the award of the degree of Doctor of Philosophy, submitted in the Department of Physics of the University is an authentic record of my own work carried out during a period from October 1986 to July 1990 under the supervision of Dr. S. K. Barthwal, Dr. V. K. Tandon and Dr. S. Ray.

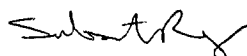
The matter embodied in this thesis has not been submitted by me for the award of any other degree.


(K. AJDARI)
29/11/90

This is to certify that the above statement made by the candidate is correct to the best of our knowledge.


(Dr. S. K. Barthwal)
Department of Physics
University of Roorkee
Roorkee


(Dr. V. K. Tandon)
Department of Physics
University of Roorkee
Roorkee

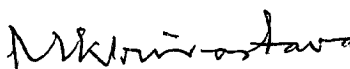

(Dr. S. Ray)
Department of Metallurgical Engineering
University of Roorkee
Roorkee

The Ph.D. Viva-Voce examination of Sri K. AJDARI Research Scholar has been held on _____

Signature of Guide(s)

Signature of External Examiner

Forwarded



Prof. & Head 30.11.90

Department of Physics
University of Roorkee

ABSTRACT

The Ternary amorphous $\text{Ni}_x\text{Co}_y\text{P}_z$ system with compositional ranges of $15.3 \leq x \leq 55.5$, $29.0 \leq Y \leq 70.0$ and $14.7 \leq z \leq 15.5$ has been prepared following an electroless deposition technique. The technique consist in using an alkaline bath containing nickel and cobalt sulphate, sodium citrate, ammonium sulphate and sodium hypophosphite through a chemical reduction on a substrates suitably sensetized by SnCl_2 and PdCl_2 . The compositional analysis was done using Inductively Coupled Plasma (ICP) with an accuracy of better than $\pm 1\%$. The samples studied are categorized into following composition ranges:

$\text{Ni}_{55.5}\text{Co}_{29.0}\text{P}_{15.5}$ $\text{Ni}_{39.0}\text{Co}_{46.0}\text{P}_{15.0}$
 $\text{Ni}_{35.6}\text{Co}_{49.1}\text{P}_{15.3}$, $\text{Ni}_{27.0}\text{Co}_{58.0}\text{P}_{15.0}$ and $\text{Ni}_{15.3}\text{Co}_{70.0}\text{P}_{14.7}$.

Differential Scanning Calorimeter (DSC) is used for a study of the kinetics of crystallization and thermal stability aspects of the system. The structure of 'as-deposited' and annealed samples have been investigated using selected area mode of Transmission Electron Microscope (TEM) and X-Ray Diffraction (XRD) techniques in the temperature range of 300 K to 823 K. The Magnetization and Electrical Resistivity behaviour of 'as-deposited' and on annealing have been investigated using Vibrating Sample Magnetometer (VSM) and Four Probe Resistivity measurements upto temperature of 850 K.

The DSC response shows a small peak followed by two strong exothermic reaction peaks (T_{PI} , T_{PII}) in the temperature range of 550-800 K. The first small peak at about 500-550 K is attributed to structural stress relaxation. The enthalpy change for first major reaction is maximum for nearly equal Nickel-Cobalt ratio where fluctuating type of trend is observed for second reaction. The limiting temperature (zero heating rate) for first reaction shows higher value of 595 K for sample containing 49.1 at% Cobalt.

Non-isothermal Kissinger's method is applied for calculation of activation energies of first and second reactions with an accuracy of better than 5.3%. The activation energy for reaction under the first peak (T_{PI}) is found to maximize to 189.7 KJ/mol for $Ni_{35.6}Co_{49.1}P_{15.3}$ where that of second peak (T_{PII}) tends to 177.0 KJ/mol for $Ni_{39.0}Co_{46.0}P_{15.0}$. The parameter 'n' is found to be $0.6 < n < 0.8$ for first reaction and $1.1 < n < 1.4$ for second reaction.

The values of 'n' indicate that the reaction under first peak taking place on pre-existing nuclei where the second one is eutectic type of transformation.

The 'as-deposited' state of thin deposits and bulk samples show diffuse ring and a broad peak under SAD mode of TEM and XRD with d-spacing matching to (0002) and (111)

planes of h.c.p. Cobalt (α -Cobalt) and f.c.c. Nickel. The samples annealed to 628 K, the region of first strong DSC peak, show separation of h.c.p. Cobalt (01 $\bar{1}1$, 0002, 01 $\bar{1}0$) and f.c.c. Nickel (111) whereas the matrix remains still amorphous. When samples heated to 823 K, the second peak region of DSC, the matrix crystallization takes place through appearance of many metastable and stable phases.

The structural annealing behaviour of amorphous Ni-Co-P system can be divided into two broad categories: 1) the alloys having the composition near to that of binary system, that is sample Ni_{55.5}Co_{29.0}P_{15.5} and Ni_{15.3}Co_{70.0}P_{14.7} show the final matrix crystallization consisting of equilibrium phases Ni₃P and Co₂P. 2) The alloys having the intermediate compositions, Ni_{39.0}Co_{46.0}P_{15.0}, Ni_{35.6}Co_{49.1}P_{15.3} and Ni_{27.0}Co_{58.0}P_{15.0} transform to many non-equilibrium phases, Ni₁₂P₅, Ni₇P₃, Ni₅P₄, CoP₄ and CoP₂ beside the equilibrium phases Co₂P and Ni₃P.

Magnetization of 'as-deposited' samples increases from 3.33 emu/g for Ni_{55.5}Co_{29.0}P_{15.5} to 49.2 emu/g for Ni_{15.3}Co_{70.0}P_{14.7} and with ' n_t ' number of electrons transferred from metalloid to be 4.5 reasonably good agreement is found between theoretical and experimental values. The annealing behaviour of magnetic moment reveals that the initial increase in magnetization at about 560 K is due to separation of h.c.p. Cobalt and f.c.c. Nickel as indicated by

TEM and XRD studies. The matrix crystallization process causes a relatively lower rate of change in magnetization.

The electrical resistivity of 'as-deposited' samples show the expected relation between resistivity ' ρ ' and Temperature Coefficient of Resistivity (TCR) and confirms the Mooij correlation for TM-M systems. The resistivity is found to be $114.5 \mu\Omega \text{ cm}$ for $\text{Ni}_{55.5}\text{Co}_{29.0}\text{P}_{15.5}$ sample and increases as Cobalt composition of the sample increases and tends to maximum value of $122.5 \mu\Omega \text{ cm}$ for $\text{Ni}_{39.0}\text{Co}_{46.0}\text{P}_{15.0}$ with reduce in TCR from $13.06 \times 10^{-5} \text{ K}^{-1}$ to $4.07 \times 10^{-5} \text{ K}^{-1}$. On annealing, the minor drop in resistivity at temperature of about 473 K may be attributed to stress relaxation. The major drops of electrical resistivity are closely associated with the crystallization process. The ternary Ni-Co-P samples with 29.0, 58 and 70.0 at % Cobalt show the separation of primary phases of h.c.p. Cobalt and Nickel distinct from that of matrix crystallization. In case of samples having nearly equal ratios of Cobalt and Nickel the two stages of crystallization are not distinct.

To conclude, our study of the mode of crystallization in ternary amorphous Ni-Co-P shows that, crystallization takes place in two distinct steps; the first step is, a primary crystallization, involving the separation of phases of α -Cobalt and Nickel from amorphous matrix. Second step, believe to be an eutectic crystallization, shows that in case of $\text{Ni}_{39.0}\text{Co}_{46.0}\text{P}_{15.0}$, $\text{Ni}_{35.5}\text{Co}_{49.1}\text{P}_{15.3}$ and $\text{Ni}_{27.0}\text{Co}_{58.0}\text{P}_{15.0}$

matrix crystallization results in appearance of a large number of metastable phases, while $\text{Ni}_{55.5}\text{Co}_{29.0}\text{P}_{15.5}$ and $\text{Ni}_{15.0}\text{Co}_{70.0}\text{P}_{15.0}$ which are much closer to a corresponding binary system Ni-P or Co-P show predominantly formation of equilibrium crystalline phases only. The addition of Cobalt in equal proportion of that of Nickel enhances the stability of the Ni-Co-P alloy and phosphorous diffusion is the slowest step at these compositions.

L I S T O F P U B L I C A T I O N S

1. 'Non-Isothermal Kinetics of the Crystallization of Ni-Co-P Amorphous Film', National Seminar on Alloy Design and Development, March 10-11, 1989, Roorkee, India.
2. 'Kinetics of Phase Separation and Matrix Crystallization in Electroless Ni-Co-15 At% P Amorphous Alloys', Presented in '7th International Conference on Liquid and Amorphous Metals', Sept. 8-11, 1989, Kyoto, Japan.
3. 'Kinetics of Phase Separation and Matrix Crystallization in Electroless Ni-Co-15 At% P Amorphous Alloy', J. Non-Cryst. Solids 117/118, (1990), 535-538.
4. 'X-Ray Studies of Transformations in Amorphous Ni-Co-P', International Confernece on Disordered Materials (Structure and Properties), Feb. 3-6, 1991, Indore, India (Communicated).
5. 'Study of Phase Transformation in Amorphous Ni-Co-P Films', (under Communication).
6. 'The Magnetic and Electrical Resistivity Behaviour of Amorphous Ni-Co-P Films During Annealing', (under Communication).

ACKNOWLEDGEMENT

It has been a matter of privilege for me to join research under Dr. S.K. Barthwal, Dr. V.K. Tandon and Dr. S. Ray, my thesis supervisors, for their expert guidance. In spite of their extremely busy schedule, they could always spare time for my research work which could not have been completed without their helpful counsel and constant cooperation.

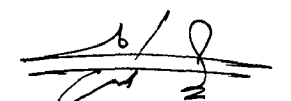
I am thankful to Head of Physics Department, for providing me all the facilities for executing the research work in the department, University of Roorkee, Roorkee.

I take the opportunity to express my thanks to Prof. Kailash Chandra, Director, University Science Instrumentation Center (USIC) for providing all facilities to work even after working hours. I am thankful to the technical staff of USIC, Mr. J.S.Saini for ICP and VSM studies, Mr.R.Joyal for TEM and Mr.Anil Kumar for carrying out XRD and DSC studies.

I am highly indebted to my father and mother for their inspiration and encouragement throughout my carrier. Their blessings could help me to achieve this goal. The constant affection of my brothers, Daneshyar, Khashayar, Naved and sisters, Mandana and Dyana was of immense help to me for completing this work.

Finally, I am deeply indebted to my wife Simin, for her patience and cooperation during the course of this work.

I am thankful to Mr. Rakesh Kaushish for untiring efforts in typing the thesis.



(KAMYAR AJDARI)

C O N T E N T S

Chapter		Page No.
1	INTRODUCTION	.. 1
2	THE AMORPHOUS TRANSITION METAL-METALLOID SYSTEM: LITERATURE REVIEW	.. 8
	2.1 METHODS OF PREPARATION	.. 8
	2.2 CRYSTALLIZATION REACTION IN AMORPHOUS ALLOYS	.. 12
	2.3 KINETICS OF CRYSTALLIZATION AND STABILITY	.. 14
	2.4 ELECTRON MICROSCOPY AND X-RAY DIFFRACTION STUDIES	.. 23
	2.5 MAGNETIZATION AND ANNEALING BEHAVIOUR	.. 26
	2.6 ELECTRICAL RESISTIVITY AND ANNEALING BEHAVIOUR	.. 29
3	EXPERIMENTAL TECHNIQUES	.. 33
	3.1 THE Ni-Co-P ELECTROLESS DEPOSITION METHODS	.. 33
	3.2 THE CHEMICAL COMPOSITION	.. 36
	3.3 DIFFERENTIAL SCANNING CALORIMETRY	.. 37
	3.4 ELECTRON MICROSCOPY AND X-RAY DIFFRACTOMETRY	.. 39
	3.5 MAGNETIC MEASUREMENTS	.. 40
	3.6 THE ELECTRICAL RESISTIVITY MEASUREMENTS	.. 42
4	CRYSTALLIZATION KINETICS OF AMORPHOUS ELECTROLESS Ni-Co-P	.. 44
	4.1 RESULTS: DIFFERENTIAL SCANNING CALORIMETRY	.. 44
	4.2 DISCUSSION	.. 47
	4.3 SUMMARY	.. 51

5	ELECTRON MICROSCOPY AND X-RAY DIFFRACTION STUDIES ON AMORPHOUS Ni-Co-P DURING ANNEALING	..	53
5.1	RESULTS: TEM AND XRD STUDIES ON 'AS-DEPOSITED' ALLOYS	..	53
5.2	RESULTS: PHASE IDENTIFICATION IN ANNEALED SAMPLES	..	54
5.2.1	TEM Studies	..	55
5.2.2	XRD Studies	..	57
5.3	DISCUSSION	..	60
5.4	SUMMARY	..	63
6	ANNEALING BEHAVIOUR OF THE MAGNETIZATION AND ELECTRICAL RESISTIVITY OF AMORPHOUS ELECTROLESS Ni-Co-P	..	65
6.1	RESULTS: MAGNETIZATION STUDIES	..	65
6.1.1	Magnetization of the "as-deposited" Samples	..	66
6.1.2	Magnetization of the Alloys during Annealing	..	68
6.1.3	Discussion	..	70
6.2	RESULTS: ELECTRICAL RESISTIVITY STUDIES	..	73
6.2.1	Electrical Resistivity of "as-deposited" samples	..	73
6.2.2	Electrical Resistivity of the Alloys during Annealing	..	75
6.2.3	Discussion	..	76
6.3	SUMMARY	..	78
7	CONCLUSIONS	..	80
	REFERENCES	..	86

CHAPTER 1

INTRODUCTION

The amorphous metallic alloys, characterized by no long range atomic order and not being in the lowest energy state are known to possess unique magnetic, electrical and mechanical properties apart from excellent corrosion resistance, not encountered in their crystalline counterparts.

Because of the lack of atomic ordering it was believed for many years that ferromagnetism could not exist in amorphous solids. However, on the basis of evidence that the electronic band structure of crystalline solids did not change in any fundamental way on transition to the amorphous state, Gubanov (1960) predicted that they would be ferromagnetic.

A real technological interest developed after Pond and Maddin (1969) reported the preparation of continuous ribbons of amorphous alloys and at this point it was clear that amorphous metallic alloys could be prepared in large quantities at low cost.

The first alloy with a substantial magnetization, further confirming Gubanov's predictions, was $\text{Fe}_{75}\text{P}_{15}\text{C}_{10}$ system. This appeared to be a typical soft ferromagnetic alloy with the large saturation magnetization of 7 KG and the relatively low coercive force of 3 Oe.

Since the discovery of melt quenched amorphous metallic alloys by Duwez and Willens (1963) in the sixties, it was the selection of various methods of preparation and detailed investigations of the properties that made amorphous alloys mature as useful products, instead of just a laboratory curiosities.

Their properties of soft magnetic materials with low magnetic losses, high tensile strength, zero thermal expansion and having electrical resistivity of three or four times higher than those of conventional iron or iron-nickel alloys, are currently the focus of intensive technological and fundamental research.

The development of amorphous magnetic alloys may be divided into three stage; the first was concerned with preparing this new state of matter by variety of techniques and confirming the existence of ferromagnetism on these alloys. The second stage started to systematize the results into an experimental and theoretical frame work. The third and perhaps present stage of work is showing an increased subdivision of interest prompted by an increased awareness of potential applications. For example, the preparation of alloys to compete for particular applications, and to evaluate and understand the stability of these alloys.

There are two important class of amorphous magnetic alloys of prime technological interests, namely, Transition Metal-Metalloid, TM-M (TM = Fe,Co,Ni and M = Si,B,P,C) and

Rare Earth-Transition Metal, RE-TM (RE = Gd, Nb, Tb).

The TM-M amorphous alloys, the class to which Ni-Co-P belongs, have been the subject of considerable investigations and consists of one or more Transition Metal Fe, Co, Ni alloyed with some Metalloid such as B, P, Si or Al.

They can be prepared by various techniques such as vapour deposition, ion implantation, melt quenching and electroless deposition. Melt quenching of molten alloy, is used for preparation of large number of amorphous alloys (known as metallic glasses) however a few binary and ternary systems are obtainable using electroless and electrodeposited methods (Watanabe and Tanabe, 1985). The electroless deposition, similar to that of Simpson and Brambley (1971) are chosen to prepare TM-M ternary system where the process parameters are optimized to get amorphous deposits.

Amorphous metallic alloys have been found to crystallize by a nucleation and growth mechanism where the driving force is the difference in free energy between the amorphous and the corresponding crystalline phase(s). Depending on the composition, crystallization have been observed to occur by one of the three commonly observed modes, Polymorphous, Primary or Eutectic.

The most promising properties of amorphous alloys, e.g. corrosion resistance, the excellent soft magnetic behaviour or the high hardness and strength combined with ductility, have

been found to deteriorate drastically during crystallization. Therefore, understanding the micro-mechanism of crystallization helps us to impede or control crystallization and to design a very special partially or fully crystallized microstructures unobtainable from liquid or crystalline solids. The most important kinetic parameters, like the activation energy, enthalpy, rate of reaction, for the amorphous-to-crystalline transformation can be deduced using Differential Scanning Calorimetry (DSC) and combining it with the observations under Transmission Electron Microscope (TEM), the study of crystallization kinetics gives an important clue to the local structure in addition to the thermal stability of amorphous alloys.

The strong exothermic peak in the response of Differential Scanning Calorimeter (DSC) can be used as a guide to find crystallization temperatures, the most important parameter, and the activation energy of the transformation reaction.

Since the change in structure governs the physical properties, the annealing behaviour of electrical resistivity, magnetization and identification of the phases formed during transformation using SAD mode of TEM supplemented by X-ray diffraction are suitable method to probe the fine scale structural variations during crystallization.

While most of the basic studies on electrodeless and electrodeposited Transition Metal-Metalloid systems are on

binary systems like Ni-P, Co-P, Ni-B etc., to achieve certain desirable properties many practical systems known are, however, either ternary or quaternary type.

In the present work an attempt is made to study the crystallization kinetics, the annealing behaviour of the 'as-deposited' structure, magnetization, electrical resistivity as the system undergoes a transition to crystalline phases through many intermediate steps of a ternary amorphous Transition Metal-Metalloid, in particular the Ni-Co-P system with the following objectives:

- a) To prepare the ternary amorphous Ni-Co-P in compositional range of Nickel from 15 at% to 60 at%, Cobalt 30 at% to 70 at% with phosphorous 15 at% using electroless deposition technique.
- b) To study the crystallization kinetics and stability of amorphous Ni-Co-P ternary system.
- c) To study the transformations to crystalline state, identification of intermediate phases involved in the crystallization process of Ni-Co-P using X-ray diffraction and selected area electron diffraction techniques.
- d) To study the magnetic and electrical resistivity of the phases observed during the annealing of the amorphous films of Ni-Co-P as it undergoes transformation to crystalline phases.

- e) To use above studies to develop an understanding of amorphous Transition Metal-Metalloid System in general and in particular of the electroless ternary Ni-Co-P from the point of view of stability and the crystallization behaviour.

The subject matter of the thesis has been arranged in seven chapters.

The first chapter, i.e. the present one, introduces the amorphous alloys and the scope and the objectives of the work.

The second chapter presents the review of the current understanding of the amorphous Transition Metal-Metalloid in respect of the preparation techniques, stability, structural, the magnetic and electrical resistivity properties, their annealing behaviour and kinetics of phase transformations. Some important experimental results for binary Ni-P, Co-P and ternary Ni-Co-P systems have been critically reviewed in view of their direct relevance to the present work.

The third chapter presents the electroless technique used for preparation of amorphous Ni-Co-P films and chemical analysis for their composition characterization, the measurement techniques used to study the calorimetric, structural, magnetic and resistivity properties of the system in the temperature ranging from 300 K to 850 K.

In chapter four, non-isothermal Differential Scanning Calorimetry techniques have been used to study the influence

of the compositional variation on the kinetics of crystallization and thermal stability in amorphous electroless Ni-Co-P alloys.

The calorimetric studies indicate that some phases are formed or transformed during the crystallization process. In order to have a qualitative idea of the related microstructural changes a detailed study of the annealing effect of the structure of 'as-deposited' amorphous Ni-Co-P is carried out using hot stage electron microscopy and X-ray diffraction techniques. The results of the study are presented and discussed in Chapter 5.

In chapter six, the results of the magnetic and electrical resistivity of electroless deposited Ni-Co-P alloys over the composition range of Cobalt varying from 29-70 at%, and on annealing upto temperature of 823 K are presented.

It is in the concluding chapter seven that the results of Differential Scanning Calorimetry, Selected Area Electron Diffraction, X-Ray Diffraction and Magnetization and Electrical Resistivity on electroless amorphous Ni-Co-P have been put in perspective for understanding the overall crystallization behaviour of amorphous metal metalloid system. In particular, the ternary system Ni-Co-P does show many features in the crystallization kinetics, structure, magnetic and electrical resistivity behaviour on annealing not observed in binary Ni-P and Co-P systems and points out that the crystallization behaviour of ternary system is more complex.

C H A P T E R 2

THE AMORPHOUS TRANSITION METAL-METALLOID SYSTEM: LITERATURE REVIEW

In this chapter we present a brief review of various methods of preparations and the work done by the earlier investigators on the calorimetric, annealing studies on the structure, magnetic and electrical resistivity of the amorphous Transition Metal-Metalloid systems. Although large number of review articles and books are available (Luborsky 1983, Duwez 1978), most of them deal with the amorphous alloys prepared by rapid quenching from the melt. In this review, however, the emphasis is on electroless ternary Ni-Co-P and binary Ni-P and Co-P and other relevant systems.

2.1 METHODS OF PREPARATION

In present section we will briefly review the physical ideas on which the techniques used to prepare amorphous alloys are based.

One of the important way of making amorphous alloys is to quench the melt fast enough (about 10^6 K/s) to avoid crystallization. The first process is the gun technique of Duwez where small droplets of liquid are accelerated and projected onto a cold surface. The next is the splat cooling process where a drop of molten liquid is smashed between two rapidly moving copper discs. Numerous compositions of

amorphous alloys were prepared using this technique.

The vacuum evaporation, some times called vapour quenching technique, gives thin films of a few tenth of microns which are studied by X-ray diffraction, resistivity or electron microscopy. These materials are produced under high vacuum with the substrate cooled by liquid nitrogen. The examples of amorphous alloys obtained by this technique are, Fe-Sn, Fe-Au, Co-Ag, and only pure Cobalt was obtained in amorphous state using this technique.

In the sputtering method, a gas at a pressure of 10^{-1} to 10^{-9} torr is ionized under a potential difference of 1 to 5 KV applied between two electrodes and high quenching rates of 10^8 K/s can be achieved by this method. This technique has been extensively used for the preparation of rare earth-transition metal films like Co-Zr, Co-Gd and Fe-Gd, which is an important class of amorphous alloys.

The ion implantation technique consists in amorphizing a metal foil by ion implanting solute atom in it. This method has been used to prepare some otherwise impossible amorphous alloys such as Cu-W or Pt-Au. This technique can be used to generate an intimate atomic mixture of controlled composition, without limitations of the conventional alloying given by equilibrium thermodynamics and provides the highest quenching rates of 10^3 - 10^{15} K/s and surface amorphization with amorphous layer thickness from 100 to 1500 Å.

The number of amorphous alloys obtained by electrolysis appears to be limited. It has been observed that the precise composition of the product depends strongly on the deposition conditions. The examples of amorphous alloys prepared by this method are, Co-P, Ni-P, Fe-P, Co-W etc.

The electroless deposition method was first extensively investigated by Brenner and Riddell (1946) and their process are modified by several authors such as Simpson and Brambley (1971) to prepare electroless Nickel and Cobalt deposits.

Only few binary and Ternary amorphous systems can be prepared by this method (Watanabe and Tanabe, 1985) and all the amorphous Ni-Co-P samples investigated in our study are prepared employing this technique.

Electroless plating is the controlled electrochemical reduction of aqueous metal ions into a suitable catalytic surface and the reaction is called autocatalytic. Typically, the electroless Nickel and Cobalt plating solution consist of a) source of metal ions b) suitable complexing agents, c) stabilizer and d) a reducing agent.

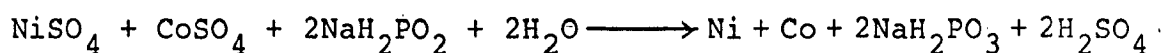
The reduction of the metal from its salts by hypophosphite is a complex process and its rate depends to a temperature and pH of the plating solution.

The composition of the solution will change during the plating and most important change is a decrease in the metal salts and hypophosphite concentration, so the continuous

replacement of the bath is necessary otherwise the rate of the deposition will go on decreasing and there will be change in composition of the deposit.

It is known that the reduction of Nickel and Cobalt salts by hypophosphite starts only on the surfaces of certain metals such as Nickel, Palladium and Aluminium where other metals can also be plated if we bring their surfaces in contact with the Nickel or metals which have more electronegativity like Palladium or Aluminium.

The main reaction for reduction of Nickel and Cobalt metals can be written as:



Ammonia may be added regularly to the bath to neutralize the acid formed in the reduction process. Although increase in the hypophosphite concentration improve the rate of deposition of the sample, large amounts of reducing agents cause the process to take place in the bulk of the solution.

From above general discussion one can conclude that for electroless plating the constituents of the bath required are as follows:

- I) Source of metal ions: for Ni-Co-P plating, Nickel and Cobalt sulfate or Nickel and Cobalt Chloride.

II) Complexing agent: a) Sodium citrate or b) Ammonium sulphate for sulphate bath and c) Ammonium chloride for chloride bath.

III) Reducing agent : Sodium hypophosphite.

Both alkaline and acidic baths have been developed and tried for deposition of Ni-P, Co-P and Ni-Co-P and have their own merits and demerits. The selection of the constituents of the bath depends on its quality, efficiency and nature of the deposits required. The results of chloride bath are arbitrary (Cziraky et al, 1980) where the sulphate bath results are reported to be systematic. The reduction of Nickel salts in acidic solutions shows non-uniform composition and is mixture of various phosphides. The nature of deposit depends on substrate used.

The rate of deposition of Ni-P and Co-P are higher in alkaline bath as compared to acid bath and it is easy to replace the solution in addition to good quality of the deposits. The presence of complex forming agents (citrate and ammonia salts) in the alkaline solution facilitate replacement and prolonged operating time.

2.2 CRYSTALLIZATION REACTION IN AMORPHOUS ALLOYS

Amorphous metallic alloys crystallize by nucleation and growth process (Jackle 1986). The driving force is the difference in free energy between the amorphous and crystalline phase(s).

Depending on the composition of amorphous phase, the crystallization can occur by following modes:

Polymorphous Crystallization

It is the crystallization of one phase with the same composition as the amorphous phase. This reaction can occur only in the concentration ranges near the same elements or compounds and proceeds by single jump of atoms across the crystallization front. As shown in Fig.2.1, polymorphous crystallization of α -Fe is possible in Iron-rich range and near the composition of Fe_3B . However, most of the amorphous alloys do not crystallize without any concentration changes into just one crystalline phase.

Primary Crystallization

This is defined as crystallization of one phase with a composition different from the amorphous matrix. During this reaction a concentration gradient is built up ahead of the crystallization front. For example, the crystallization of α -Fe in amorphous $\text{Fe}_{86}\text{B}_{14}$ (Fig.2.1). Here amorphous phase will be enriched in boron until crystallization is stopped after reaching equilibrium and subsequently the boron enriched matrix transforms by one of the other mechanisms. Three types of growth; diffusion interface and mixed control are observed in primary crystallization. This reaction occurs in many amorphous systems in the initial stage of crystallization

(Koster and Herold, 1981). The dispersed primary crystallized phase may act as the preferred nucleation site for the oncoming crystallization of the amorphous matrix.

Eutectic Crystallization

Here two crystalline phases grow cooperatively by a discontinuous reaction. There is no difference in the overall concentration across the reaction front, diffusion takes place parallel to the reaction front and the two components have to separate into the two phases, thus reducing the growth rate of the reaction. For example, amorphous $\text{Fe}_{80}\text{B}_{20}$ crystallize simultaneously to $\alpha\text{-Fe} + \text{Fe}_3\text{B}$ or $\alpha\text{-Fe} + \text{Fe}_2\text{B}$. This reaction has the large driving force and usually should take more time compared to the other reactions.

These three types of crystallization reactions are shown schematically in Fig. 2.1 for amorphous Fe-B system. However, these reactions are not limited to specific amorphous alloy and one or the other has been observed to occur in all amorphous alloys investigated so far.

2.3 KINETICS OF CRYSTALLIZATION AND STABILITY

The stability of amorphous alloys are important topics both theoretically and technologically. The theoretical analysis of the factor controlling the stability of the resultant amorphous alloys from the thermodynamic view point have been reviewed and discussed in many articles.

The use of non-isothermal thermal analysis for calculation of kinetics of reaction parameters have been strong theoretical and experimental interests in last decade. The rapidity of performing the non-isothermal experiment, the extent of temperature beyond that accessible in isothermal case and knowing that the industrial process often depend on the kinetic behaviour of the system undergoing phase transformation under non-isothermal conditions are advantages of this method which can even detect many phase transformations occurring too rapidly to be detected under isothermal experiments.

The application of DSC to the characterization of phase transformation has been examined by several workers (Henderson 1979 , Miyazaki et al 1986, Calka and radlinski 1987, Greer 1982, Russew 1985). Here the experimentally imposed conditions are the change of temperature of transformation 'T' at constant heating rate ' β ' with respect to time i.e. $\beta = dT/dt$. If the sample size is relatively small and good thermal contact is maintained between the sample and rest of the system, the thermal behaviour of the system can be used to accurately determine the transformation kinetics of the sample and is a convenient method for obtaining information on reaction kinetics in amorphous alloys. Kissinger (1957) developed a thermal analysis method to determine the most important kinetic parameters, activation energy of reaction 'E' and order reaction 'n' using formula given below:

$$\frac{d(\ln p / T_p^2)}{d(1/T_p)} = - E/R \quad (2.1)$$

Where the slope of graph of $\ln p / T_p^2$ Vs $1/T_p$ gives value of E. Here T_p is peak temperature, R = gas constant. The value of 'n' can be calculated from 'shape index' as shown by Criado and Ortega (1987) using formula, $n = 1.26 S^{1/2}$ (2.2)

where $S = a/b$

Since the type of reaction for which Kissinger demonstrated his method is homogeneous, there was confusion about validity of this non-isothermal method for heterogeneous reactions which generally occur in solid state transformations (Wandlant, 1974 and Sharp, 1972). Meisel and Cote (1983) followed by Criado and Ortega (1987) have provided the theoretical basis justifying the use of Kissinger's method for determining the kinetics of reaction in amorphous alloys.

Criado and Ortega started with the reaction rate formula for solid state transformation obeying Johnson-Mehl-Avrami (JMA) kinetics.

$$\frac{d\alpha}{dt} = A n (1-\alpha) [-\ln(1-\alpha)]^{n-1/n} \exp(-E/RT) \quad (2.3)$$

where, α = the fraction reacted

t = time

A = the pre-exponential factor

n = a parameter depending on exact mechanism of nucleation and growth

E = the activation energy

R = the gas constant = $8.3143 \text{ JK}^{-1} \text{ mol}^{-1}$

T = the absolute temperature

For a reaction taking place under constant heating rate β , one can apply Kissinger's method. The maximum rate of reaction is observed when $d(d\alpha/dt)/dt$ is zero;

Differentiating (2.3) one gets,

$$\frac{d^2\alpha}{dt^2} = \left[\frac{E\beta}{RT^2} + \frac{n \ln(1-\alpha) + n - 1}{[-\ln(1-\alpha)]^{1/n}} A \exp(-E/RT) \right] \frac{d\alpha}{dt} \quad (2.4)$$

At $T = T_m$, when maximum reaction rate is reached,

$$\frac{d^2\alpha}{dt^2} = 0, \quad \text{then,}$$

$$\frac{E\beta}{RT_m^2} = - \frac{n \ln(1-\alpha_m) + n - 1}{[-\ln(1-\alpha_m)]^{1/n}} A \exp(-E/RT_m) \quad (2.5)$$

where α_m is the reacted fraction at maximum reaction rate. Taking logarithm of both sides of equation (2.5) and rearranging one gets,

$$\ln \frac{\beta}{T_m^2} = - \frac{E}{RT_m} + \ln \frac{AR}{E} + \ln \left[\frac{n \ln(1-\alpha_m) + n - 1}{[-\ln(1-\alpha_m)]^{1/n}} \right] \quad (2.6)$$

If we assume that the influence of heating rates used in non-isothermal analysis ' β ', on T_m does not lead to any dramatic change in E/RT_m obtained from constant heating rates, then formula (2.6) can be written as:

$$\ln \left[- \frac{n \ln (1 - \alpha_m) + n - 1}{[-\ln (1 - \alpha_m)]^{1/n}} \right] = C_1 \frac{E}{R T_m} + \ln C_2 \quad (2.7)$$

where, C_1 and C_2 are constant.

If this relationship is fulfilled one obtains from equation (2.6) and (2.7);

$$\ln \frac{\beta}{T_m^2} = - \frac{(1 - C_1)E}{R T_m} + \ln \frac{C_2 A R}{E} \quad (2.8)$$

comparison of equation (2.8) with (2.6) allows us to conclude that the plot of $\ln \beta / T_m^2$ Vs $1/T_m$ gives straight line whose slope yields an apparent activation energy $E_a = E (1 - C_1)$ and percentage error in activation energy determined from Kissinger Method would be

$$e = \frac{E_a - E}{E} 100 = -100 C_1 \quad (2.9)$$

The percentage of error (e) in activation energy and values of C_1 and C_2 calculated by the least square fit according to equation (2.7) for different 'n' are shown in Table 2.1 .

The above results show that the errors involved in activation energy using Kissinger's method depends on the value of both 'n' and ' E/RT_m ' and in general, the method gives accurate values for kinetic parameters of a solid state transformation.

The parameter 'n' depends on a number of factors and in

general, can be expressed by the relationship,

$$n = a + bp$$

Where a is 0 for zero nucleation and 1 for constant nucleation, b is the dimensionality of the transformation 1, 2 or 3 and $p = 1/2$ for diffusional growth and 1 for interfacial growth.

Kissinger's non-isothermal method has been used by several researchers to calculate the activation energies of the transformation especially crystallization in amorphous alloys. Luborsky and Walter (1977) showed that the activation energies for crystallization correlate well with the value of crystallization temperature (T_x) for stability of amorphous alloys and indicates that the more complex the alloy, the greater is activation energy. Similar correlations between thermal stability and crystallization parameters were discussed by Chen (1973,1976a,1976b).

More quantitative approach for binary transition metal and rare earth transition metal is proposed by Buschow (1979, 1980).

The activation energies for binary Ni-P and Co-P are dependent on metalloid percentage and their values are presented and discussed in Chapter 4.

There is no such a study for ternary Ni-Co-P so far, however, attempt is made by researchers to study the

compositional dependence of kinetics parameters for many ternary and quaternary amorphous systems. It is shown by Chen (1977) that the ternary addition of B to Fe-P ($\text{Fe}_{83}\text{P}_{14.7}\text{B}_{2.3}$) and Ni to Fe-B ($\text{Ni}_{40}\text{Fe}_{40}\text{B}_{20}$) increases the crystallization temperature by about 50 K higher than those of the corresponding binary alloys.

A study of the effect of composition on the change in activation energy (Orehotsky and Rowlands, 1982) reveals that in case of $\text{Fe}_{80}\text{B}_{20}$ system when Fe is partially replaced by Nickel to $\text{Fe}_{60}\text{Ni}_{20}\text{B}_{20}$ or metalloid B is replaced by P, to $\text{Fe}_{80}\text{B}_{15}\text{P}_5$ there is remarkable increase in activation energy of the system. Recently Panek et al (1985) pointed out that even slight variation in composition for $(\text{Fe}_{100-x}\text{Co}_x)_{100-y}\text{B}_y$ affects the crystallization temperature and activation energy. They reported that for $y = 17$, two crystallization peaks are observed whereas for $33 \geq y \geq 20$ only one reaction taking place. Low Boron content alloys show a decrease in activation energy with increasing Cobalt content from 70 to 90. However, for alloys with $y = 25$ and 33 the activation energy for crystallization tends to increase at the composition above $x = 75$.

Crystallization temperature, activation energy, heat and volume change of crystallization of amorphous Fe-Ni-B system is determined by Warlimont and Gordelik (1985). The results are concluded as: 1) The first phases to crystallize are likely to be structurally related to the amorphous matrix

phase. 2) The magnitude of volume change by crystallization and heat of crystallization are small if the amorphous and crystalline structures are closely related; 3) The rate of atomic motion during relaxation and nucleation are high for disordered amorphous structures and low for intermetallic compound structures, activation energies result accordingly; 4) The magnitude of heat of relaxation affected by the degree of relaxation having occurred during production.

The crystallization kinetics of quaternary $\text{Fe}_{40}\text{Ni}_{40}\text{P}_{14}\text{B}_6$ system is investigated by Russew et al (1985) using both isothermal and non-isothermal conditions in order to gain quantitative information about nucleation mechanism and growth phenomena. The activation energy of growth of crystalline particles under isothermal conditions was calculated to be 300 KJ/mol where the same was determined according to Kissinger, yielding the value of 280 KJ/mol. It is found that these two values are in good agreement with the activation energy of growth of crystallites and self diffusion of Boron in similar systems.

There are three kinds of stability of significance for amorphous magnetic alloys: their resistance to the initiation of crystallization, structural relaxation effects and the reorientation of directional order.

Numerous investigations have therefore been devoted to finding a description of the stability of amorphous alloys. The temperature of first crystallization is a measure for the

relative stability of amorphous state of different composition, provided the heating rate is kept constant (Khan et al, 1981). Cohen and Turnbull, (1961) and recently Buschow (1985) noted that the composition most favourable for amorphous formation is near the eutectic where they show higher crystallization temperature and activation energy of crystallization and at these points the glassy alloys are stable against crystallization.

There have been different approaches to relate the stability of amorphous alloy to its microstructure. The first is based on Bernal's model of randomly packed hard sphere and in the second approach Chen (1974) discusses the effect of atomic sizes and interatomic interaction by investigation on systems like Pd-M-P (M=Fe, Co, Ni). The third approach was suggested by Nagel and Tauc (1975) and it is based on the role of the electron gas.

Luborsky and Walter (1977) has clearly shown that the end of life as far as magnetic application are concerned corresponds to the onset of crystallization and activation energies obtained correlate well with the stability of amorphous system. The activation energy values appear to correlate well with the number of atomic species; the more complex the alloy, the greater is the activation energy.

The effect of compositional variation on the crystallization temperature has been studied by Naka et al

(1976) in the series of amorphous $\text{Fe}_{80-x}\text{M}_x\text{P}_{13}\text{C}_7$ and by Luborsky and Walter (1977) in $\text{Fe}_{80-x}\text{Ni}_x\text{P}_{14}\text{B}_6$ and $\text{Fe}_{80-x}\text{Ni}_x\text{B}_{20}$ alloys. They concluded that the atomic size of the alloying elements and electronegativity had little or no effect on crystallization temperature.

2.4 ELECTRON MICROSCOPY AND X-RAY DIFFRACTION STUDIES

In situ observations of annealing behaviour in heating stage of Transmission Electron Microscope reveal some valuable informations on the micromechanisms of the reactions.

However, it is necessary to examine the bulk state using X-ray diffraction, because there may be local changes due to inhomogeneity which will be detected by TEM but will not be representation of the film. However, X-ray diffraction cannot detect a phase change if the amount is small. Thus, the use of both TEM and XRD is very useful to detect new phases forming during crystallization and identify their structures.

There are some systematic study reported on binary Ni-P and Co-P amorphous alloys prepared by different methods. Bakonyi et al (1986) and Makhsoos et al (1978) studied the crystallization of electrodeposited amorphous Ni-P alloys. In 'as-deposited' Ni-22 at%P alloy, Bakonyi observed that the amorphous state had two kinds of regions having similar diffraction patterns but different contrasts, where Makhsoos observed two to three diffuse rings and

they concluded that the diffuse rings could be attributed either to amorphous state or microcrystalline state with a very fine grain size.

Graham et al (1965) analyzed the electron and X-ray diffraction patterns of 'as-deposited' electroless Ni-P and concluded that the structure of alloys upto 12 at%P is supersaturated solid solution of P dissolved in f.c.c. Nickel but Albert et al (1967) on the basis of X-ray studies showed that the 'as-deposited' films with P content from 0.5 to 14 at% had a strained single phase f.c.c. structure.

While most of X-ray studies show the 'as-deposited' high P, Ni-P films are amorphous, Bagley and Turnbull (1970) followed the mode of transformation by electron microscopy to the stable state and concluded that only a sample with 25 at%P was initially amorphous. The other samples containing 21.2 and 24.9 at%P contents on isothermal annealing, showed crystallite coarsening, suggesting an original microcrystalline structure.

Tyagi (1986) prepared the Ni-P films using electroless alkaline bath and reported that these films can be divided into four regions: polycrystalline for alloys containing less than 11 at%P, microcrystalline for 11-14 at%P, mixed microcrystalline and amorphous having 14-18 at%P and amorphous for more than 18 at%.

In a study of the electroless Ni-P films by Agarwala and Ray (1989) they found that the alloys with 17.8 to 19.8 at%P showing mixed state with amorphous phase and some metastable phases like Ni_{12}P_5 as a common phase and alloys with more than 22.4 at% phosphorous are primarily amorphous.

There is not as much work reported on Co-P. Simpson and Brambley (1971) were the first to report that the Co-P alloys prepared by electroless alkaline method are amorphous for films containing more than 9.0 at%P and alloy with less than 8.8 at%P show single-phase supersaturated solid solution of cobalt having h.c.p. structure. On annealing the amorphous materials transforms to Cobalt-rich h.c.p. and Co_2P at high temperatures.

The electrodeposited Co-P deposit prepared by Bestgen (1985) shows that the samples with 5 at%P consists of supersaturated solid solution of phosphorous in h.c.p. Cobalt and small fraction of Co_2P but samples with 10 at%P is micro-crystalline with randomly oriented crystallites. According to X-ray and electron diffraction patterns the sample $\text{Co}_{86}\text{P}_{14}$ is amorphous.

Thus even for binary system of Ni-P and Co-P the clear composition separating the amorphous and crystalline regions and specific modes of crystallization process have not yet been established. As far as ternary Ni-Co-P is concerned

there is no systematic structural study on this system. The X-ray analysis of ternary Ni-Co-P of composition ranging between 13 and 94 at% Cobalt and phosphorous from 6 at% to 22 at% have been studied by Clements and Cantor (1976) and are reported to be completely amorphous. However, no attempt was made to identify the phases formed on crystallization during annealing.

The phases obtained during crystallization transformation for multi-component TM-M amorphous alloys are studied by various workers, namely, Fe-B-Si and Ni-B-Si (Quivy et al. 1985), Fe-B-Si-C (Fouquet et al. 1985) and Ni-Cr-Co-Ta-B (Geoffroy 1983).

In order to carry out the study of different phases in Ni-Co-P ternary system it is important to have a knowledge about the possible crystalline phases. The structure of different possible phases in Ni-Co-P system are given in Table 2.2 .

2.5 MAGNETIZATION AND ANNEALING BEHAVIOUR

Bagley and Turnbull (1965) reported that amorphous Ni-P alloys in contrast to Co-P, are non-ferromagnetic at room temperature with a phosphorous concentration of 25 at% and above. The study of the composition and temperature dependence of magnetic behaviour are followed by many researchers for binary Ni-P (Bagley and Turnbull 1965, Tyagi

et al 1989, Huller and Dietz 1985, Huller et al 1985) and Co-P (Huller and Dietz 1985, Huller et al 1985, Pan and Turnbull 1974) alloys.

The magnetic moments of most amorphous alloys are lower than those of the pure crystalline transition metals and it is because of the change in the local chemical environmental provided by the presence of metalloid. These alloys are known to fall in the category of weak itinerant ferromagnets.

Different simplified models have been developed to describe the phenomena of lowering the magnetic moment on alloying. Malozemoff et al. (1984) have argued that Friedel's modification of the rigid band model should also apply to Transition Metal-Metalloid alloys.

In this model the average number n_{av} of Bohr magnetons per atom should linearly decrease according to

$$n_{av} = n_0 - x [10 - (Z_{TM} - Z_x)]. \quad (2.10)$$

Where, n_0 is the magnetization in Bohr magneton/atom, of the pure metal, x is the concentration of the metalloid, Z_x and Z_{TM} are respectively the valence of the metalloid and the metal. Number of experiments on Fe-P, Co-P and Ni-P show that the effect of P on magnetic moment per atom is weaker than that predicted by this model. The proposed relation based on rigid band model by Yamauchi and Mizoguchi (1975) for calculation of magnetic moment with alloy compositions are presented and discussed in Chapter 6.

A variety of ternary alloy with a single transition metal elements were prepared and the observed magnetization agree reasonably well with rigid band Model if it is assumed that the number of electrons transferred from metalloids as; 1 for B, 2 for C, 2 for Si and 3 for P.

Becker et al (1977) studied the magnetic moment and Curie temperatures of amorphous alloys of $(\text{Fe-Ni})_{80}(\text{P-B})_{20}$ and their data are in good agreement with the rigid band model. For the Fe rich alloys in the Fe-Ni (Fe-Ni-P-B) series of amorphous alloy, the reduction of moment is greater for $-\text{P}_{14}\text{B}_6$, less for $-\text{P}_{13}\text{B}_8$ and least for $-\text{B}_{20}$ alloys.

Albert et al (1967) studied Ni-P films prepared by different methods, and observed that spontaneous magnetization decreased with increasing phosphorous and films become non-magnetic at 15 at% P. Pan and Turnbull (1974) studied electrodeposited Ni-P for $12 < P < 23$ at% and Co-P for $18 < P < 25$ where their magnetic properties were examined with vibrating sample magnetometer under the applied field of upto 8 K Oe. They showed that in case of Ni-P the low temperature magnetization decreases with phosphorous concentration and ferromagnetism almost disappears at about 17 at% P.

For amorphous Co-P system, the coercive force, and ratio of remanence to saturation of these alloys are several hundred times lower as compared to the 'as-crystallized' states and a more rapid decrease of magnetization with composition is

observed than that expected from rigid band model for $P > 23$ at%.

The electroless amorphous Ni-Co-P with 22.3 at% P is prepared by Simpson and Clements (1975) and the magnetostriction and temperature dependence of the saturation magnetization were measured. The magnetization values depend on the composition with the trend similar to that of crystalline alloys, where the magnetostriction were found to be roughly twice the magnitude of those for crystalline sample.

O' Handley et al (1977) reported the magnetic properties of $\text{Co}_{80-x}\text{Ni}_x\text{P}_{20}$ with $20 \leq x \leq 60$ prepared by rapidly quenching technique. The values of magnetization ' σ ' at 295 K are 3.7, 24 and 46 emu/g for $X = 20, 40$ and 60 respectively for the applied field of 8 K Oe. The comparison of results reported with that prepared by our group is presented in Chapter 6.

2.6 ELECTRICAL RESISTIVITY AND ANNEALING BEHAVIOUR



The electronic transport properties of amorphous alloys have been characterised in terms of electrical resistivity, its magnitude, their temperature and composition dependence. The alloys in amorphous state have small Temperature Coefficient of Resistivity (TCR) which could be positive, zero or negative depending on the concentrations and for some amorphous alloys TCR can be changed continuously by varying the alloy composition. The overall change in resistivity

from the lowest temperature to the crystallization temperature is usually less than 10 per cent.

Mooij (1973) established a correlation between the magnitude of electrical resistivity ' ρ ' and TCR ' $\alpha = \partial \rho / \partial T \cdot \rho^{-1}$ ', by analyzing available data in amorphous transition metal alloys.

This remarkable correlation can be summarized as:

- (a) Positive TCR for ρ less or about $100 \mu\Omega \text{ cm}$
- (b) Negative TCR for ρ greater than $150 \mu\Omega \text{ cm}$
- (c) About zero TCR for ρ around $150 \mu\Omega \text{ cm}$.

Most of the works on the transition metal alloys deal with those having Ni, Fe, Pt or Pd and Metalloids P, B, or Si.

In the binary systems, amorphous Ni-P alloys are typical and the temperature and composition dependence of their electrical resistivity measured by Cote (1976) shows that, TCR (α) changes from positive to negative at $P \approx 24 \text{ at}\%$ and resistivity minima are seen near 15 K.

The electroless Ni-P alloys containing upto 16 at% phosphorous studied by Pai and Marton (1972) shows a drastic change in resistivity accompanied by structural transformation of the film from a single phase f.c.c. structure to a two phase microstructure containing f.c.c. Nickel and tetragonal Ni_3P .

The electroless Ni-P alloys containing both microcrystalline and amorphous regions, with $5 < P < 23.5$ at% prepared by Tyagi (1986) show the following temperature dependences: 1) the resistivity is found to increase from an initial value of $71 \mu\Omega \text{ cm}$ to $187 \mu\Omega \text{ cm}$ at 21.5 at% P. 2) TCR decreases to a value of $12 \times 10^{-5} \text{ K}^{-1}$ with increasing phosphorous to 22%, 3) As pointed out by Mooij, higher resistivity samples are found to have linear TCR. At lower phosphorous the transport is primarily through microcrystalline regions.

The electrical resistivity measurements of Co-P for different compositions are reported for samples prepared by electrodeposition (Riveiro et al 1986, Kuhnast et al 1984, Sonberger and Dietz 1985) and vacuum evaporation (Rivory and Bouchet 1979) methods. The resistivity of 'as-prepared' samples increases with increasing phosphorous. The initial sharp drop in electrical resistivity observed at temperatures of 523-593 K are associated with phase separation of h.c.p. Cobalt from amorphous alloy and then its transformation to h.c.p. Cobalt and Co_2P .

Majority of the investigations on electrical resistivity of amorphous alloys reported so far on TM-M ternary or quaternary systems are prepared by melt quenching techniques. Composition and temperature dependence of electrical transport properties of Fe-Ni based amorphous alloys have been

extensively studied because of their technological importance (Malmhall et al 1979). Studies of resistivity with temperature have been carried out to correlate the resistivity changes with the exothermic DSC peaks in order to identify the crystallization process and phases formed during this reaction (Heimendahl and Maussner, 1978). Also, the kinetic parameters like activation energy has been found out by resistivity technique.

The results of electrical resistivity for 'as-deposited' samples and TCR values and annealing behaviour from room temperature upto 850 K is presented in Chapter 6 for the amorphous electroless Ni-Co-P.

TABLE 2.1 VALUES OF C_1 , C_2 AND PERCENTAGE OF ERROR IN THE ACTIVATION ENERGY (ϵ) CALCULATED BY THE LEAST SQUARE METHOD ACCORDING TO EQUATION (2.7)

KINETICS		E/RT				
		2	5	10	30	60
n						
0.5	C_1	-0.307	-0.239	-0.053	-0.007	-0.002
	C_2	28.160	10.311	2.976	1.472	1.313
	ϵ	30.7	23.9	5.3	0.7	0.2
1.5	C_1	0.132	0.028	0.008	0.001	0.0003
	C_2	0.542	0.723	0.838	0.935	0.966
	ϵ	13.2	2.8	0.8	0.1	0.03

TABLE 2.2 THE STRUCTURE OF DIFFERENT POSSIBLE PHASES INVOLVING NICKEL, COBALT AND PHOSPHOROUS.

DESIGNATION	CRYSTAL SYSTEM	LATTICE PARAMETERS	REFERENCES
α -Co (e)	HEXAG- -ONAL	a = 2.507 , C = 4.07	ASTM DATE CARD TECHNICAL MANUAL
Co P ₂	MONOC- -LINIC	a = 5.61, b = 5.591, c = 6.43	ASTM DATA CARD
Co P ₃	CUBIC	a = 7.707	"
Co P ₄	CUBIC	a = 7.711	"
Co ₂ P(e)	ORTHOR- -HOMIC	a = 6.638 , b = 5.670, c = 3.52	"
Ni (e)	F.C.C.	a = 3.5238	"
Ni ₃ P(e)	TETRA- -GONAL	a = 8.93 c = 4.39	MAKHSOOS et al (1978)
Ni ₅ P ₄	HEXAG- -ONAL	a = 6.789 c = 10.986	ASTM DATA CARD
Ni ₇ P ₃	CUBIC	a = 8.647	"
Ni ₁₂ P ₅	TETRA- -GONAL	a = 8.646 c = 5.020	"
Ni P ₂	CUBIC	a = 5.4706	"
Ni P	ORTHOR- -HOMIC	a = 6.05, b = 4.881 c = 6.890	"

(e) DENOTES EQUILIBRIUM PHASE

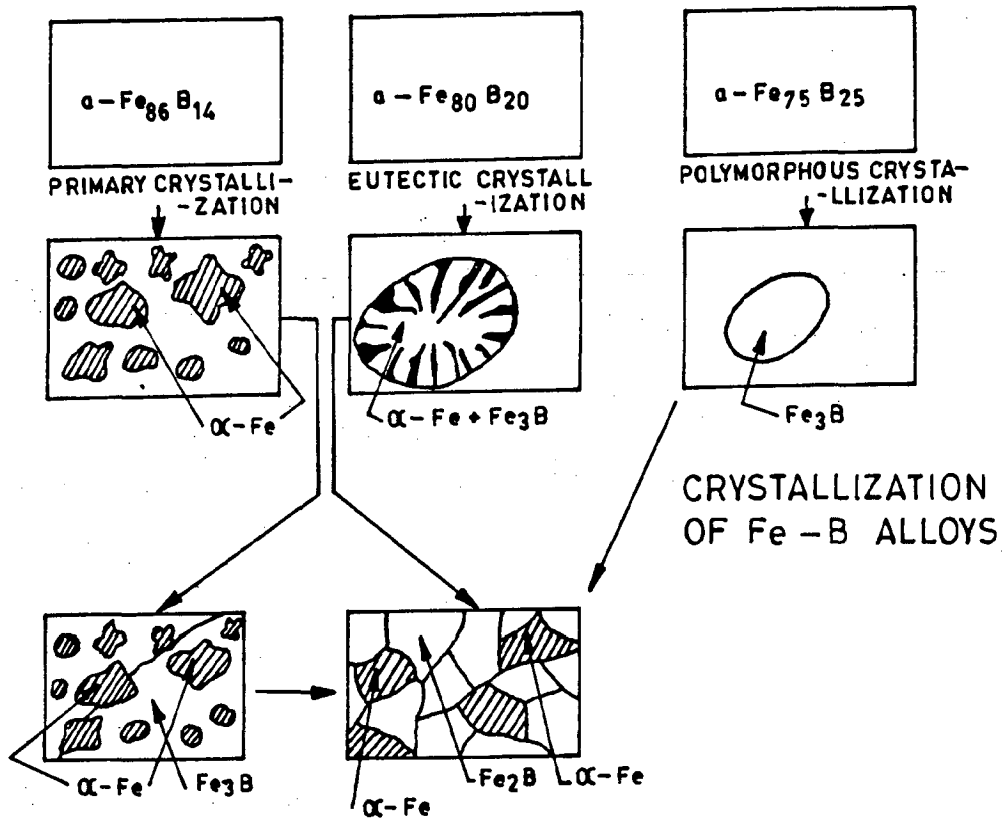


FIG. 2.1 SCHEMATIC DIAGRAM OF TYPICAL CRYSTALLIZATION REACTION IN AMORPHOUS Fe-B ALLOYS (KOSTER AND HEROLD, 1981)

CHAPTER 3

EXPERIMENTAL TECHNIQUES

In this chapter we present the details of our sample preparation method, the electroless deposition, its elemental analysis and measurement techniques used for crystallization kinetics, phase transformations, electrical resistivity and magnetization study of Ni-Co-P system.

3.1 THE Ni-Co-P ELECTROLESS DEPOSITION METHODS

Keeping all the consideration in view, as discussed in chapter 2, an alkaline sulphate bath has been used in our work to prepare Ni-Co-P amorphous films.

The compositions and condition of the bath selected for sample preparation is shown in Table 3.1. All the chemical used were of ANALAR grade. pH value is maintained throughout the deposition time by suitable addition of ammonia solution to the bath. Both Aluminium foils and glass slides were used as substrate for the deposition of amorphous Ni-Co-P films. Constituents of the bath used in our study is adjusted to get an optimum rate of deposition and strain free amorphous alloys. In our bath as Nickel salt increases the rate of deposition also increases.

The phosphorous content of all the samples was about 15 at% since samples of less than 14 at% P are mixture of

amorphous and crystalline phases whereas deposits of more than 15.5 at% P were not stress free.

To have uniform deposit, the proper cleaning of substrate is essential. The procedure of cleaning of glass slides are as follows:

- I) They were rubbed with cotton dipped in liquid detergent and are washed with water.
- II) Putting in hot chromic acid for 15 hours and then washed thoroughly in hot deionized water.
- III) Passing the slides through hot solution of 10% NaOH and again washed thoroughly in hot deionized water.
- IV) The glass substrates are dried with hot air.

Before immersing the glass slides in the bath they have to be first sensitized in a 1% SnCl_2 solution for 1 minute and then activated by immersing in a 0.1% PdCl_2 solution for about 30 seconds, followed each time by a rinse in deionized water.

Aluminium foils (99.955 pure) of 0.3mm thick and 3 cm wide strips have been used and cleaning of aluminium substrates is done by following steps:

- a. degreasing with organic solvent and rubbing with Vim Powder
- b. washing with running water followed by deionized water
- c. etching in 1:1 nitric acid

- d. final washing with deionized water and drying with hot air.

For Aluminium substrates the sensitization is not necessary, however, immersing in PdCl_2 solution for about 30 seconds is desirable.

- a) Sample preparation for Electron Microscopy Studies:

For transmission electron microscopy cleaned glass slides are dipped on Formvar solution (4.0g polyvinyl formal in 1 liter ethylene dichloride). This transparent layer of Formvar will form on the glass slides and about 15-20 minutes of deposition on Formvar coated glass slides were found to be suitable for TEM study. After deposition the Formvar layer was dissolved in suitable organic solvent and microscope grid is used to support the sample for insertion into the microscope.

The typical appearance of 'as-deposited' Ni-Co-P alloys is shown in transmission electron micrographs of Fig.3.1 (a) to (c). The growth starts at isolated nuclei on the substrate Fig. 3.1(a), and covers it progressively by growth of colony as is evident from deposits of longer times shown in Fig.3.1(b) and (c). This shows that the discontinuity in the deposit decreases with time and at longer deposition times the deposit become continuous as revealed in Fig.3.1(c).

b) Sample Preparations for XRD, DSC, VSM and Electrical Resistivity Studies.

In case of deposits on Aluminium foils, the foil was dissolved in hot NaOH solution, whereas for the case of deposits on glass slides samples are physically removed.

Using both the glass slides and Aluminium foils the thick films of 25 mm x 70 mm x (3 - 8 μm) are obtained for purpose of compositional analysis. X-ray diffractometry, differential scanning calorimetry, resistivity and magnetization studies. The foil samples and thin deposits for electron microscopy have been assumed to have same composition as they have been deposited in same bath for each sample.

3.2 THE CHEMICAL COMPOSITION

The Inductively Coupled Plasma (ICP) Model 8410 is used for elemental analysis of all the samples. It is a sequential Inductively Coupled Plasma Atomic Emission Spectrometer which can perform rapid estimation of most elements in the periodic table.

Here power from a radio frequency generator is coupled to a flow of ionized Argon gas inside a quartz tube encircled by an induction coil. To initiate the plasma, Argon is ionized by a momentary high voltage discharge. The ionized gas passing through the high frequency magnetic field, absorbs energy and this causes further local heating and ionization to form a ball of electrically conducting gas, or plasma. Liquid

samples are injected into a high temperature environment of the plasma. Here the analyte forms free atoms and ions emit characteristic spectra and is viewed by the optical system which covers the wavelength range of 170-820 nm, with resolution of 0.01 nm, and selectability of 0.005 nm per step can be achieved.

A multi-processor computer system controls the monochromator and autosampler. It has sample volume 10-15 μ l, Injection rate of 240 sample/hour and relative standard deviations of less than 1.5 %. Detection limits of 0.1 mg/l with 10 μ l injections.

Here metal salts are used as a standard and all electroless deposited samples are dissolved in suitable solvent. The chemical composition of amorphous electroless films prepared are listed in Table 3.2. As can be seen samples composition in atomic percent are, Ni_{55.5}Co_{29.0}P_{15.5}, Ni_{39.0}Co_{46.0}P_{15.0}, Ni_{35.6}Co_{49.1}P_{15.3}, Ni_{27.0}Co_{58.0}P_{15.0} and Ni_{15.3}Co_{70.0}P_{14.7}. Total number of 20 samples are prepared where care was taken to use central portions for all the investigations.

3.3 DIFFERENTIAL SCANNING CALORIMETRY

Because of large enthalpy of crystallization which is highly exothermic, Differential Scanning Calorimetry (DSC) is a standard method to monitor the crystallization process and kinetics.

The calorimeter used was a Stanton Redcraft DSC-1500 model with working range from room temperature to 1500 °C and facility of controlling atmosphere.

The DSC signal is derived from a temperature difference between the sample and an inert reference (Alumina) and designed to give an output in milliwatts. The microprocessor based DSC lineariser is included as a standard part of the instrument unless connected to a computer system.

Specimens of mass 4.0 mg were annealed in a Platinum crucible under a static air atmosphere. The temperature and power axis of the calorimeter were calibrated from melting endotherms of pure Pb, Sn, Zn and thermal lag is linear with heating rate. All amorphous Ni-Co-P samples were heated at different heating rates ranging from 5 to 40 Kmin⁻¹. The area enclosed by the peak and base line is proportional to the enthalpy change of the reaction and planometer is used to measure the area and calculate the enthalpy with respect to pure Lead and Tin.

In order to study the origin of the heat effects observed during DSC measurement we repeated the DSC runs several times with new pieces of amorphous Ni-Co-P films and stopped at various stages of the heating process. After cooling to room temperature these pieces were subjected to investigation by means of X-ray diffraction.

3.4 ELECTRON MICROSCOPY AND X-RAY DIFFRACTOMETRY

The structural study of the electroless Ni-Co-P films has been carried out using Transmission Electron Microscopy and X-Ray Diffraction. The Transmission Electron Microscope used was Philips EM 400 T/ST model with a heating holder attachment PW6592 operated at 100 KV. The electron micrographs have been taken at magnifications from 16000 to 27000 and for selected area diffraction patterns the camera lengths used are 290 mm and 410 mm. A temperature control and measuring unit is attached with the heating holder which contains the current supply for the heater and also the circuitry to measure the voltage generated by the thermocouples and we have the advantage of precise information of the sample temperature.

Two types of patterns i.e. ring and spot patterns are obtained when examined by Selected Area Diffraction (SAD) mode in TEM.

I) Indexing Ring Patterns:

The radius of each ring is characteristic of the spacing of the reflecting planes in the crystal and setting of microscope lenses and this was calibrated by using gold specimen. The diameter of ring R_1 , R_2 and R_3 etc. are measured from negatives. The parameter R is characteristic of inter planar spacing d_{hkl} of reflecting plane and magnification due to the lens setting, i.e. Camera Constant

λL , where λ is the wavelength of the electron beam and L is the distance between the specimen and screen. These distances are converted into interplaner spacings using camera constant as $d = \lambda L/R$. From the ASTM index cards, starting with the most likely phases, the phases present in the deposits were identified.

II) Indexing Spot Patterns:

The distance R_1, R_2, R_3 etc. are the distance of diffracted spots from transmitted beam (i.e. from the center spot (000)). The angles between lines drawn from the center to the diffracted spots are the angles between planes and beam direction \vec{B} is approximately the zone axis of the reflecting planes. If the camera constant is known accurately by the calibration with gold specimen, d values can be calculated by measuring R_1, R_2, R_3 etc. values from negatives and substituting in $Rd = \lambda L$. Checking the d -values with the ASTM cards and angles between the reflecting planes must be correct to provide a cross check.

X-Ray Diffractometer Model 1140/90 PHILIPS, equipped with a Scintillation Counter, Zr filter, and Cu- K_α radiation have been used for x-ray study of our 'as-deposited' and annealed samples.

3.5 MAGNETIC MEASUREMENTS

Foner Type Vibrating Sample Magnetometer (VSM) Model 155 Princeton Applied Research Corporation with RE 0091 X-Y

recorder are used for magnetization study. It has five calibration ranges and minimum detection limit of 0.00001 emu.

When a sample is placed in a uniform magnetic field, a dipole moment proportional to the product of the sample susceptibility times the applied field is induced in the sample. If the sample is made to undergo sinusoidal motion as well, an electrical signal can be induced in suitably located stationary pickup coils. This signal, which is at the vibration frequency, is proportional to magnetic moment, vibration amplitude and frequency. By approximately processing, the effects of vibration amplitude and frequency shifts are cancelled and readings are obtained which vary only with the magnetic moment, the quantity of our interest.

With this model, reproducibility is better than 1% where absolute accuracy is less than 2%. Temperature oven with chromel-alumel thermocouple under low vacuum is used for annealing study where heating rate is 2.0 ± 0.5 K/min.

Constant magnetic field of 5 K Oe which is sufficient to saturate the samples has been applied for the measurement of magnetic moment with temperature from ambient to 850 K.

The semi-micro METTLER balance model-H 54R, with a resolution of 0.00001 gm, has been used for weighing the samples.

3.6 THE ELECTRICAL RESISTIVITY MEASUREMENTS

The change on annealing of the resistivity is studied using a standard four probe DC method. Typically, the samples were 25 mm long, 5 mm wide with thickness of about 3-8 μm and for each alloy measurements were made on several specimens cut from central portion of the deposited samples.

The thickness of each specimen was measured at several points along its length using surface profile measurement system DEKTAK IIA. The DEKTAK IIA is a microprocessor-based instrument used for making accurate measurements on very small vertical features ranging in height from less than 100 \AA to 655000 \AA .

The set up used for electrical resistivity measurements in the temperature range 300 K through 850 K shown in Fig.3.2 and Fig.3.3. The copper cold finger supported by heating coil is used to heat the sample where glass slides are used as a sample holder. The temperature of the heater and the sample was monitored using chromel-constantan (type E) thermocouples connected to the microprocessor based digital thermocouple meter (Model AD2050).

A constant current source of about few miliampere is applied and voltage drop was measured using digital Keithley microvoltmeter (Model 197).

The sample holder assembly of cryostat is evacuated by

rotary pump and the electrical and thermocouple connections are carried out through a vacuum seal. A four point probe with an interprobe spacing of 4.0 mm was constructed so that by using the long rectangular samples it was possible to calculate the resistivity using the simple relation.

$$\rho = Vwt/Il$$

where V is the voltage between the inner probes. I is the current along the length of the sample, l is the interprobe spacing, w is the width of the sample, and t is the thickness of the sample.

Parasitic thermoelectric voltage were eliminated by either reversing the current or noting the zero-current voltage reading at each temperature. The heating rate was kept in 20 ± 3 K/min for all the samples. Considering all the sources of error, our accuracy is about 7-8% in estimation of resistivity. However, in studying the temperature dependance of the sample resistance the precision is 1% or better and temperature values are good to about 2 K.

TABLE 3.1 GENERAL COMPOSITION OF THE BATH
USED FOR DEPOSITING Ni-Co-P.

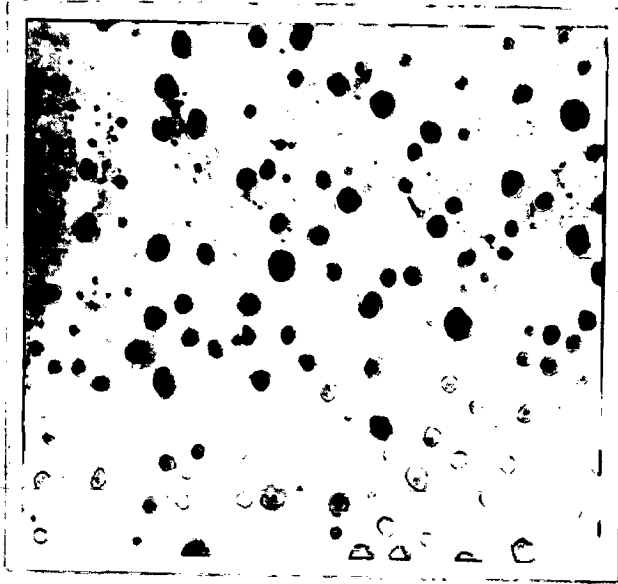
$\text{NiSO}_4 \cdot 7\text{H}_2\text{O}$	(2.5-15) g/l
$\text{CoSO}_4 \cdot 6\text{H}_2\text{O}$	(10-22.5) g/l
$\text{Na}_3\text{C}_6\text{H}_5\text{O}_7 \cdot 2\text{H}_2\text{O}$	90 g/l
$(\text{NH}_4)_2\text{SO}_4$	47 g/l
NaH_2PO_2	(28-32) g/l
pH VALUE	8.0 ± 0.1
TEMPERATURE	$(358.0 \pm 2.0\text{K})$

SLOW STIRRING

TABLE 3.2 ATOMIC COMPOSITION ($\pm 1\%$) OF THE AMORPHOUS ELECTROLESS Ni-Co-P.

SAMPLE	Ni (at%)	Co (at%)	P (at %)
A	55.5	29.0	15.5
B	39.0	46.0	15.0
C	35.6	49.1	15.3
D	27.0	58.0	15.0
E	15.3	70.0	14.7

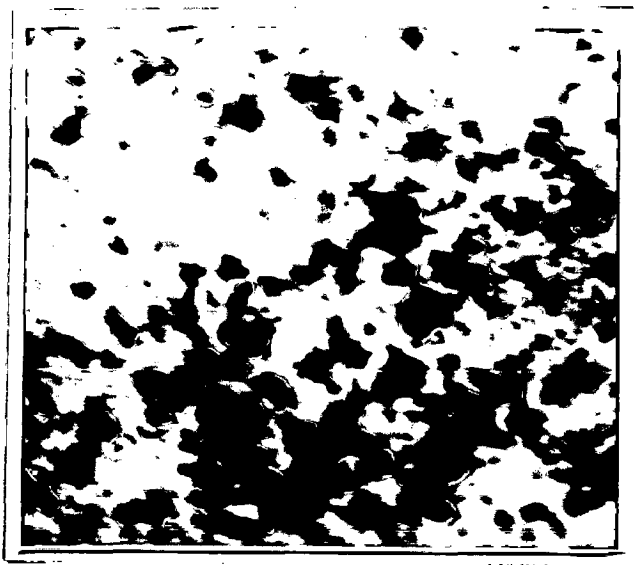
TRACES OF Fe AND Mn (less than 1 at%)



(a)



(b)



(c)

FIG. 3.1 TRANSMISSION ELECTRON MICROGRAPHS OF TYPICAL
Ni-Co-P ALLOYS.
(a) START OF DEPOSITION (X 16000)
(b) DEPOSITED FOR 10 MINUTES (X 27000)
(c) DEPOSITED FOR 30 MINUTES (X 27000)

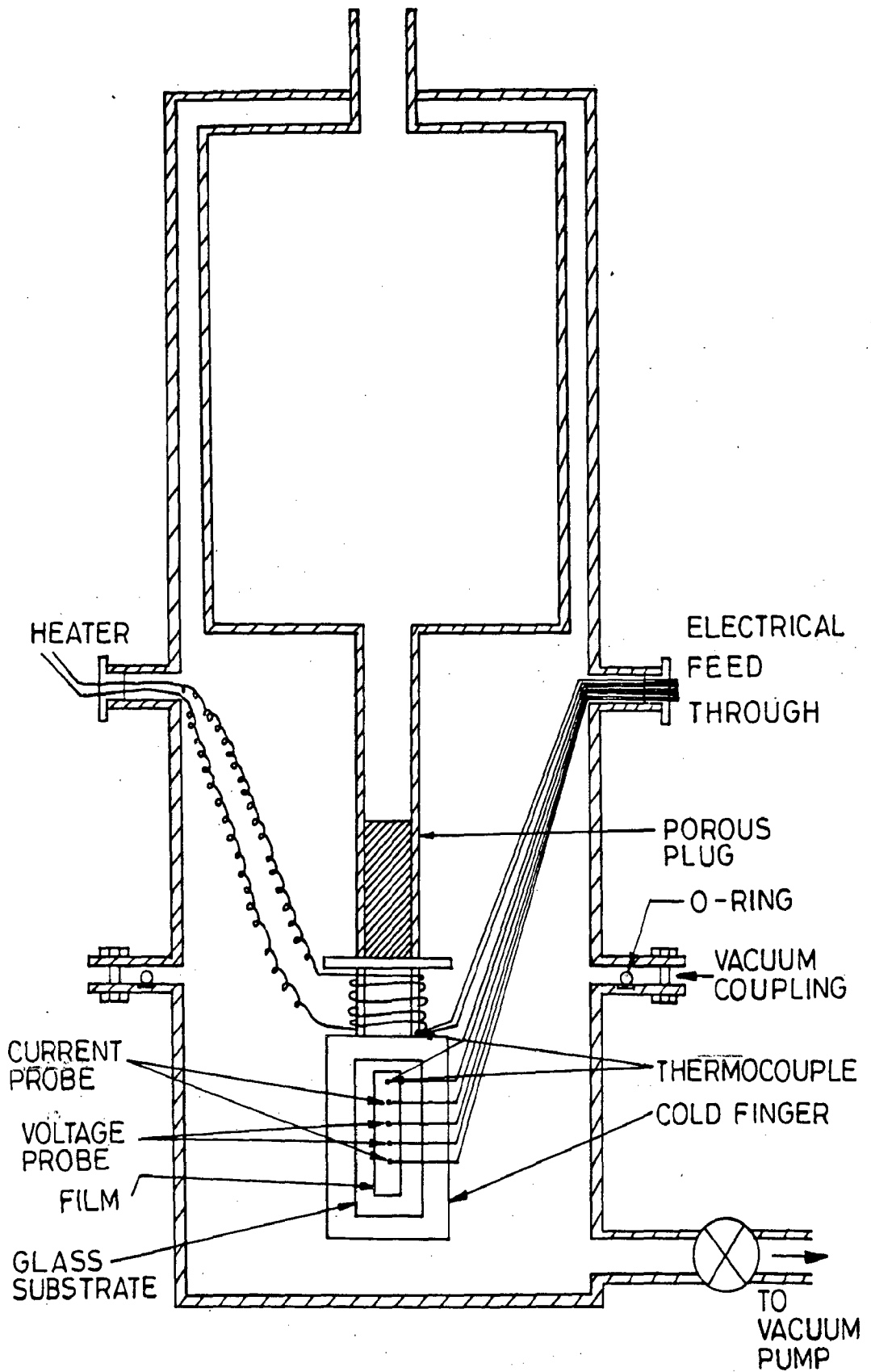


FIG.3.2 DIAGRAM OF THE RESISTIVITY SET-UP FABRICATED IN THE LOBORATORY BY THE CANDIDATE.

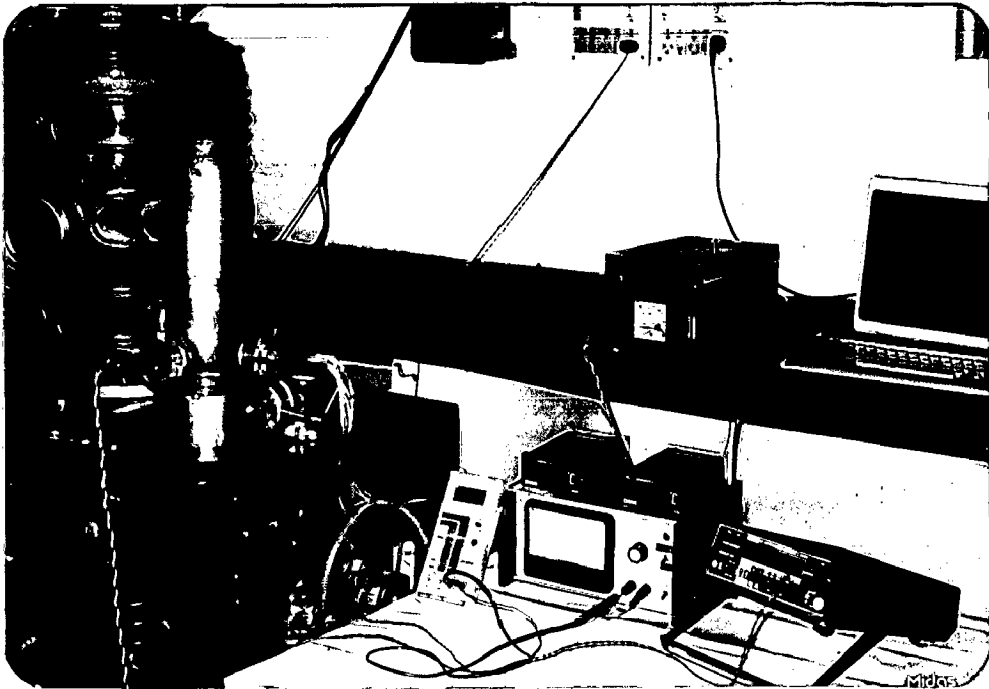


FIG. 3.3 A PHOTOGRAPH OF RESISTIVITY SET UP.

CHAPTER 4

CRYSTALLIZATION KINETICS OF AMORPHOUS ELECTROLESS Ni-Co-P

The metastable nature of amorphous alloys is a major disadvantage and knowledge of their thermal stability prior to any application is of prime technological importance.

The study of amorphous-to-crystalline transformation by calorimetric method (DSC) gives rise to a strong exothermic peak T_p at the crystallization temperature. The kinetic parameter, the activation energy of crystallization which is the energy that must be crossed by the atoms to transfer them from amorphous to crystalline state, is a good measure of the stability of amorphous state.

The aim of present chapter is to understand how compositional variation influences the kinetics of crystallization and thermal stability of amorphous electroless Ni-Co-P ternary alloy.

4.1 RESULTS: DIFFERENTIAL SCANNING CALORIMETRY

Typical plots of DSC in the temperature range of 300-850 K for Ni-Co-P samples heated at a rate of 20 K/min are shown in Fig.4.1. The curves show two strong exothermic transformation peaks (T_{PI} and T_{PII}) in the temperature range starting from 550 K up to 800 K. A small peak in the temperature range of 500-550 K can also be observed. However

this small peak believed to be due to atomic relaxation (Fouquet et al. 1985, Tyagi et al. 1989), was not further investigated.

The first and second peaks are taken to correspond to crystallization reactions and kinetics of the transformations associated with these peaks are focus of our present investigation. The values of peak temperatures for first and second peak (T_{PI} , T_{PII}) for compositionally different Ni-Co-P samples are shown in Table 4.1.

Enthalpies of the reactions under first and second peaks have been obtained following the procedure given in the chapter 3 and the values are presented in Table 4.1. It is observed that the reaction taking place under the first peak involves a smaller enthalpy change compared to that occurring under the second peak. Further, the peak temperature of the first reaction increases with the increase in cobalt content of the film till about 49.1 at% cobalt content (sample C) and then reduces a little but no such trend has been observed in the peak temperature for the second reaction. The enthalpy change per unit weight of the sample for the first reaction shows a maximum when Nickel and Cobalt at roughly in equal atomic proportion i.e. sample B, but the enthalpy change for the second shows a similar fluctuating type of trend as it is observed for its peak temperature. Fig.4.2 shows the described variation of enthalpies with change in composition.

Fig. 4.3 shows a plot of first peak temperature (T_{PI})

with heating rate for the films containing different amounts of Cobalt. When the plots extrapolated to almost zero heating rate one obtains a limiting temperature which is also a measure of thermal stability. Fig.4.4 shows the variation of limiting temperature with composition. This limiting temperature is higher in values for the samples containing 49.1 at% Cobalt.

Since the reactions occurring under the peaks are thermally active, the Kissinger's method (Kissinger, 1957) is applied and slope of $\ln \beta / T_p^2$ Vs $1/T_p$ is used for calculation of activation energies involved in the first and second reaction. The typical Kissinger's plot for $\text{Ni}_{35.6}\text{Co}_{49.1}\text{P}_{15.3}$ sample are shown in Fig. 4.5. The values of activation energy as obtained by least square fit and that of parameter 'n' are listed in Table 4.2. To have an idea of accuracy in calculation of activation energies, as described in Chapter 2, the values of E/RT for different heating rates are calculated and minimum values are listed in Table 4.2. The overall accuracy is better than 5.3% as estimated from Table 2.1. The variation of activation energy with composition is shown in Fig. 4.6. Where the activation energy of the reaction for both the peaks maximizes at almost equal composition of Nickel and Cobalt (46, 49.1 at% Cobalt).

For the sake of comparison in Table 4.3, we have listed the value of activation energy for binary Ni-P and Co-P as determined by us along with that of other worker. Our

values of activation energy in case of ternary Ni-Co-P are lesser than that reported by others for binary Ni-P and Co-P but show higher values for the Ni-P (Am. + Cryst.) and amorphous Co-P prepared by our group.

4.2 DISCUSSION

For binary Ni-P, Bakonyi et al (1986) reported the samples prepared by electrodeposition show three different types of DSC responses corresponding to phosphorous content of $P < 20$ at%, $P = 20$ at% and $P > 20$ at%. For the compositions below 20 at% P, the DSC shows a broad maximum which represents some process preceding the amorphous-crystalline transformation which occurs at a much lower temperature than crystallization temperature (T_x). For $P \approx 20$ at% the one step crystallization is observed where for P contents beyond 20 at%, the crystallization is completed in two steps corresponding to crystallization and grain growth process. Simpson and Brambley (1972) reported that $Ni_{85}P_{15}$ prepared by electroless technique, under DTA shows two peaks at 573 K and 661 K .

In Ni-P system Clements and Cantor (1976) has observed one broad peak at 480-600 K depending on heating rate and two major peaks at around 600 K or above in DSC for films with $P < 15$ at% prepared by electroless technique. However, for films containing phosphorous in excess of 15 at%, the broad peak disappears and the other two peaks eventually merge to a single peak.

Study on binary Co_{91}P_9 by Simpson and Brambley (1971) also show two peaks at 533 and 683 K. In general, Metal-Metalloid amorphous systems with relatively lower Metalloid content crystallizes by two stage processes as it has been observed in Fe-B, Ni-P, Ni-B and Fe-Ni-B systems. The initial primary phase which probably is equivalent to separation of pre-eutectic phase when transformation takes place from metastable liquid. The remaining amorphous phase does not appear to transform polymorphously to phosphide - say Ni_3P in Ni-P system as evident from magnetic change accompanying the second reaction in crystallization. It appears that this second reaction may be an eutectic type of reaction giving rise to a mixture of phases Ni_3P and Nickel in Ni-P system. This two stage process is characteristic of crystallization of ternary Ni-Co-P films as investigated by us (Azhdary et al., 1990). The appearance of a broad peak in the initial stage of annealing electroless Ni-P films with lower phosphorous as observed by both Bakonyi and Clements may be due to mixed state of Ni-P films with less than 15 at% P. As observed by Tyagi et al (1985), Agarwala and Ray (1989) phosphorous may be coming out of the supersaturated crystalline regions with the separation of complex phosphides as it has been observed by a number of investigators (Agarwala and Ray 1989, and Masui et al 1985).

Since Co-P system becomes amorphous at a lower phosphorus content than Nickel, the ternary system in the

composition range investigated has always resulted in completely amorphous film. It is possible that if the investigation would have covered low Cobalt and high Nickel end of the ternary system one could obtain a mixed crystalline and amorphous film whose crystallization could show a broad peak in addition to those two peaks observed by us. It will be interesting to investigate into this conjecture.

A few binary Ni-P and Co-P alloys have been prepared with similar phosphorous content as those of Ni-Co-P for the sake of comparison of data. The $\text{Ni}_{84.2}\text{P}_{15.8}$ films show a mixture of amorphous and crystalline regions where as Co-P samples are completely amorphous even with a phosphorous content of 14.2 at%.

In the ternary electroless Ni-Co-P films prepared by Clements and Cantor (1976) DSC response is reported to show one peak at 640 K for $\text{Co} < 26$ at%, ($\text{P} = 20$ & 22 at%) and three distinct peaks at 570, 640 and 680 K for $\text{Co} > 26$ at%, ($\text{P} = 20, 21, 12, 6$ at%). It is possible that at the compositions investigated by Clements and Cantor primary Nickel and Cobalt separates out over different temperature ranges.

As can be seen from table 4.2 and 4.3 addition of Nickel to Co-P and Cobalt to Ni-P increases the value of activation energy to 189.7 KJ/mole for ternary $\text{Ni}_{35.6}\text{Co}_{49.1}\text{P}_{15.3}$ from 132.7 KJ/mole and 102.33 KJ/mole respectively. In case of other ternary systems, for example, addition of Nickel to

Fe-B amorphous alloys (Orehotsky and Rowlands, 1982) the value of activation energy increases to 355.8 KJ/mole for ternary $\text{Fe}_{60}\text{Ni}_{20}\text{B}_{20}$ from 188.4 KJ/mole and comparatively similar trend is found by Warlimont and Gordelik (1985).

Addition of phosphorous to Cobalt apparently produces larger strain in lattice resulting in amorphous phase at lower phosphorous content. In addition, the alloying of Nickel with Cobalt and vice-versa is going to produce additional lattice strain. Both these elements, Nickel and Cobalt has similar eutectic phase diagrams when alloyed with metalloid phosphorous and even, the eutectic temperatures are almost the same. Thus, keeping the phosphorous content the same, the variation of composition from Nickel to Cobalt end in the ternary system will highlight the effect of alloying the binary Ni-P and Co-P systems with Cobalt and Nickel respectively.

The variation of activation energy with the Cobalt content in the film as shown in Table 4.2 and Fig.4.6 indicates that Cobalt enhances the stability of the film both with respect to separation of primary phase and also, the first reaction occurring under the second peak of the DSC curve. But from the Cobalt end the addition of Nickel does not produce such large impact on stability. Any further alloying of the amorphous system with new elements enhances the stability of the amorphous phase in general, because diffusion of the new alloying element will be required to cause the amount partition accompanying phase separation. So,



245694

the element having a higher activation energy for diffusion in the alloy should give larger stability to the amorphous phase. However, the activation energy for crystallization in each of its two stages reflects that of its slowest step. The magnitude of activation energy is similar to those of activation energy for diffusion of phosphorus in Ni, Co and Ni-Co alloys (Masui et al, 1985) and thus, Phosphorous diffusion may be the slowest step in the reactions involved.

The values of 'n' for the reaction under first peak due to primary phase separation is lower than 1 so it appears that this transformation is taking place on pre-existing nuclei. The index 'n' for the reaction occurring under the second peak is less than 1.5. It is also possible that the eutectic type of transformation may have been nucleated by the already formed primary phases.

4.3 SUMMARY

The kinetics of crystallization for the amorphous Ni-Co-P have been investigated with the help of Differential Scanning Calorimeter. The small peak observed are attributed to stress relaxation followed by exothermic crystallization reactions (T_{PI} , T_{PII}). The enthalpy change of the samples for first reaction shows maximum for Nickel - Cobalt where fluctuating type of trend is observed for second reaction. The limiting temperature (zero heating rate) shows higher value of 595 K for sample containing 49.1 at% Cobalt.

Applying Kissinger's non-isothermal method the activation energy of first and second reaction are calculated with an accuracy of better than 5.3 % . Where the activation energy for the reaction under the first peak (T_{PI}) is found to maximize at 49.1 at% Cobalt, that of second peak attains maximum at a nearly equal Cobalt and Nickel composition. These results show that addition of Cobalt in equal proportion of that of Nickel enhances the stability of the films and phosphorous diffusion will be the slowest step in these reactions.

The values of 'n' indicates that the reaction under first peak (T_{PI}) taking place on pre-existing nuclei where the second one is eutectic type of transformation.

TABLE 4.1 THE CHARACTERISTIC PARAMETERS OF TRANSFORMATION PROCESS FOR AMORPHOUS Ni-Co-P FILMS.

SAMPLE COMPOSITION	T_{P_I} K	ΔH_I J/g	$T_{P_{II}}$ K	ΔH_{II} J/g
Ni _{55.5} Co ₂₉ P _{15.5} (A)	578	103.84	713	788.72
Ni _{39.0} Co _{46.0} P _{15.0} (B)	586	182.69	673	763.94
Ni _{35.6} Co _{49.1} P _{15.3} (C)	613	173.62	733	785.32
Ni _{27.0} Co _{58.0} P _{15.0} (D)	598	128.09	678	728.81
Ni _{15.3} Co _{70.0} P _{14.7} (E)	598	128.31	713	823.1

THE VALUES T_p AND ΔH ARE FOR 20 K min^{-1} HEATING RATE.

TABLE 4.2 THE VALUES OF KINETIC PARAMETERS n , E
AND E/RT FOR DIFFERENT Ni-Co-P ALLOYS.

SAMPLE COMPOSITION	0.6 < n < 0.8		1.1 < n < 1.4	
	E_I KJ mol ⁻¹	E_I/RT	E_{II} KJ mol ⁻¹	E_{II}/RT
Ni _{55.5} Co _{29.0} P _{15.5} (A)	112.50	20	112.2	17
Ni _{39.0} Co _{46.0} P _{15.0} (B)	171.0	34	177.0	30
Ni _{35.6} Co _{49.1} P _{15.3} (C)	189.7	36	154	24
Ni _{27.0} Co _{58.0} P _{15.0} (D)	147.0	29	142.0	25
Ni _{15.3} Co _{70.0} P _{14.7} (E)	135.0	21	130.37	20

TABLE -4.3 VALUES OF ACTIVATION ENERGY FOR BINARY
Ni - P AND Co - P

BINARY COMPOSITION	METHOD OF PREPARATION	ACTIVATION ENERGY K J mol ⁻¹	REFERENCE
Ni ₈₅ P ₁₅	ELECTROLESS	220,227	MEISEL AND COTE (1983)
Ni ₈₄ P ₁₆		183.3	CLEMENTS AND CANTOR (1976)
Ni ₈₃ P ₁₇	„	192.9	„
Ni ₈₂ P ₁₆		154.4	„
Ni _{84.2} P _{15.8}	„	102.33	OUR GROUP
Co ₈₈ P ₁₂	ELECTRODEPOSITED	231.56	SONNBERGER AND DIETZ (1985)
Co ₇₆ P ₂₄	„	192.97	„
Co _{85.8} P _{14.2}	ELECTROLESS	132.74	OUR GROUP

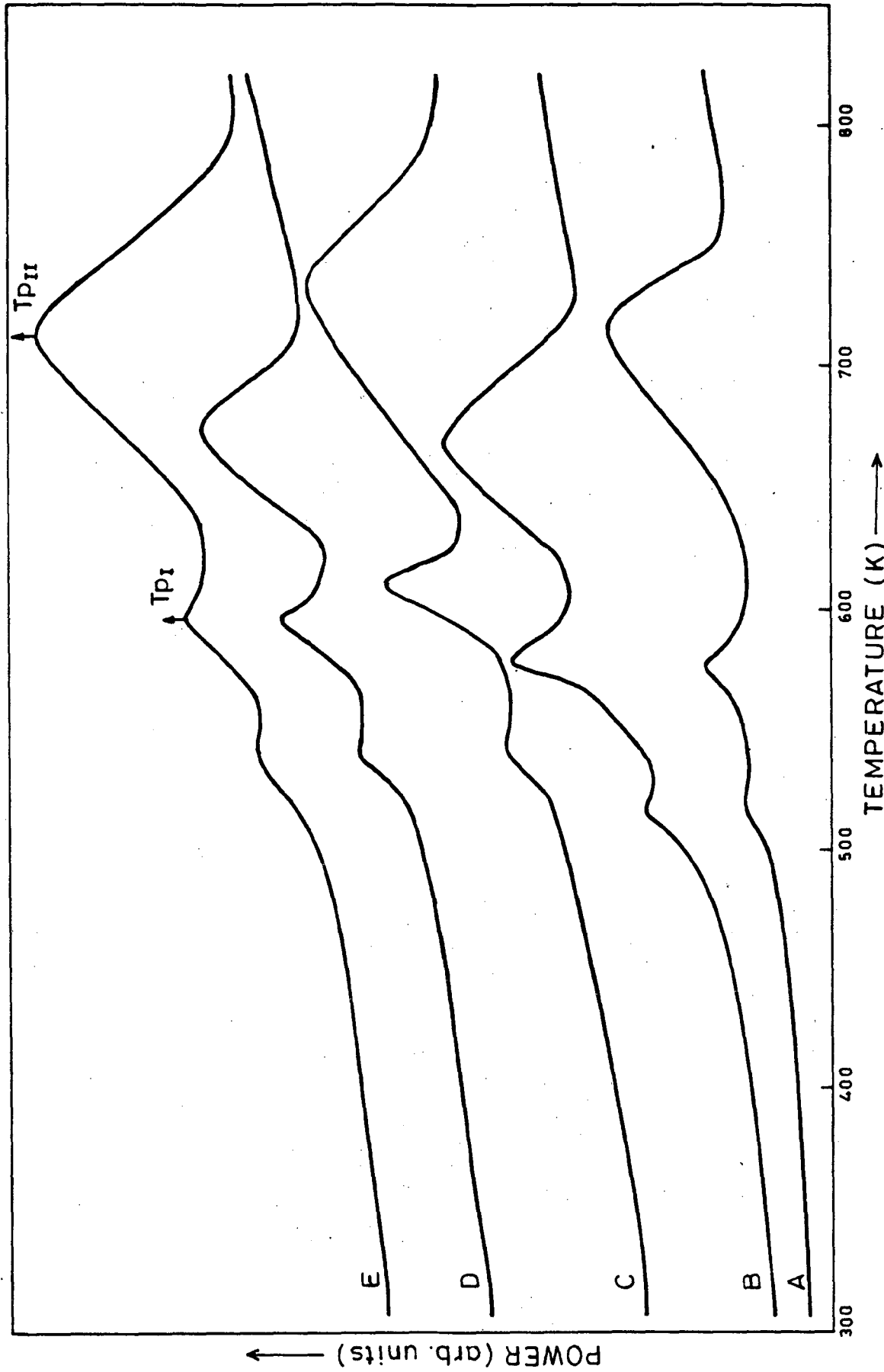


FIG. 4.1 DSC THERMOGRAMS OF FIVE Ni-Co-P ALLOYS HEATED AT 20 K/min.

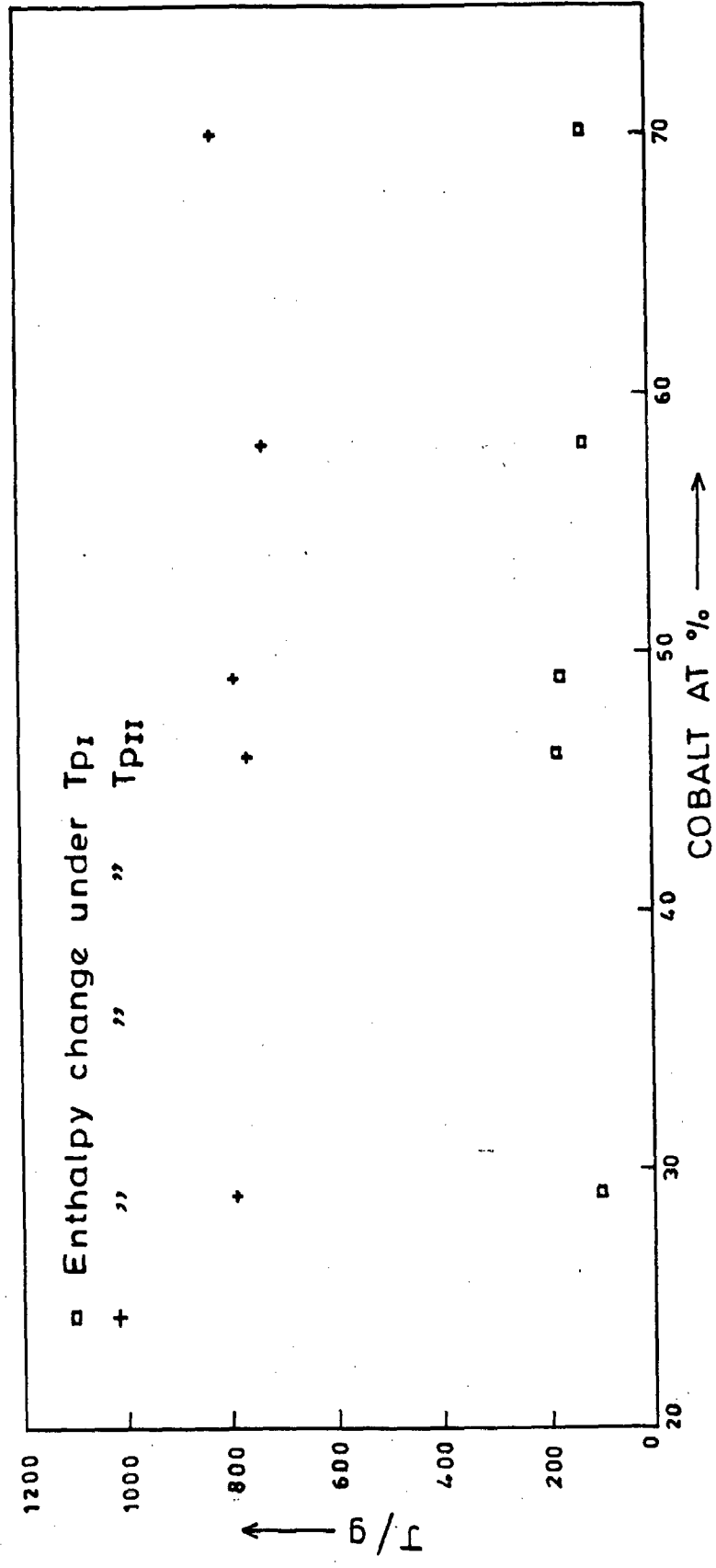


FIG. 4.2 THE CHANGE IN ENTHALPY WITH COMPOSITION FOR THE REACTION OCCURRING UNDER FIRST AND SECOND PEAK.

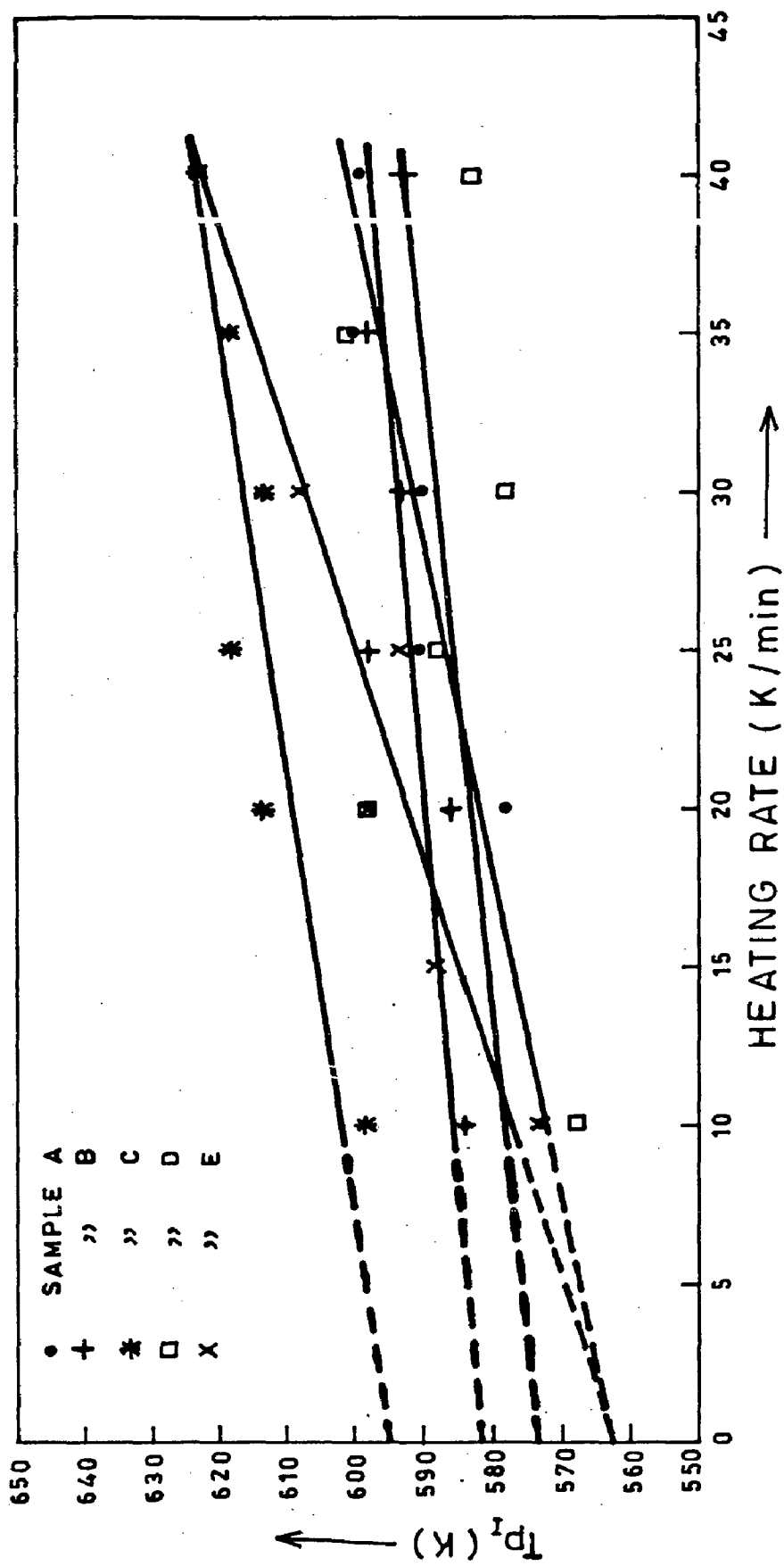


FIG. 4.3 VARIATION OF FIRST PEAK TEMPERATURE (T_{P1}) WITH HEATING RATE FOR AMORPHOUS Ni-Co-P ALLOYS.

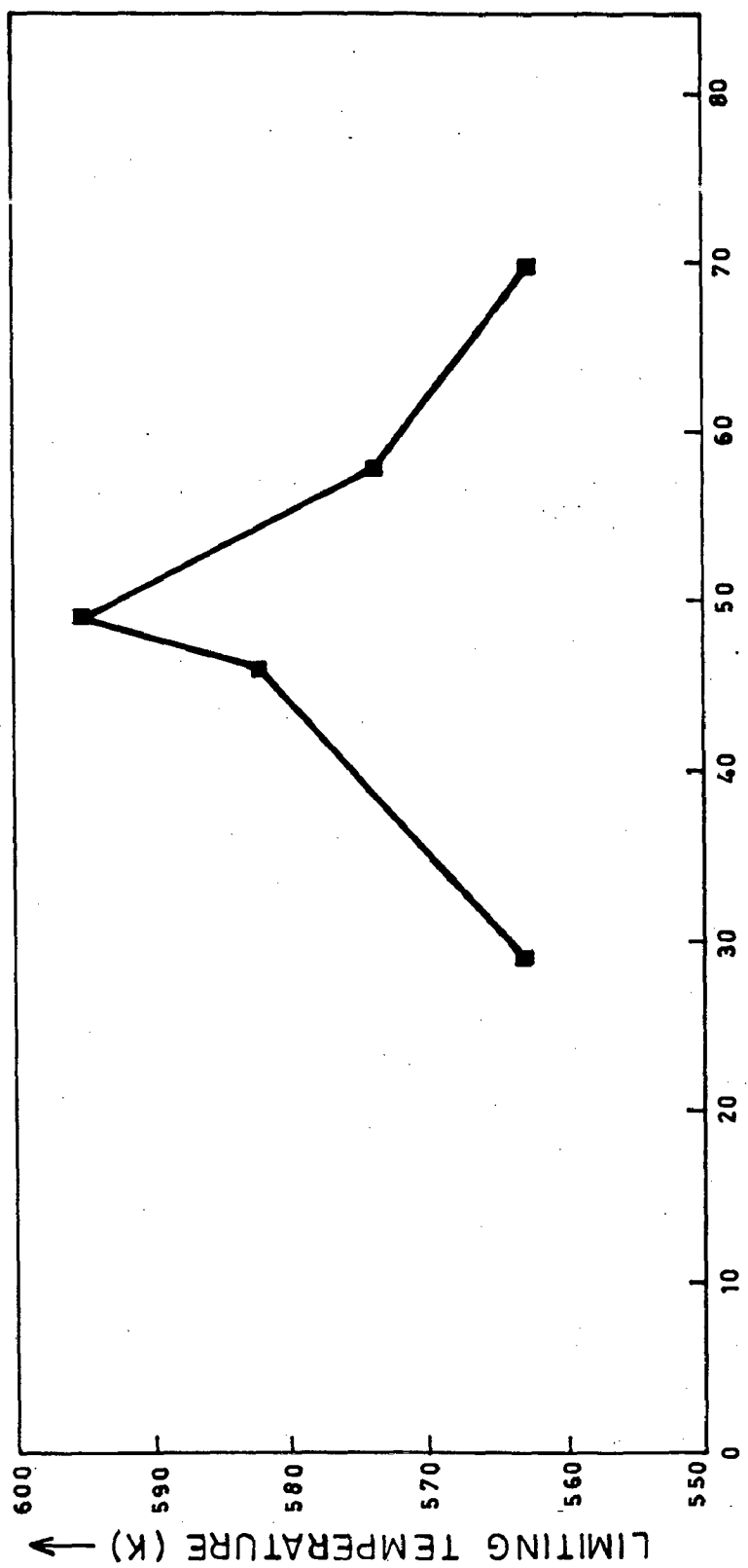


FIG. 4.4 THE VARIATION OF LIMITING TEMPERATURE WITH COMPOSITION OF COBALT IN AMORPHOUS Ni - Co - P ALLOYS .

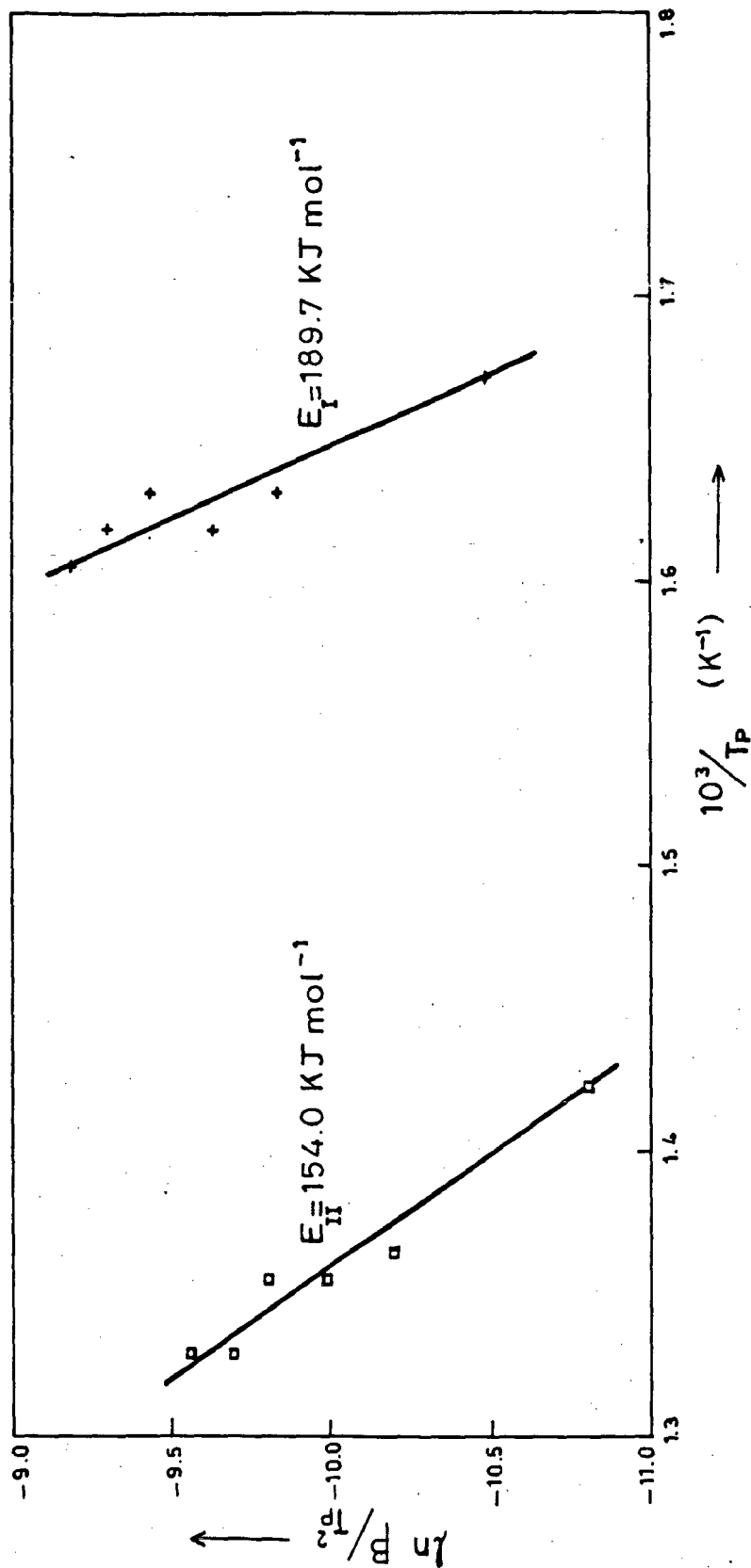


FIG. 4.5 A KISSINGER PLOT FROM THE VARIATION OF THE TEMPERATURE CORRESPONDING TO THE MAXIMUM OF THE DSC PEAK, T_p , AS A FUNCTION OF SCAN RATE, β , IN AMORPHOUS $\text{Ni}_{35.6}\text{Co}_{49.1}\text{P}_{15.3}$ (SAMPLE C).

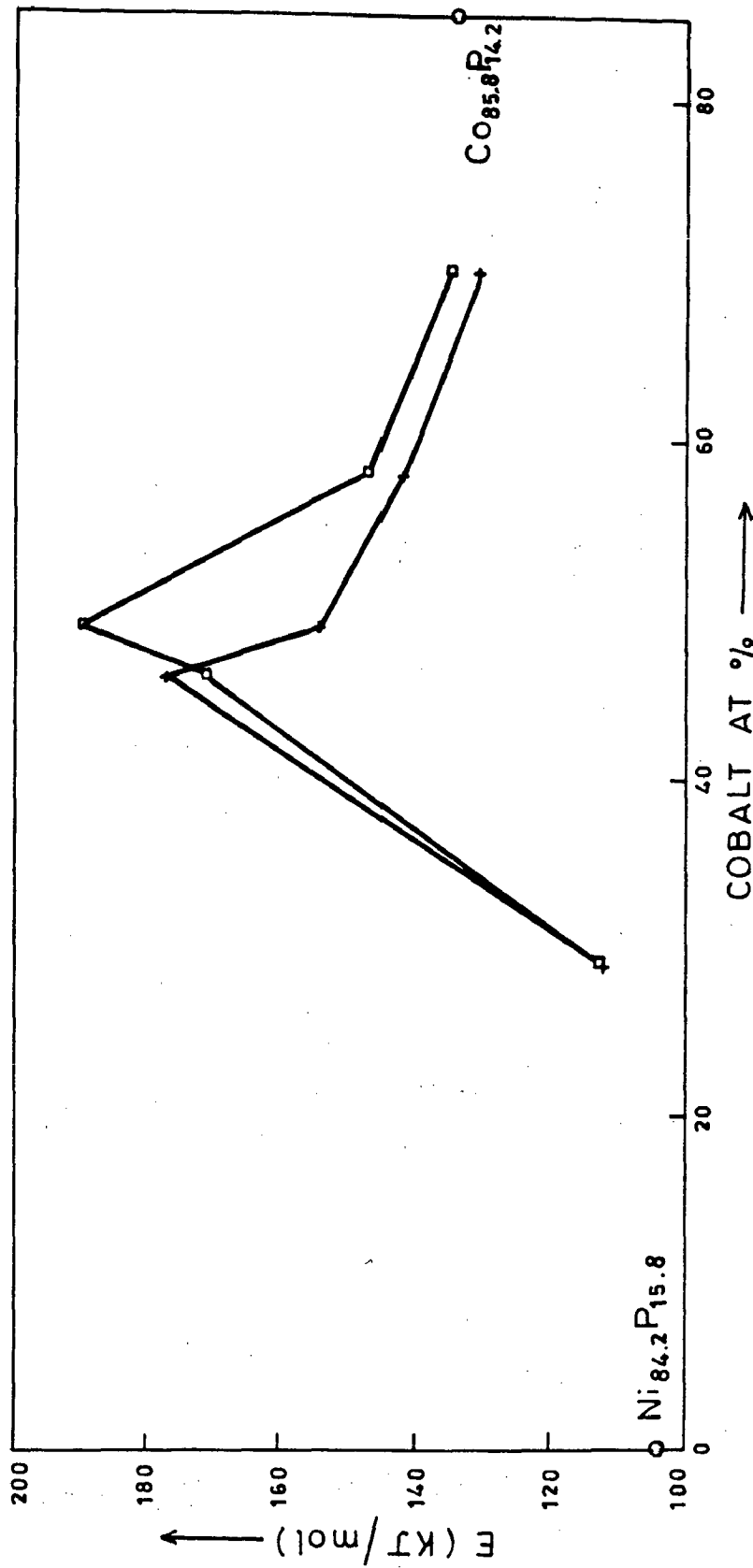


FIG. 4.6 COMPOSITIONAL DEPENDENCE OF ACTIVATION ENERGY FOR AMORPHOUS Ni - Co - P SYSTEM. (\square) ACTIVATION ENERGY OF THE REACTION UNDER T_{pI} , (+) ACTIVATION ENERGY OF THE REACTION UNDER T_{pII} .

C H A P T E R 5

ELECTRON MICROSCOPY AND X-RAY DIFFRACTION STUDIES ON AMORPHOUS Ni-Co-P DURING ANNEALING

The calorimetric studies have indicated that some phases have formed or transformed during crystallization of ternary TM-M systems. In order to have a qualitative idea of the related microstructural changes a detailed study of the ternary Ni-Co-P system using electron microscopy and X-ray diffraction techniques was carried out.

In this chapter the results of phase identification, using SAD mode in TEM and X-ray diffraction of the bulk 'as-deposited' and annealed amorphous electroless Ni-Co-P films are presented in order to get an integrated information on the micromechanisms of crystallization process in these alloys.

In the present work the sample temperature was monitored throughout the study on the heating stage of the microscope where annealed thick deposits were subjected to X-ray diffraction and phases obtained were indexed. The details of the techniques used have already been discussed in Chapter 3.

5.1 RESULTS: TEM AND XRD STUDIES ON 'AS-DEPOSITED' ALLOYS

The electroless Ni-Co-P films with different TM content have been deposited with the bath conditions described in 3.1.

The thin deposits and bulk samples are examined under electron microscope and X-ray diffractometer without any pre-treatment.

The 'as-deposited' films were investigated under SAD mode of TEM at ambient temperature and show a diffuse ring throughout the sample region scanned which is characteristic of amorphous nature. A typical SAD pattern for sample B with Cobalt content of 46 at% is shown in Fig. 5.1(a).

Thick samples obtained from same bath for each composition were subjected to X-ray diffraction analysis and a broad peak with scattering vector $Q = (4\pi \sin \theta) / \lambda = 3.1 \text{ \AA}^{-1}$ is observed.

The d-value corresponding to the diffuse ring in TEM and broad peak in XRD matches with the interplanar spacing of (0002) and (111) plane of h.c.p. Cobalt (α -Cobalt) and f.c.c. Nickel. Fig. 5.1(b) shows the XRD for the 'as-deposited' sample containing 46 at% Cobalt. The values of width at half maximum $\Delta(2\theta)$ are found to be about 5.5-6.5° for the Ni-Co-P samples where no other maxima is observed.

5.2 RESULTS: PHASE IDENTIFICATION IN ANNEALED SAMPLES

In order to investigate the nature of changes taking place corresponding to each peak in DSC, samples were heated to the relevant temperature ranges where considerable reaction takes place and the phases so formed were indexed using SAD under TEM and XRD.

5.2.1 TEM Studies

When 'as-deposited' samples are heated to a temperature of 553 K, the temperature region in which a small peak was observed in DSC prior to the first major exothermic peak, in the heating holder of TEM with 20 ± 3 K/min heating rate and viewed from SAD mode, all the films show no apparent changes in microstructures. The nature of the diffuse ring and corresponding plane spacing is same as that in 'as-deposited' samples and no indication of phase transformation has been observed.

To probe further the samples are heated to 628 K, the region of the start of the first major exothermic peak in DSC, and kept for 30 minutes. SAD mode shows separation of some crystalline phases beginning at about 573 K. A typical appearance of this starting stage and transmission electron micrographs are shown in Fig. 5.2 (a) & (b) for the sample containing 46 at% Cobalt. The presence of the diffuse ring indicates that although some crystalline precipitate has separated but the matrix is still amorphous. The separated phases are indexed and it is mainly h.c.p. Cobalt (α -Cobalt) and f.c.c. Nickel for the samples of different composition. In case of samples with 49.1, 58 and 70 at% Cobalt (i.e. sample C, D and E), α -Cobalt is common phase.

The typical appearance of α -Cobalt which is common phase for $\text{Ni}_{27.0}\text{Co}_{58.0}\text{P}_{15.0}$ sample is shown in Fig. 5.3(a). It is

observed that the first spots are coinciding over the diffuse ring in most of the regions when these initial phase separates out of amorphous matrix.

The sample B with 46 at% Cobalt showing the metastable phases of tetragonal Ni_{12}P_5 in α -Cobalt microcrystalline matrix, Fig. 5.3(b), where the few region of only microcrystalline α -Cobalt is found in case of sample E containing 70 at% Cobalt (Fig. 5.3(c)).

The samples of different composition is heated further to 823 K i.e. beyond the last peak in DSC and kept for 30 minutes and different regions of each thin samples are scanned throughly under TEM with SAD mode.

Sample A having a composition of 55.5 at% Nickel shows that complete crystallization takes place and beside the phases observed earlier the new crystalline phases are forming. The twinned orthorhombic Co_2P phase and metastable Ni_{12}P_5 are observed as it is revealed from Fig. 5.4(a & b) and the most of the regions showing the equilibrium Ni_3P , Fig. 5.4(c). The phases like Ni_{12}P_5 and Ni_3P are observed for binary electroless Ni-P system too (Agarwala and Ray, 1989).

In case of $\text{Ni}_{39.0}\text{Co}_{46.0}\text{P}_{15.0}$ sample, amorphous matrix crystallize through large number of phases as shown in Fig. 5.5. The common phases are found to be non-equilibrium strained cubic Ni_7P_3 and equilibrium tetragonal Ni_3P , Fig. 5.5 (a) & (b). Other phases as it is shown in Fig. 5.5 (c), (d) & (e) are

non-equilibrium cubic CoP_4 , Ni_{12}P_5 and stable Co_2P phases.

The sample having the composition near to B, that is sample C with 49.1 at% Cobalt also crystallizes through the formation of same phases as shown in Fig. 5.6 .

The non-equilibrium Cobalt phosphides are twinned CoP_2 and CoP_4 (Fig. 5.6 (a) & (b)) where strained hexagonal Ni_5P_4 and cubic Ni_7P_3 in f.c.c. Nickel matrix are observed from different regions of the sample (Fig. 5.6 (c) & (d)). The expected equilibrium phases of Ni_3P and Co_2P are also observed which are common phase in that sample, the SAD pattern of such a regions are shown in Fig. 5.6 (e) & (f) .

When samples of 58 at% Cobalt, i.e. sample D, is heated to 823 K for 30 minutes there are regions found to contain CoP_4 (Fig. 5.7 (a)). The Ni_3P and $\text{Co}_2\text{P} + \alpha\text{-Cobalt}$ is found from other regions and shown in Fig. 5.7 (b) & (c). To investigate the effect of transition metal percentage on matrix crystallization, the annealing process is repeated for the sample E with the highest of Cobalt percentage (70 at%). Some new polycrystalline $\alpha\text{-Cobalt}$ precipitates appeared (Fig.5.8 (a)), where most of the samples annealed are showing $\text{Co}_2\text{P} + \alpha\text{-Cobalt}$ and $\alpha\text{-Cobalt}$ SAD patterns as are shown in Fig.5.8 (b) & (c).

5.2.2 XRD Studies

The thick films of amorphous electroless Ni-Co-P were

annealed in DSC with 20 K/min upto a temperature where the reaction takes place as shown by the exothermic peaks and then examined by X-ray diffraction analysis. No sharp peak characteristic of crystalline phase has been observed when samples are heated upto 553 K.

The bulk samples are then heated to 628 K, cooled to room temperature and subjected to X-ray diffractometer. Three small crystalline peaks superimposed over a broad maxima have been observed for all the samples but the intensity of each peak is different for different samples. These peaks are indexed and found that they are corresponding to the Nickel (111) and α -Cobalt (01 $\bar{1}$ 1, 0002, 01 $\bar{1}$ 0). The intensity is measured in arbitrary units from the base line for each peak and are shown in Fig. 5.9 (I) and (II). As can be seen that intensity of Nickel (111) peak is more compared to the rest of the peaks for sample A containing 55.5 at% Nickel, where as in rest of the samples α -Cobalt (01 $\bar{1}$ 1) and (01 $\bar{1}$ 0) planes are showing relatively higher intensities.

For the samples heated to 823 K and cooled to room temperature many peaks can be observed. Because of the complexity of the pattern it was not possible to identify the phases present unambiguously, although an attempt was made to identify them with calculation of interplaner d-spacing for each peak and comparing with the data (Table 2.2) for the most likely phases of Nickel and Cobalt phosphides.

In case of $\text{Ni}_{55.5}\text{Co}_{29.0}\text{P}_{15.5}$ sample the new phases present are Ni_3P and Co_2P where some lower intensity peaks of α -Cobalt and Nickel are appearing for the first time which indicates the growth of these crystallites. The peaks correspond to Ni_{12}P_5 is not found as it is observed in TEM. For sample B, i.e. 46 at% Cobalt, new crystalline phases identified as Ni_7P_3 , Ni_3P and Co_2P . The metastable Ni_7P_3 was observed by TEM but the CoP_4 and Ni_{12}P_5 phases were not present in XRD for the said sample. There was a slight increase in peak length for α -Cobalt (01 $\bar{1}$ 1) plane as comparing to that of phase separation case.

The amorphous sample $\text{Ni}_{35.6}\text{Co}_{49.1}\text{P}_{15.3}$ which is showing large number of stable and metastable phases in TEM are investigated under XRD. The only phases observed during the complete crystallization, beside the previous α -Cobalt and Nickel, were the Co_2P , Ni_3P and CoP_4 and no other phases could be identified (Fig. 5.10(I)). When the annealed D samples are examined by XRD, the Co_2P and Ni_3P new phases are dominant and the peak corresponding to CoP_4 which are identified in thin samples under TEM, are not observed here in Fig. 5.10(II). For high Cobalt ternary system, $\text{Ni}_{15.3}\text{Co}_{70.0}\text{P}_{14.7}$, many new peaks of α -Cobalt and Co_2P are observed where there is no indication of any Ni_3P peaks. Further, Nickel present in 'as-deposited' sample is precipitated out on annealing and the remaining amorphous matrix is poor in Nickel.

5.3 DISCUSSION

When thin films as well as bulk samples of different transition metal contents were annealed at various temperatures, the 'as-deposited' samples underwent definite structural changes and various phases present after annealing treatments are systematically listed in Table 5.1. The mark (*) on different phases tabulated indicate that these phases are seen in many regions of the same specimen under SAD mode of TEM and therefore called a common phase. Number of phases are found to be present in thin samples which are not present in their bulk state. This may be because of closed surfaces and effect of surface crystallization in thin samples and an indication that surfaces in thin samples have a strong influence on path of crystallization. For example, in amorphous $\text{Fe}_{40}\text{Ni}_{40}\text{B}_{20}$ the increase in Nickel concentration near the surfaces increases the crystallization temperature of the sample (Koster and Herold, 1981). The crystallization behaviour changes drastically in thin foils because of rise of the free energy due to the surface energy term. For example, on thinned $\text{Fe}_{80}\text{B}_{20}$ foil, in situ annealing in a hot stage of electron microscope the primary crystallization of α -Fe followed by eutectic or polymorphous is observed where in ribbons annealed in the bulk state one observes only eutectic α -Fe + Fe_3B transformation.

The compositional inhomogenities which is result of electroless preparation favour the formation of number of

phases in our samples locally depending on the composition of the regions under study in TEM.

As it is observed in careful TEM study and reveals from our results, the h.c.p. Cobalt and f.c.c. Nickel separates out from Cobalt and Nickel rich regions which are softer to crystallize. In matrix crystallization reaction, the new crystals nucleate randomly in locally different composition parts of the amorphous phase and grow until impinge and consume all the matrix.

No indication of, which crystalline phase appears preferentially near the boundary between the 'amorphous-phase separation' and 'phase separation-matrix crystallization' could be obtained by electron microscopy observations.

The crystallization behaviour of electroless Ni-Co-P films can be tentatively divided into two broad categories: I) the amorphous alloys having the composition near to that of binary systems of Ni-P and Co-P like $\text{Ni}_{55.5}\text{Co}_{29.0}\text{P}_{15.5}$ (sample A) and $\text{Ni}_{15.3}\text{Co}_{70.0}\text{P}_{14.7}$ (sample E), show the final matrix crystallization transformation as consisting of equilibrium phases, II) the amorphous alloys having the intermediate composition, i.e. approximately equal transition metal concentration going to the many non-equilibrium (Ni_{12}P_5 , Ni_7P_3 , Ni_5P_4 , CoP_2 , CoP_4) and equilibrium (Co_2P , Ni_3P) phases at about 823 K. The compositional dependence of crystallization behaviour for binary Ni-P and Co-P are reviewed in details in Chapter 2.

The crystallization behaviour of other multicomponent systems are studied by various workers, in case of, Fe-B-Si-C using XRD it is observed that crystallization transformation goes through two steps; a) primary crystallization of α -Fe and b) formation of stable, metastable phases like $\text{Fe}_2(\text{B,C,Si})$ - $\text{Fe}_3(\text{B,C,Si})$ or $(\text{Fe,Si})_2(\text{B,C}) - (\text{Fe,Si})_3(\text{B,C})$ (Fouquet et al, 1985). In case of ternary $\text{Ni}_{78}\text{B}_{14}\text{Si}_{13}$ (Pilz and Ryder, 1985) and $\text{Ni}_{81.5}\text{P}_{18.5-x}\text{B}_x$ (Fogarassy et al, 1985) it is shown that the crystallization path depends to the metalloid content.

For multi-transition metal system like Ni-Cr-Co-Ta-B (Geoffroy et al, 1983) the crystallization process is complex and the final crystalline product depends to the both transition metal and metalloid composition.

The studies reported so far as it is briefly noted above for some systems are supporting our results and the fact that, more the elements in amorphous system, more complex is the crystallization behaviour.

In chapter 4, while discussing the stability of amorphous Ni-Co-P we have seen that kinetic of crystallization parameter like activation energy are higher in value for intermediate compositions. Further that, there are two exothermic reaction peaks identified with the process of crystallization. The phase identification by TEM and XRD in this chapter clearly confirms that the first reaction

constitutes of separation of primary phases like Nickel and α -Cobalt. The room temperature stable form of Cobalt has hexagonal structure which is also the structure of room temperature primary phase of Cobalt in Co-P system. At elevated temperature f.c.c. primary phase exists in the phase diagram and this transforms to h.c.p. Cobalt when it is cooled (Masui et al, 1985). The primary phases of f.c.c. Nickel and h.c.p. Cobalt are separating out from ternary Ni-Co-P as it would happen in a mechanical mixture of Ni-P and Co-P binary amorphous films. The second reaction in crystallization corresponds to compound formation (probably as a part of eutectic type of reaction) as it has been observed in binary amorphous metal-metalloid alloys. The interesting effect of ternary addition is appearance of metastable compounds like Ni_7P_3 or CoP_4 in Nickel or Cobalt rich compositions respectively around Nickel - Cobalt ratio of 50:50. Near binary ends of the composition these metastable phosphides are not observed.

From our structural analysis it appears that the starting compositions that results in formation of many non-equilibrium phases in case of amorphous electroless Ni-Co-P are more stable and resistant to crystallization. A summary of the composition ranges over which different phases are forming is given in Fig. 5.11.

5.4 SUMMARY



The structural study of the electroless amorphous

Ni-Co-P of different transition metal composition with phosphorous of about 15 at% has been carried out using a transmission electron microscope and X-ray diffraction in the 'as-deposited' state and after annealing at 628 K and 823 K.

The 'as-deposited' state of thin deposits and bulk samples are examined under SAD mode of TEM and XRD show a diffuse ring and a broad peak with interplaner spacing matching with the (0002) and (111) planes of h.c.p. Cobalt and f.c.c. Nickel. The samples heated to 628 K, the region of first peak (T_{PI}) in DSC, shows separation of h.c.p. Cobalt (01 $\bar{1}$ 1, 0002, 01 $\bar{1}$ 0) and f.c.c. Nickel (111). For the samples heated to 823 K, the second peak (T_{PII}) region of DSC, the crystallization of matrix takes place through appearance of many metastable and stable phases.

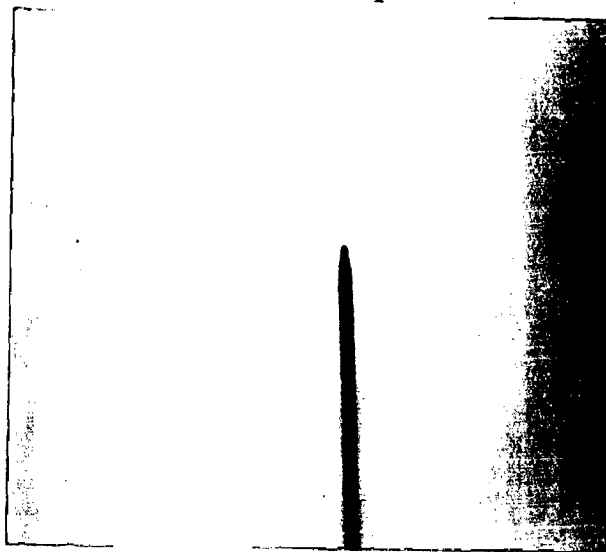
The crystallization annealing behaviour can be tentatively divided into two broad categories: I) The alloys having the composition near to that of binary systems show the final matrix crystallization transformation as consisting of equilibrium phases, II) The alloys having the intermediate composition transform to the many non-equilibrium and equilibrium phases.

Our structural investigations indicate that, more the elements in amorphous alloys, makes the crystallization transformation more complex and the starting compositions that results in formation of many non-equilibrium phases are more stable and resistant to crystallization.

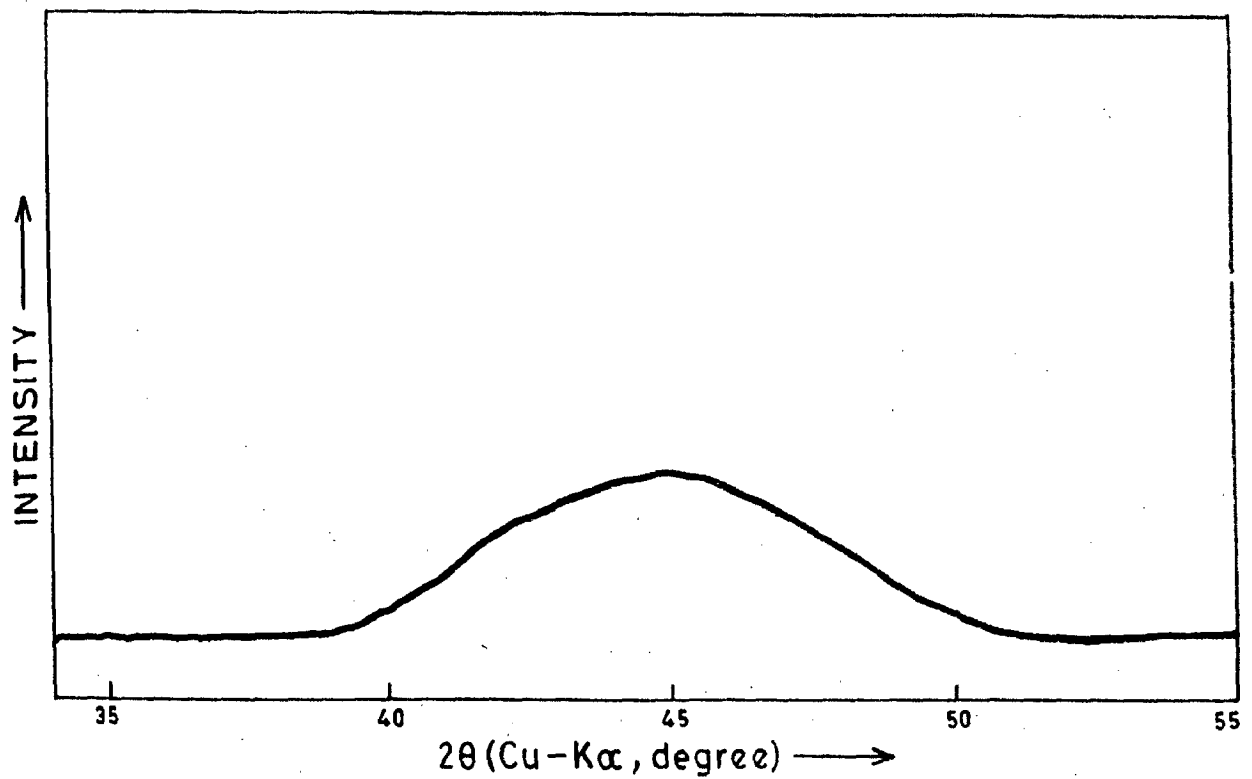
TABLE 5.1 THE PHASES OBSERVED DURING ANNEALING OF AMORPHOUS Ni-Co-P.

SAMPLE COMPOSITION (AT %)	ANNEALED TO 628 K		ANNEALED TO 823 K	
	XRD	TEM	XRD	TEM
Ni _{55.5} Co _{29.0} P _{15.5}	Ni α-Co	Ni (*) α-Co	Ni, α-Co Ni ₃ P Co ₂ P	Ni, α-Co Co ₂ P Ni ₃ P (*) Ni ₁₂ P ₅
Ni ₃₀ Co ₄₆ P ₁₅	Ni α-Co	Ni Ni ₁₂ P ₅ in α-Co matrix	α-Co Ni Co ₂ P Ni ₇ P ₃	Ni, α-Co Ni ₇ P ₃ (*) CoP ₄ in Ni ₃ P MATRIX Ni ₃ P (*) Ni ₁₂ P ₅ Co ₂ P
Ni _{35.6} Co _{49.1} P _{15.3}	Ni α-Co	Ni α-Co (*)	Ni, α-Co Co ₂ P Ni ₃ P CoP ₄	Ni, α-Co CoP ₄ (*) Ni ₇ P ₃ Co ₂ P (*) Ni ₃ P (*) Ni ₅ P ₄ CoP ₂
Ni ₂₇ Co ₅₈ P ₁₅	Ni α-Co	Ni α-Co (*)	Ni, α-Co Co ₂ P Ni ₃ P	Ni, α-Co CoP ₄ Ni ₃ P Co ₂ P (*)
Ni _{15.3} Co _{70.0} P _{14.7}	α-Co Ni	α-Co (*) Ni	Ni, α-Co Co ₂ P	Ni, α-Co Co ₂ P (*)

(*) STANDS FOR COMMON PHASE IN THAT COMPOSITION.



(a)



(b)

FIG. 5.1 (a) SAD PATTERN OF 'AS-DEPOSITED' $\text{Ni}_{39.0}\text{Co}_{46.0}\text{P}_{15.0}$ (SAMPLE B)

(b) X-RAY DIFFRACTION PATTERN OF 'AS-DEPOSITED' $\text{Ni}_{39.0}\text{Co}_{46.0}\text{P}_{15.0}$ (SAMPLE B)



(a)



(b)

FIG. 5.2 INITIATION OF PHASE SEPARATION IN $\text{Ni}_{39.0}\text{Co}_{46.0}\text{P}_{15.0}$
(SAMPLE B) AT 573 K.

(a) SAD PATTERN

(b) TRANSMISSION ELECTRON MICROGRAPH (X 21000)

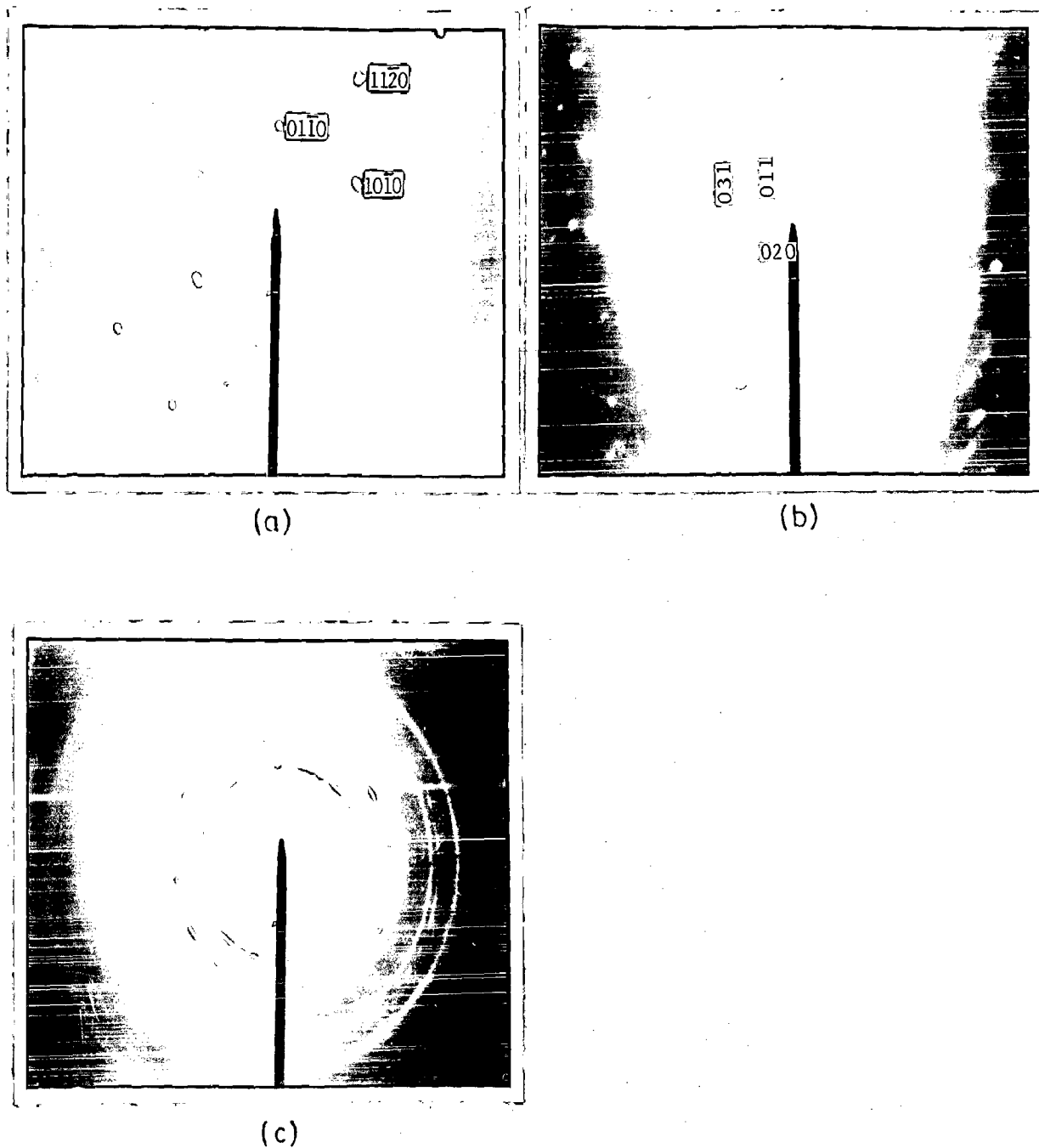
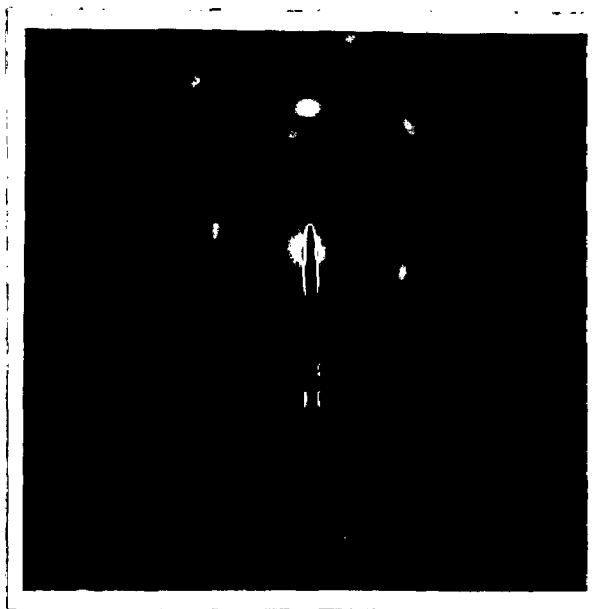
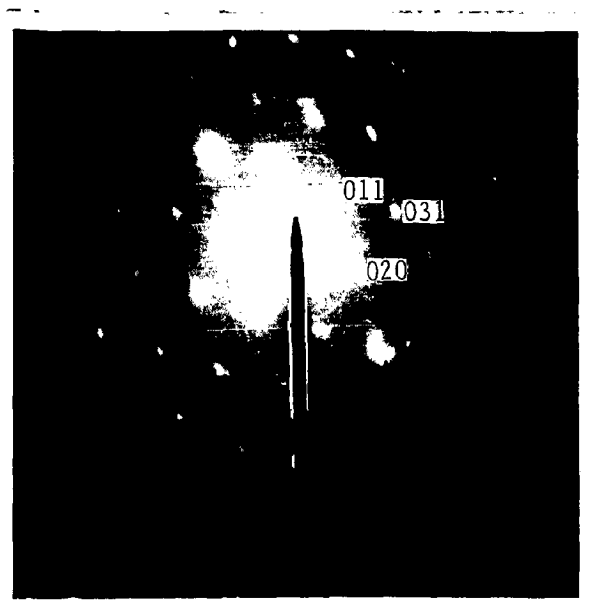


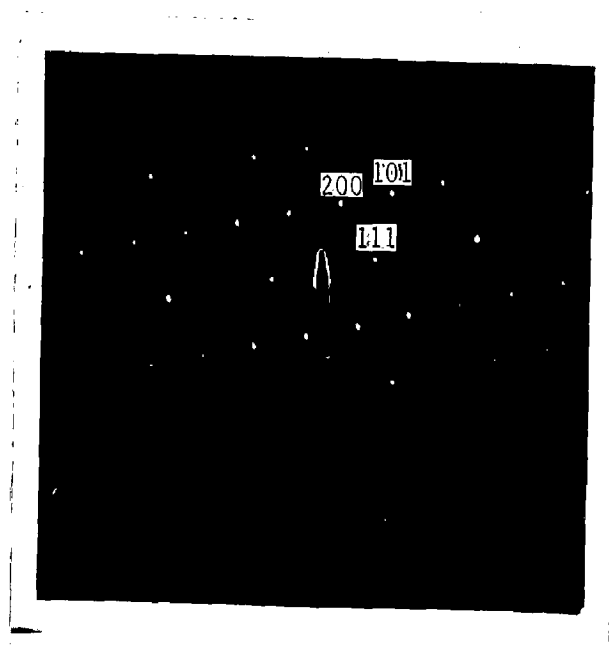
FIG. 5.3 SAD PATTERNS OF THE SAMPLES ANNEALED AT 628 K SHOWING (a) α -COBALT FOR $\text{Ni}_{27.0}\text{Co}_{58.0}\text{P}_{15.0}$, (b) Ni_{12}P_5 IN α -COBALT MICROCRYSTALLINE MATRIX FOR $\text{Ni}_{39.0}\text{Co}_{46.0}\text{P}_{15.0}$ AND (c) MICROCRYSTALLINE α -COBALT FOR $\text{Ni}_{15.3}\text{Co}_{70.0}\text{P}_{14.7}$.



(a)

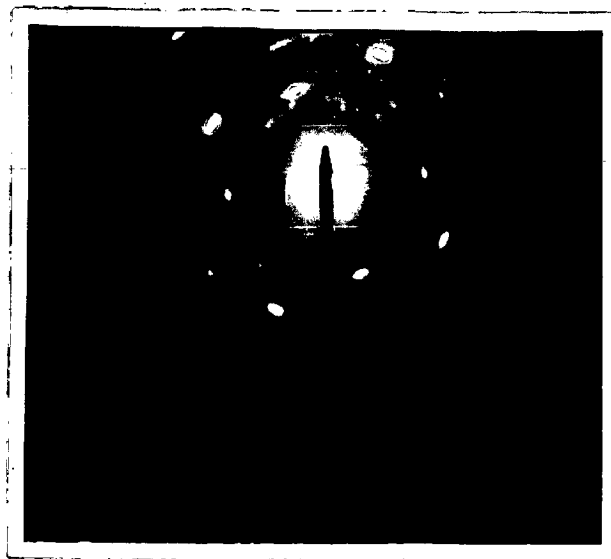


(b)

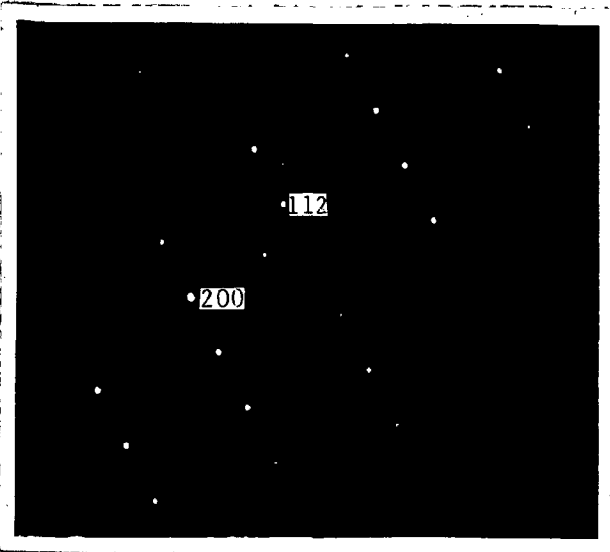


(c)

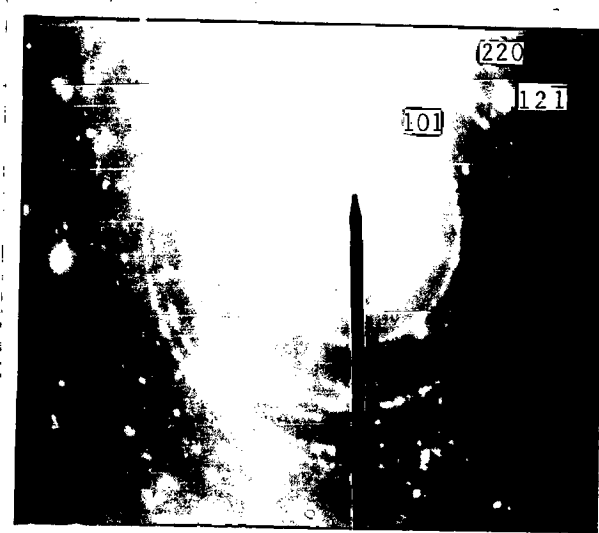
FIG. 5.4 SAD PATTERNS OF THE $\text{Ni}_{55.5}\text{Co}_{29.0}\text{P}_{15.5}$ (SAMPLE A) ANNEALED AT 823 K, (a) TWINNED Co_2P , (b) Ni_{12}P_5 AND (c) Ni_3P .



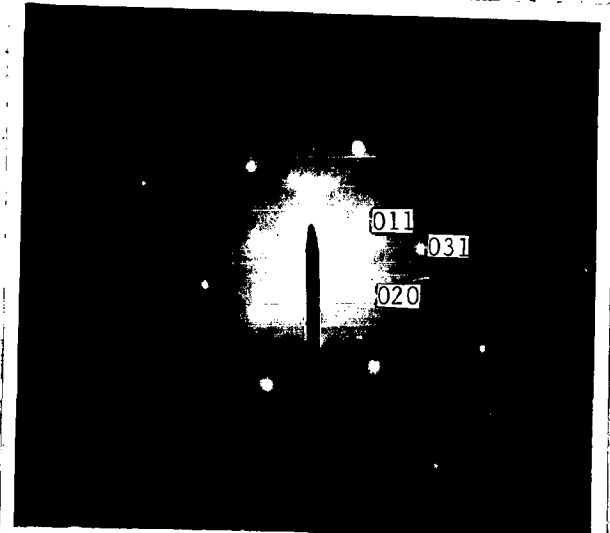
(a)



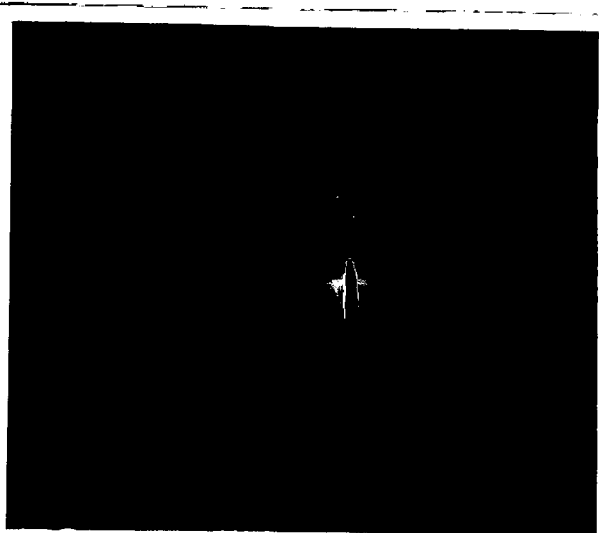
(b)



(c)



(d)



(e)

FIG. 5.5 SAD PATTERNS OF THE $\text{Ni}_{39.0}\text{Co}_{46.0}\text{P}_{15.0}$ (SAMPLE B) ANNEALED AT 823K, (a) STRAINED Ni_7P_3 , (b) Ni_3P , (c) CoP_4 IN Ni_3P MATRIX, (d) Ni_{12}P_5 , (e) Co_2P .

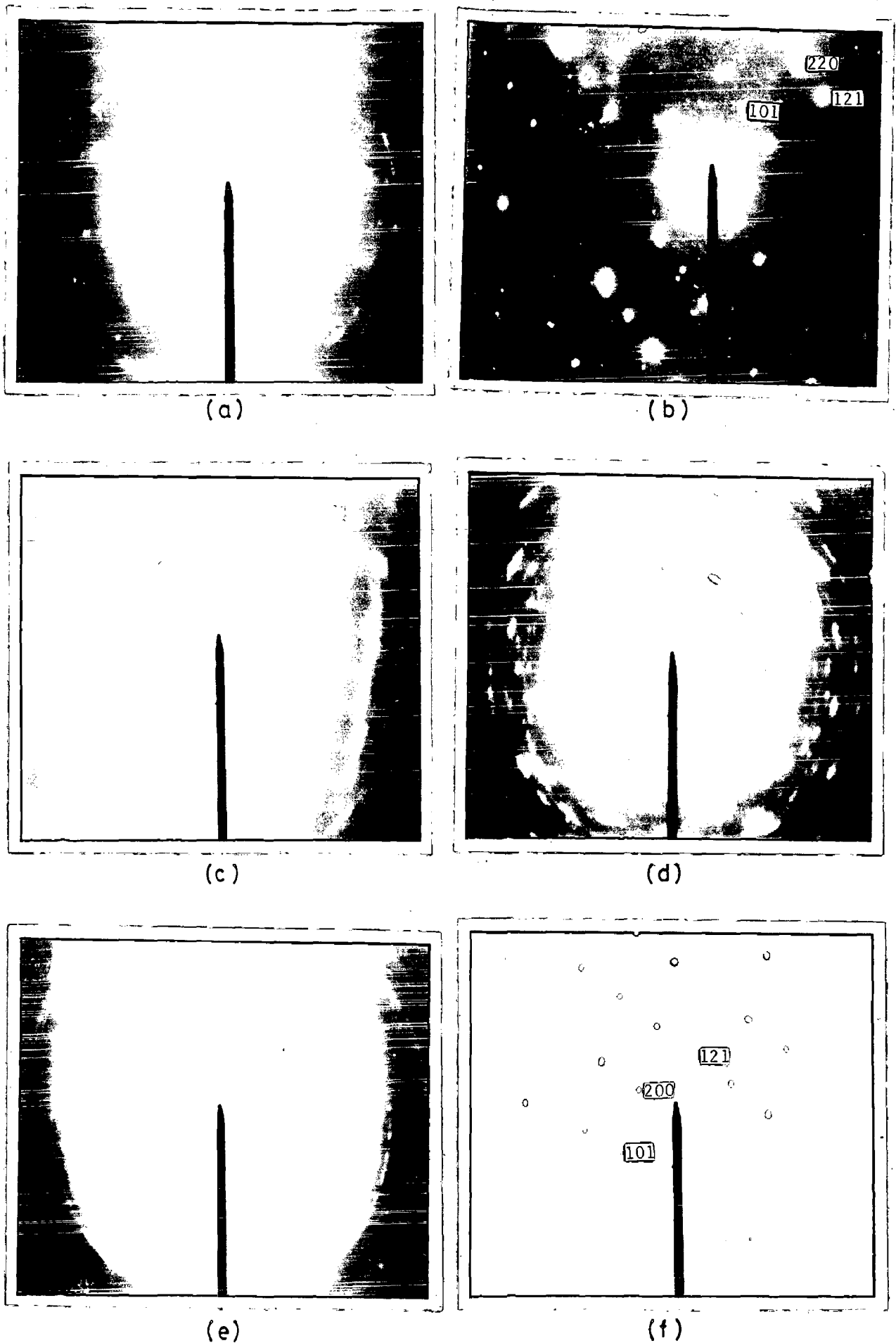


FIG. 5.6 SAD PATTERNS OF THE $\text{Ni}_{35.6}\text{Co}_{49.1}\text{P}_{15.3}$ (SAMPLE C) ANNEALED AT 823 K, (a) TWINNED Co_2P , (b) CoP_4 , (c) STRAINED Ni_5P_4 , (d) Ni_7P_3 IN NICKEL MATRIX, (e) $\text{Co}_2\text{P} + \infty$ -COBALT AND (f) Ni_3P .

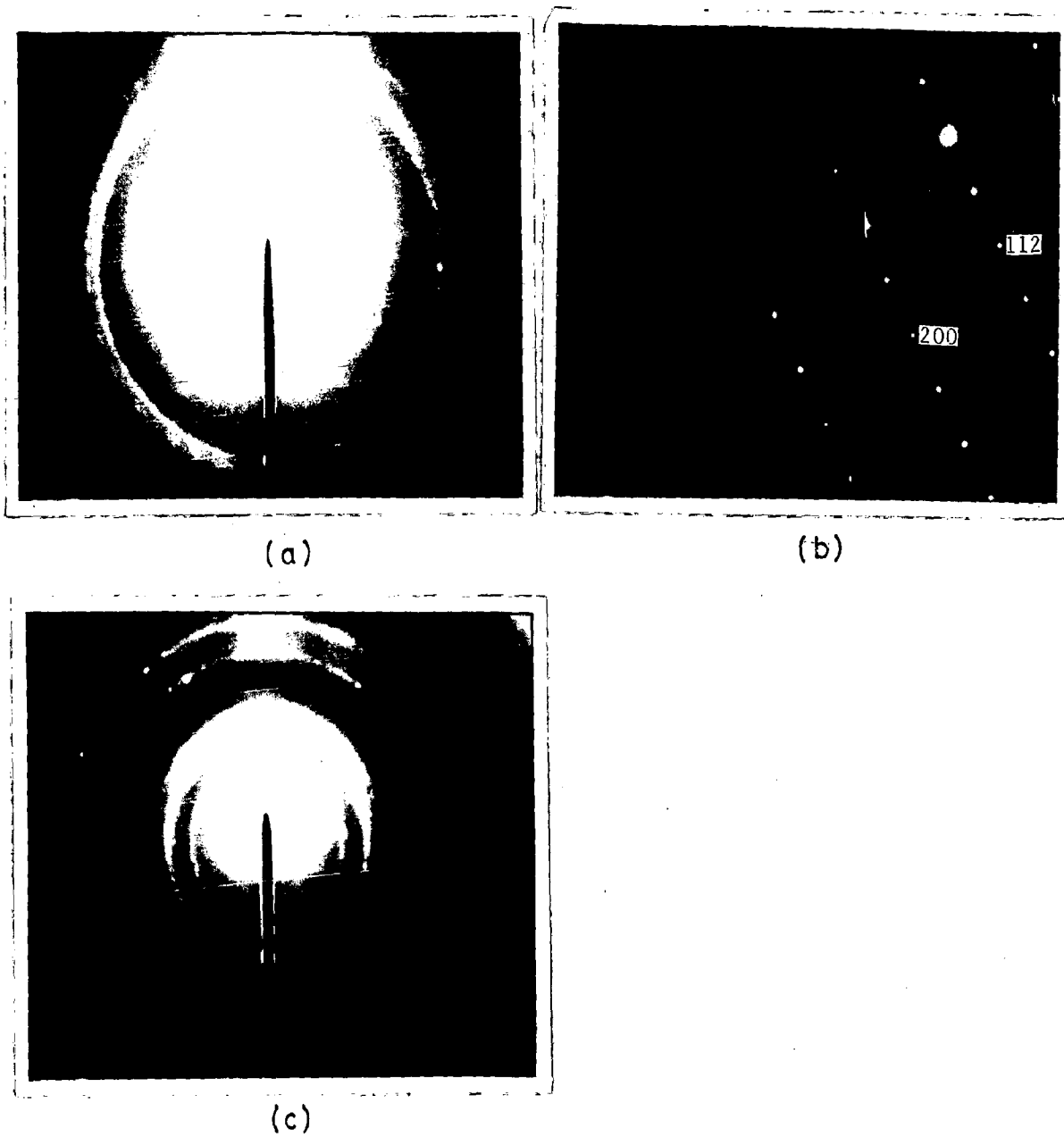


FIG. 5.7 SAD PATTERNS OF THE $\text{Ni}_{27.0}\text{Co}_{58.0}\text{P}_{15.0}$ (SAMPLE D) ANNEALED AT 823 K, (a) CoP_4 , (b) Ni_3P AND (c) $\text{Co}_2\text{P} + \alpha\text{-COBALT}$.

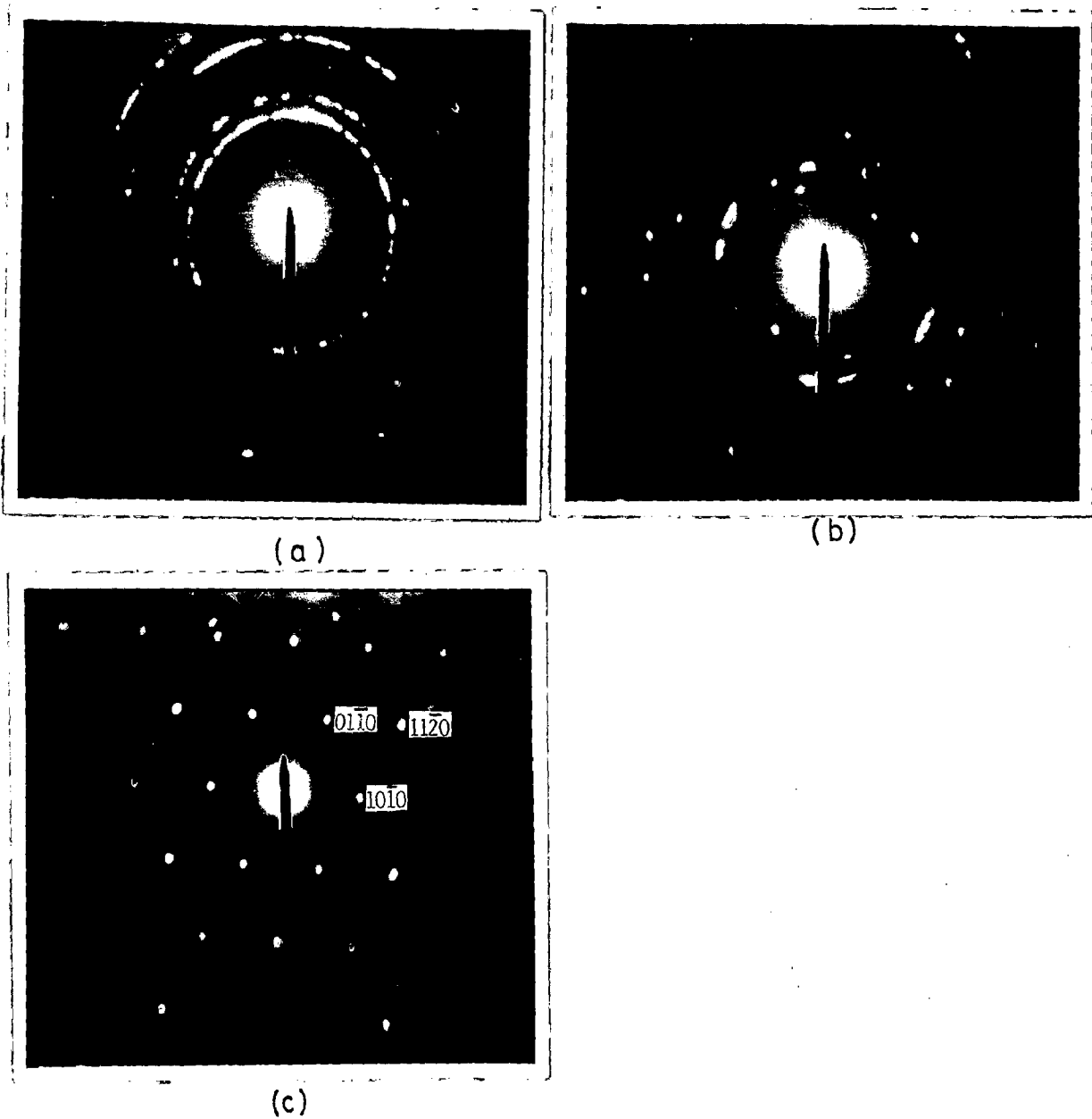


FIG. 5.8 SAD PATTERNS OF THE $\text{Ni}_{15.3}\text{Co}_{70.0}\text{P}_{14.7}$ (SAMPLE E) ANNEALED AT 823 K, (a) POLYCRYSTALLINE α -COBALT, (b) $\text{Co}_2\text{P} + \alpha$ -COBALT AND (c) α -COBALT.

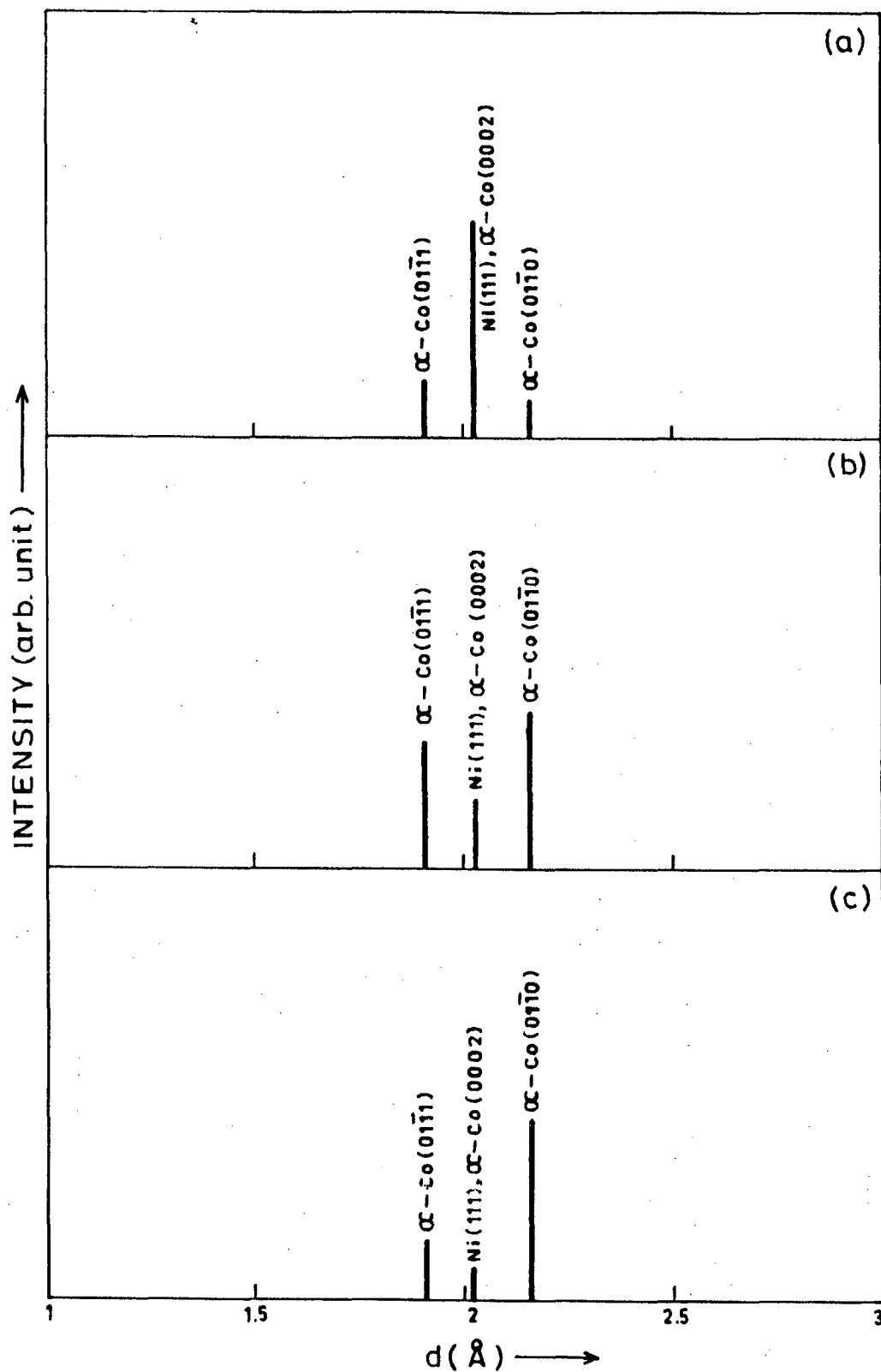


FIG. 5.9 (I) X-RAY DIFFRACTION PATTERNS OF THE SAMPLES, (a) $\text{Ni}_{55.5}\text{Co}_{29.0}\text{P}_{15.5}$, (b) $\text{Ni}_{39}\text{Co}_{46}\text{P}_{15}$ AND (c) $\text{Ni}_{35.6}\text{Co}_{49.1}\text{P}_{15.0}$ ANNEALED AT 628 K.

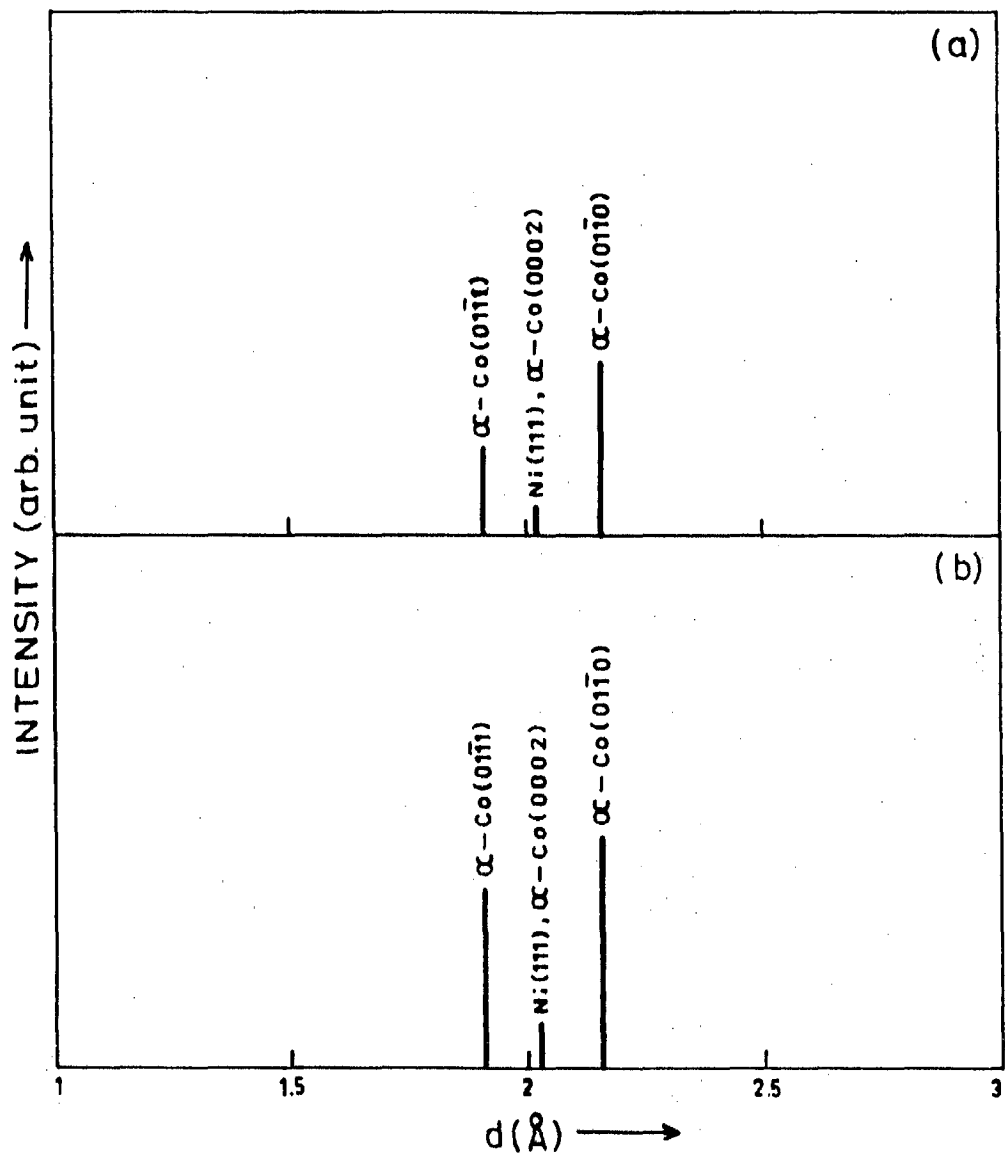


FIG. 5.9 (II) X-RAY DIFFRACTION PATTERNS OF THE SAMPLES, (a) $\text{Ni}_{27.0}\text{Co}_{58.0}\text{P}_{15.0}$ AND (b) $\text{Ni}_{15.3}\text{Co}_{70.0}\text{P}_{14.7}$ ANNEALED AT 628 K .

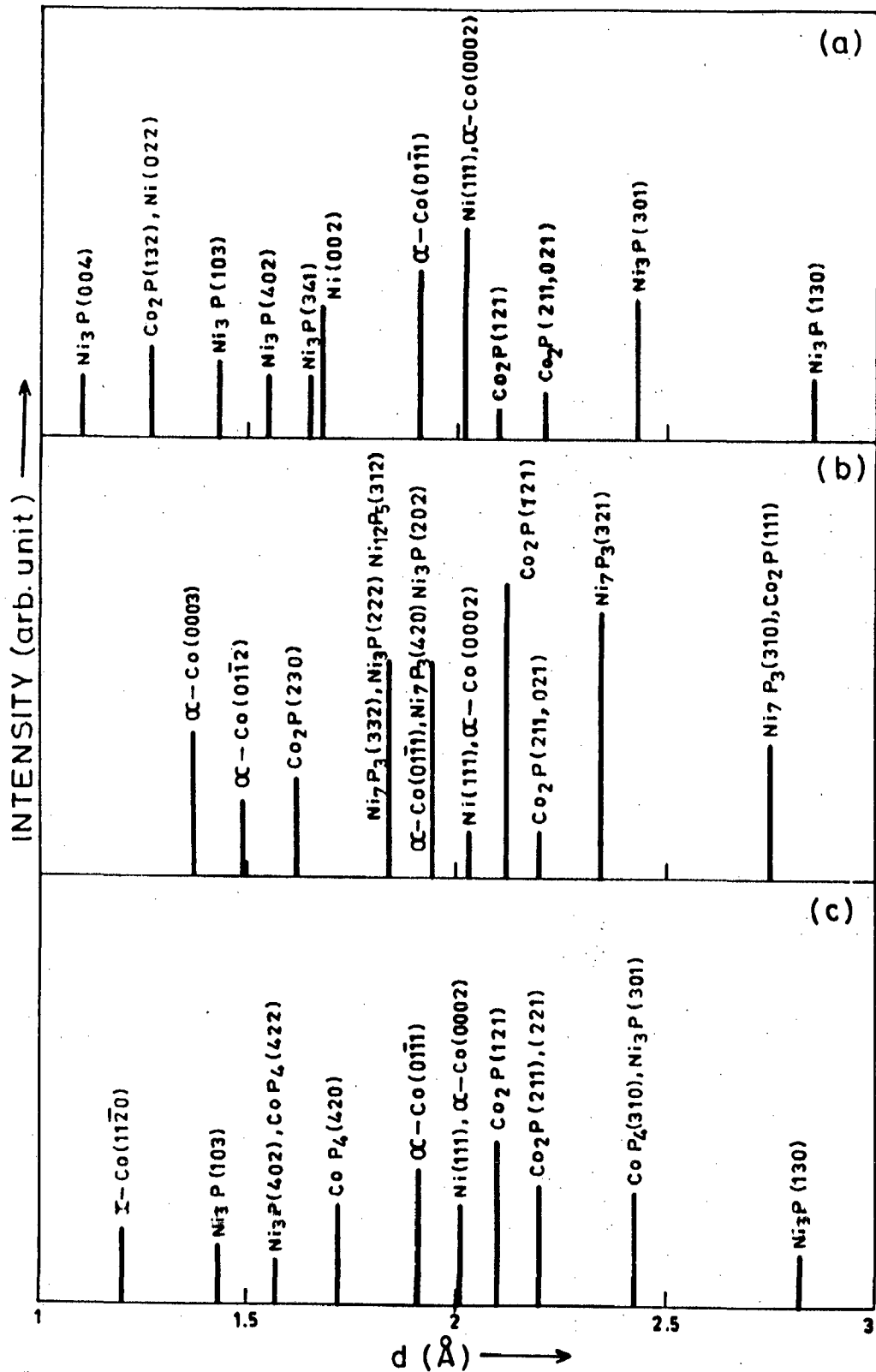


FIG. 5.10 (I) X-RAY DIFFRACTION PATTERNS OF THE SAMPLES, (a) $\text{Ni}_{55.5}\text{Co}_{29.0}\text{P}_{15.5}$ (b) $\text{Ni}_{39}\text{Co}_{46}\text{P}_{15}$ AND (c) $\text{Ni}_{35.6}\text{Co}_{49.1}\text{P}_{15.3}$ ANNEALED AT 823 K.

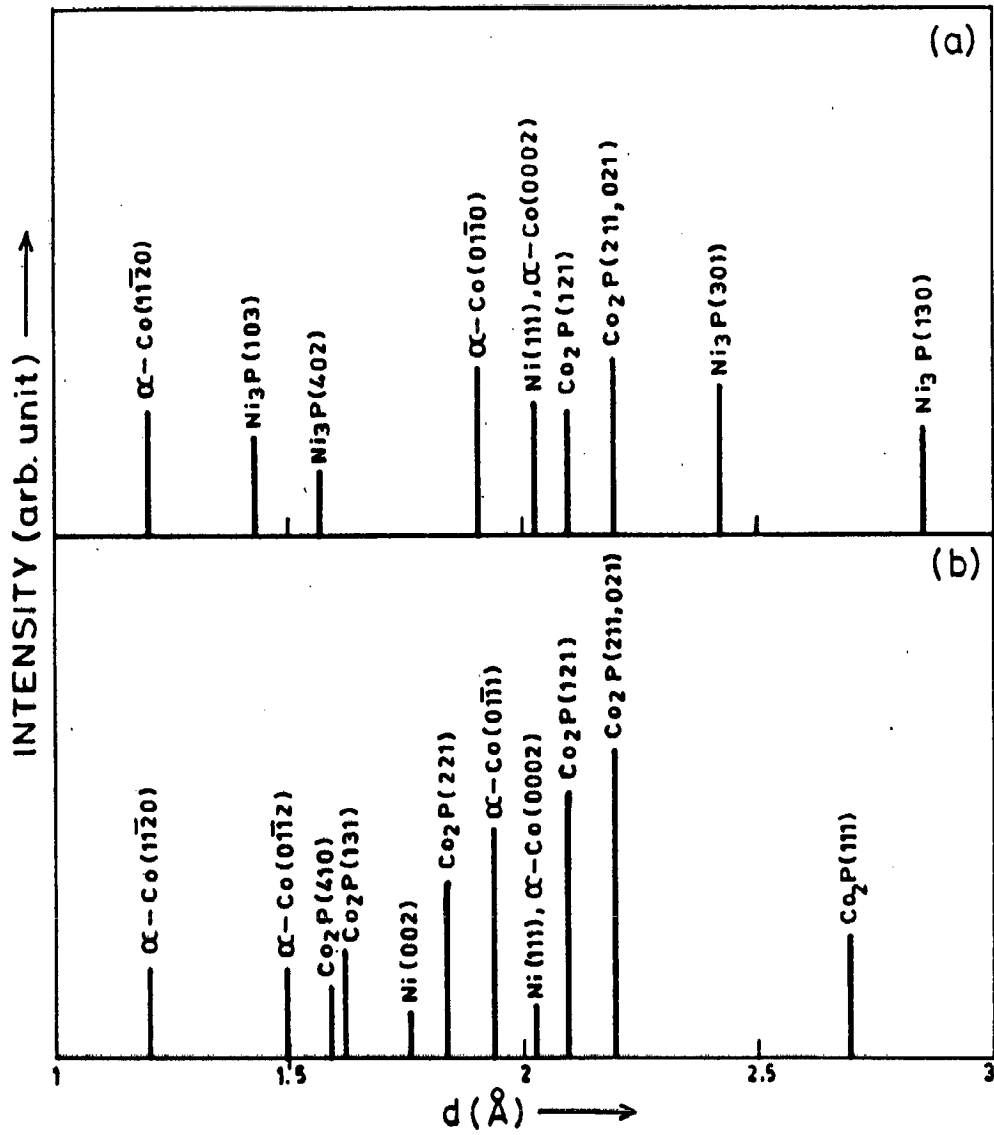


FIG. 5.10 (II) X-RAY DIFFRACTION PATTERNS OF THE SAMPLES, (a) $\text{Ni}_{27.0}\text{Co}_{58.0}\text{P}_{15.0}$ AND (b) $\text{Ni}_{15.3}\text{Co}_{70.0}\text{P}_{14.7}$ ANNEALED AT 823 K .

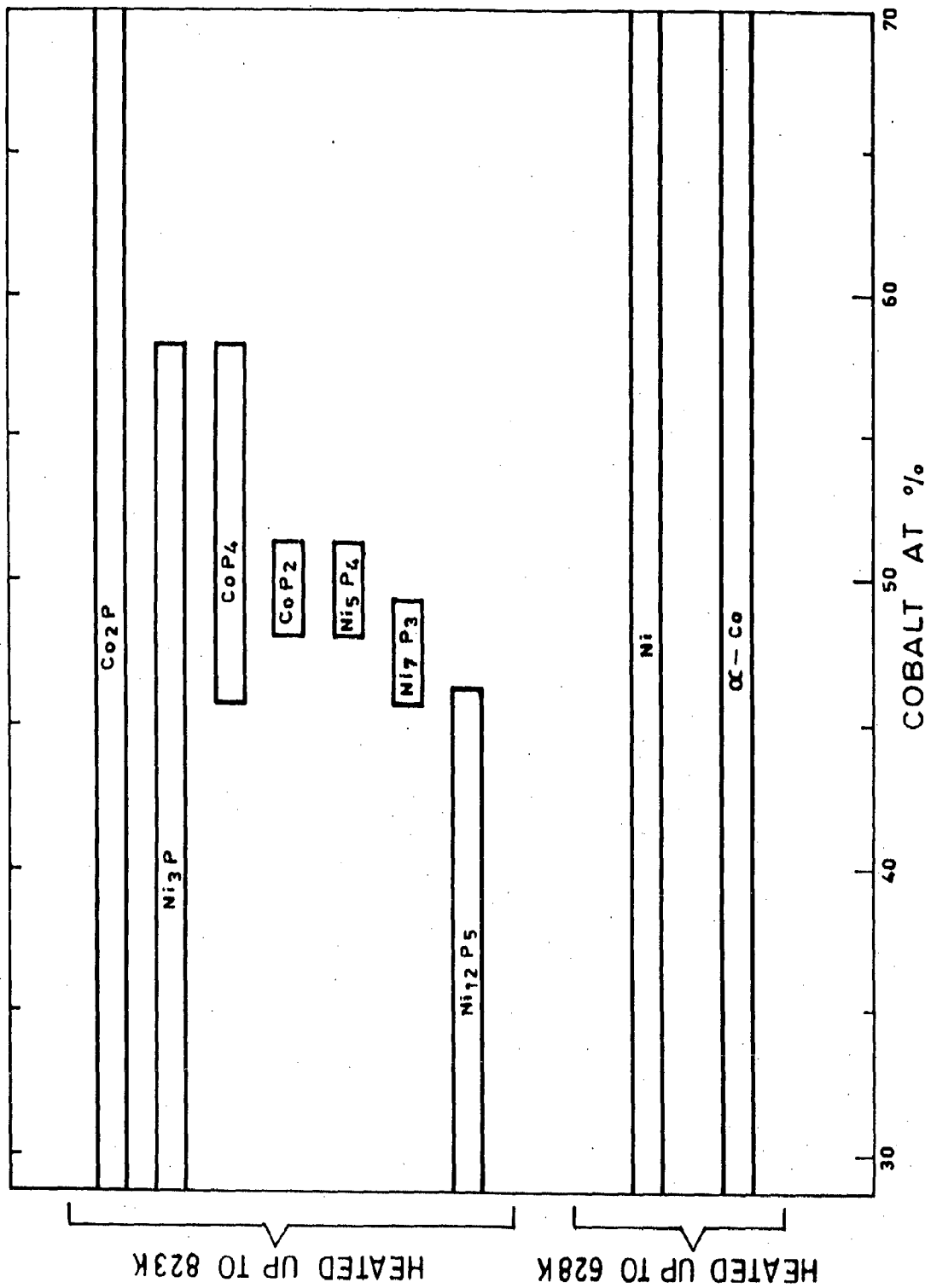


FIG. 5.11 SUMMARY OF THE COMPOSITION RANGES OVER WHICH DIFFERENT PHASES FORMED DURING ANNEALING OF THE AMORPHOUS Ni - Co - P SYSTEM.

C H A P T E R 6

ANNEALING BEHAVIOUR OF THE MAGNETIZATION AND ELECTRICAL RESISTIVITY OF AMORPHOUS ELECTROLESS Ni-Co-P

This chapter contains results of investigations on the magnetic and electrical resistivity behaviour of the electroless deposited amorphous Ni-Co-P system over the composition range of Nickel 15-56 at%, Cobalt 29-70 at% with about 15 at% phosphorous. The magnetic moment, their compositional dependence for the amorphous 'as-deposited' phase, and their change on annealing for these alloys are investigated and discussed. The results of compositional and temperature dependence of electrical resistivity are also presented and compared with similar ternary systems.

6.1 RESULTS: MAGNETIZATION STUDIES

Increasing evidence indicates that amorphous structures vary considerably with composition and it is to be expected that structure sensitive magnetic properties, their magnitudes and rate of change should be susceptible to variations in composition and thermal treatment.

In this section the results of the magnetic moment measurements on amorphous electroless deposited ternary Ni-Co-P films are presented. Magnetic moment measurements are carried out, as detailed in chapter 3, using Forner type Vibrating Sample Magnetometer (VSM) for the 'as-deposited' and

the annealed samples in the temperature range of 300 K to 850 K. The review of the magnetic behaviour of amorphous Ni-Co-P and related systems are discussed in 2.5.

6.1.1 Magnetization of the 'as-deposited' samples

Table 6.1 presents the measured values of magnetic moment for Ni-Co-P samples and the same data of variation of magnetic moment with composition is shown in Fig.6.1. The experimental values of Ni-Co-P system reported by O'Handley (1977) has been shown in the same figure for comparison. Our magnetic moment results are lower than that of prepared by melt quenching and do not show that good a linearity. Similar attempt is made to study the change in magnetic moment of binary electroless deposited Ni-P (Tyagi 1986, Simpson and Brambley 1972) and Co-P (Simpson and Brambley 1971) alloys. However, large number of research works are reported for these binary Ni-P and Co-P systems prepared by other techniques (Pan and Turbull 1974, Huller et al 1985, Cargill and Cochrane 1974) and the magnetic moment of 'as-deposited' samples decreases with increasing phosphorous content. The magnetic moments approach zero at phosphorous concentration of 20 at% in Ni-P alloys and 35 at% for Co-P alloys.

Studies of variation of magnetic moment for ternary TM-M systems carried out by Simpson and Clements (1975) for Co-Ni-P and Fe-Co-Ni-P have shown that average magnetic moment per atom increases by decreasing the number of 3d and 4s electrons contributed by the transition metal atoms.

Based on rigid band model, Yamauchi and Mizoguchi (1975) proposed that the magnetic moment ' σ ' of an amorphous binary alloy having the composition $M_{1-x}G_x$ is given by,

$$\sigma = \frac{m(1-x) - n_t x}{(1-x)} \quad (6.1)$$

Where M represents 3d transition metal and G the metalloid element, n_t is the average number of electrons transferred from metalloid atom to fill the m holes of the transition metal. The m values which is original number of unpaired spins, are 0.6 and 1.6 for Nickel and Cobalt respectively. Taking into account the change in individual moment varying with composition i.e., $m = m_{Ni}(1-\alpha) + m_{Co}$, where α is the fraction Cobalt replacing Nickel.

The magnetic moments have been calculated for 'as-deposited' amorphous Ni-Co-P using above formulas. The experimentally observed, and calculated values for $n_t = 4.5$ for our ternary system is shown in Fig. 6.1.

Assuming a number of electrons transferred from metalloid to be 4.5 ($n_t = 4.5$) a reasonably good agreement is found between the magnetic moments calculated for ternary Ni-Co-P amorphous alloys following equation 6.1 and the experimentally observed values. However, there appears to be a discontinuous change in the values of n_t when one moves in composition from Nickel majority to Cobalt majority side.

Assuming that the rigid band model is valid, the values

of $n_t = 3$ for amorphous Ni-P (Yamauchi and Mizoguchi, 1975) and $n_t = 5$ for amorphous Co-P (Simpson and Brambley 1971, Pan and Turnbull 1974) are reported for binary TM-M systems and the average value of $n_t = 4.5$ in ternary Ni-Co-P appears quite reasonable.

In case of multicomponent TM-M system these values for number of electron transferred from phosphorous are found to be 2.4 for Fe-Ni-B-P and Fe-Co-B-P and 3.0 for (Fe, Co, Ni)-B-P. One should note that there are large variations in the values of number of electrons transferred depending on various Metalloid (P,B,Si,C) and Transition Metal constituents participating.

6.1.2 Magnetization of the alloys during annealing

The Ni-Co-P electroless deposits were heated under vacuum from room temperature to 850 K. The variation of the magnetic moment of different amorphous alloys while sample is heated gradually (2.0 ± 0.5 K/min) are described here.

Fig. 6.2(a) and (b) showing the variation of magnetic moment with annealing temperature for sample A with 29 at% Cobalt and the sample B having 46 at% Cobalt. Both the samples show an initial decrease in magnetic moment with increase in temperature upto about 560 K. But further heating of sample A results in an increase in magnetic moment which have a peak value of 20 emu/g at about 710 K and

finally decreases with temperature as shown in Fig. 6.2(a). The magnetic moment increases in two stages at a rapid rate and then at a relatively slower rate. However, the sample B shows a larger increase in magnetic moment during its first stage and then the increase in magnetic moment is relatively slow with increase in temperature.

The annealing behaviour of magnetic moment for the samples having 49.1 and 58 at% Cobalt i.e. Sample C and D are shown in Fig. 6.3(a) and (b), where in both the cases two maxima in magnetization are observed. Sample C ($\text{Ni}_{35.6}\text{Co}_{49.1}\text{P}_{15.3}$) shows the increase of magnetic moment from 5 emu/g to 27 emu/g between 560-615 K temperature intervals with second maxima at about 830 K. The sample having 8.9 at% Cobalt more than the sample C i.e. sample D ($\text{Ni}_{27.0}\text{Co}_{58.0}\text{P}_{15.0}$) shows the occurrence of second peak at about 800 K.

The sample E with Cobalt content of 70 at% shows the initial decrease upto 560 K which is similar to other samples. Further heating causes an increase in magnetic moment by about 19 emu/g from 560 to 605 K as shown in Fig.6.4. The second maxima occurs at about 760 K which is lower than of that observed for sample C and D.

For the comparison purpose in Fig. 6.5(a) and (b) we also shown the typical changes in magnetization in $\text{Ni}_{84.2}\text{P}_{15.8}$ and $\text{Co}_{85.8}\text{P}_{14.2}$ electroless alloys. The temperature dependence of magnetization for binary microcrystalline and

amorphous Ni-P (Tyagi et al, 1989) and amorphous Co-P (Pan and Turnbull, 1974) have been extensively studied and show different trends for different phosphorous concentration.

6.1.3 Discussion

The magnetization in 'as-deposited' electroless Ni-Co-P system shows, the specimens with low cobalt concentration display rather weak ferromagnetism. The experimental results obtained in this study have consistently lower values as compared to that of O'Handley (1977) and the reason may be the difference in preparation and experimental conditions resulting in difference in structural state of the sample.

In Ni-Co-P and in general for amorphous alloys, though they are poor conductors, yet their 3d electrons are itinerant as in a crystalline transition metal alloys. The best fit for the number of electrons transferred from metalloid to TM atoms in rigid band model ' n_t ', in case of amorphous electroless Ni-Co-P is 4.5 which is intermediate between that of binary Ni-P ($n_t = 3$) and Co-P ($n_t = 5$) amorphous systems. This shows that the Cobalt atoms having larger number of unpaired spins invites larger number of electrons from metalloid atom to its 3d band as compared to Nickel. The results also indicate that rigid band model describe the magnetic behaviour of this ternary system reasonably well. However, the detailed nonlinear change in magnetic behaviour particularly when composition shifts from Nickel rich to

Cobalt rich side may call for more accurate description of electrons in this system. This could be a reflection of extra stability as seen in DSC data for the composition having almost equal Nickel-Cobalt ratio (i.e. sample B & C).

The samples heated with heating rate of 2.0 ± 0.5 K/min show different behaviour which depends on their initial compositions. The temperature range over which these changes take place and the rate of change of magnetization depend upon the rate of heating. Thus, annealing behaviour of magnetic moment reveals certain crystallization characteristics.

The initial increase in magnetization at about 560 K for all the amorphous electroless Ni-Co-P is due to separation of h.c.p. Cobalt and f.c.c. Nickel magnetic phases as indicated by electron microscopy and X-ray diffraction studies. The temperature range over which first increase in magnetization is observed corresponds to the first exothermic peak of DSC as shown in Fig. 4.1 of Chapter 4.

In the specimen containing 29 at% Cobalt, i.e. sample A, the rate of increase in magnetization reduces at around 625K indicating the onset of crystallization of the remaining amorphous phase. If this change would have been purely polymorphous to Ni_3P or Co_2P the magnetization should have reduced. The increase in magnetization clearly indicates transformation to some magnetic phase apart from Ni_3P and Co_2P . The evidence of TEM indicates that this phase could only be primary phase of Nickel or α -Cobalt. Thus, it

appears that the mode of transformation of the remaining amorphous phase is eutectic.

Figures 6.2(b) and 6.3(c) indicate that after separation of primary phases, crystallization of the remaining amorphous phase causes a lower rate of change in magnetization upto 850 K.

The similar transformation in Co-P samples shown in Fig. 6.5(b) has a similar flat type of region in magnetization temperature curve. The increase in Cobalt content and corresponding lowering of Nickel can explain the difference in nature of variation in magnetization as shown in Fig. 6.2(a) and (b). However, there appears a third stage of increase in magnetization marked by a different rate in sample C,D,E having a cobalt content of 49.1 at% or higher. In this samples the crystallization of the matrix amorphous phase after separation of primary phases, do not result in equilibrium phases directly and thus, these compositions have a three stage crystallization process.

The evidence that the temperatures corresponding to different stages of crystallization are much less for Ni-P and Co-P as compared to those for Ni-Co-P amorphous samples supports the general observation that addition of ternary elements in binary Ni-P or Co-P system enhances the stability of the amorphous state.

6.2 RESULTS: ELECTRICAL RESISTIVITY STUDIES

In this section electrical resistivity of 'as-deposited' samples have been characterized and the progress in crystallization of amorphous Ni-Co-P samples has been followed by monitoring the resistivity changes which show discrete discontinuities.

The results of composition and temperature dependence of electrical resistivity are presented in sections 6.2.1 and 6.2.2.

6.2.1 Electrical resistivity of 'as-deposited' samples

This section presents the results of electrical resistivity measurements using d.c. four probe method on electroless amorphous Ni-Co-P ternary system of different composition at room temperature. The measurements at temperature higher than 300 K which related to the amorphous-to-crystalline phase transformations are described in section 6.2.2. The details of measurement have already been covered in Chapter 3.

The values of resistivity and the TCR at about 300 K for different samples are shown in Table 6.2. The variation of these values with composition is illustrated in Fig. 6.6 alongwith the corresponding electrical resistivity values for binary Ni-P and Co-P prepared for the sake of comparison.

As can be seen from Fig. 6.6 the electrical resistivity increases with increase in Cobalt composition for sample A ($\text{Ni}_{55.5}\text{Co}_{29.0}\text{P}_{15.5}$) to B ($\text{Ni}_{39.0}\text{Co}_{46.0}\text{P}_{15.0}$). Further, addition of Cobalt does not change the resistivity of 'as-deposited' films significantly for the samples with 49.1, 58.0 and 70.0 at% Cobalt (i.e. sample C, D and E). The electrical resistivity of Ni-P prepared by electroless method is comparatively low because 'as-deposited' state is a mixture of amorphous and crystalline phases. But the Co-P films having 14.2 at% Phosphorous is amorphous and so, has a relatively higher resistivity.

The temperature coefficient of resistivity

' $\alpha = \left(\frac{\partial \rho}{\partial T} \right)_{T=300} \rho^{-1}$ ' is observed to decrease from

$13.06 \times 10^{-5} \text{K}^{-1}$ for $\text{Ni}_{55.5}\text{Co}_{29.0}\text{P}_{15.5}$ sample to $4.07 \times 10^{-5} \text{K}^{-1}$ for $\text{Ni}_{39.0}\text{Co}_{46.0}\text{P}_{15.0}$ sample and remains almost constant for other compositions. The value of TCR for sample A is near to that reported for Ni-P alloys of having a high phosphorous content of 20 at% (Tyagi, 1986). However, different values of TCR are reported for Ni-P samples prepared by other methods (Cote, 1976).

Although the present data does not extend upto negative values of the TCR, and there are no samples with resistivity greater than $150 \mu\Omega \text{ cm}$, one can clearly observe that samples with higher resistivity values have lower temperature coefficients.

6.2.2 Electrical resistivity of the alloys during annealing

The changes in resistivity of various amorphous electroless Ni-Co-P alloys are shown in Figs. 6.7-6.11. Beside the difference in value of 'as-deposited' electrical resistivity, the different annealing behaviour is also observed for different samples when they are heated upto about 850 K with heating rate of 20 ± 3 K/min. There is no major change in resistivity upto 553 K however a slight deviation from linear behaviour is observed from 450 K onwards upto 550K (Fig.6.7). A reduction in electrical resistivity is observed to occur between 553 K to about 600 K beyond which there is large reduction in resistivity upto a temperature of about 750 K.

In case of samples B and C there are similar drops in resistivity as observed in sample A but the different stages of drop in resistivity are less distinct as shown in Figs. 6.8 and 6.9. The variation of electrical resistivity with temperature for the samples with high Cobalt percentage as shown in Figs. 6.10 and 6.11 for sample D and E, are qualitatively similar to that of Fig. 6.7 and the different stages of crystallization are quite distinct.

As it is observed, electrical resistivity increases upto 450 K which is mainly because of thermal vibrations. The values of TCR related to this extend of increase is shown in Fig. 6.6. The lowering of electrical resistivity starts at 473 K and continuous upto about 553 K. This decrease in

electrical resistivity values are more pronounced for sample A, D and E as comparing to the sample B and C. This little drop in electrical resistivity is observed to coincide with the region of small peaks in DSC experiments and can be attributed to atomic relaxation prior to crystallization process.

In order to get better idea about this atomic relaxation process, the samples are heated upto 533 ± 2 K, before the sharp decrease in electrical resistivity takes place and held at that temperature to study the annealing behaviour with respect to time. The typical values for sample C and A is shown in Fig. 6.12. The sample B, C, D and E show a similar behaviour. In case of sample C, $\rho = 121.2 \mu\Omega \text{ cm}$ for $t = 0$, as this annealing time increases, the electrical resistivity decreases and saturates to $122.4 \mu\Omega \text{ cm}$ at $t = 200$ min with $\rho = -1.2 \mu\Omega \text{ cm}$. The similar curve is shown for sample A with $\rho = -2.24 \mu\Omega \text{ cm}$ and saturation time, $t = 300$ min.

6.2.3 Discussion

Broadly speaking, the results of electrical resistivity measurements on electroless amorphous Ni-Co-P alloys in 'as-deposited' state can be discussed in the light of broad features shown by amorphous transition metal-metalloid system. The increase in electrical resistivity from low Cobalt-to-high Cobalt concentration follows the trend of experimental values of electrical resistivity of liquid transition metals

(Guntherodt and Kunzi, 1978). Due to increased disorder, the sample of equal atomic ratio of Nickel and Cobalt show peak in electrical resistivity.

This system is observed to show the expected correlation between resistivity ' ρ ' and temperature coefficient of resistivity ' α ' as it was first reported by Mooij (1973). This is believed to be a result of electron mean free path approaching the inter-atomic distances as the disorder cannot reduce the mean free path any further. This correlation has been observed for relatively low resistivity alkali metals too. Therefore, the plot of ρ with TCR confirms the Mooij observation for electroless amorphous Ni-Co-P samples as well.

Since amorphous alloys are thermodynamically unstable spontaneous transformation to stable phases occur at elevated temperatures. The drop in resistivity observed at relatively low temperatures of about 473 K may be attributed to stress relaxations as indicated also by DSC response. The structural investigations under TEM and XRD reveal that no phase transformation has taken place till about 553 K. However the atomic relaxation is not accompanied by any change in electron states or their occupation and so magnetization measurements do not detect it.

The major drops in resistivity are closely associated with the crystallization process. Sample A, D and E shows separation of primary phases of Cobalt and Nickel distinctly

from the following stage where the remaining amorphous matrix crystallizes. These transformations have resulted into clearly distinct two steps in electrical resistivity. However, it seems that in case of samples having nearly equal ratios of Cobalt and Nickel these two steps corresponding to two stages of crystallization are not distinct. This is may be because of formation of metastable crystalline phases as can be seen from the annealing studies using TEM and XRD (Chapter 5).

6.3 SUMMARY

The magnetization and electrical resistivity of 'as-deposited' and annealed amorphous electroless Ni-Co-P samples of different TM compositions have been investigated with the help of Vibrating Samples Magnetometer and four probe dc setup.

The rigid band model for the case of $n_t = 4.5$ describes reasonably well the magnetic behaviour of ternary Ni-Co-P system. The annealing behaviour of magnetic moment reveals that the initial increase in magnetization at about 560 K is due to separation of h.c.p. Cobalt and f.c.c. Nickel as indicated by TEM and XRD studies. The crystallization of matrix causes a relatively lower rate of change in magnetization where the extend of this variation is different for compositionally different samples.

The results of electrical resistivity of 'as-deposited' samples show the expected correlation between resistivity ' ρ '

and TCR ' α ' and confirms the Mooij observation for TM-M systems. The minor drop in resistivity at temperatures of about 473 K may be attributed to stress relaxations where the major drops are closely associated with the crystallization process. Samples with 29.0, 58.0 and 70.0 at% Cobalt show the separation of primary phases distinct from that of matrix crystallization. However, in case of samples having nearly equal ratios of Cobalt and Nickel, the two stages of crystallization are not distinct. This is may be because of formation of metastable phases observed during annealing studies using TEM and XRD.

TABLE 6.1 VARIATION OF ROOM TEMPERATURE
MAGNETIC MOMENT WITH COMPOSITION
OF AMORPHOUS Ni-Co-P ALLOYS

SAMPLE	MAGNETIC MOMENT($\pm 2\%$) emu/g
Ni _{55.5} Co _{29.0} P _{15.5} (A)	3.33
Ni ₃₉ Co ₄₆ P ₁₅ (B)	10.14
Ni _{35.6} Co _{49.1} P _{15.3} (C)	13.7
Ni ₂₇ Co ₅₈ P ₁₅ (D)	37.9
Ni _{15.3} Co _{70.0} P _{14.7} (E)	49.2

TABLE - 6.2 ELECTRICAL RESISTIVITY (ρ) AND THE TEMPERATURE COEFFICIENT OF RESISTIVITY (α) OF AMORPHOUS ELECTROLESS Ni-Co-P SYSTEM.

SAMPLE	ρ $\mu\Omega$ cm at 300K	$-\rho^{-1} \left(\frac{\partial \rho}{\partial T} \right)_{T=300}$ 10^{-5} K^{-1}
Ni _{55.5} Co _{29.0} P _{15.5} (A)	114.5	13.06
Ni _{39.0} Co _{46.0} P _{15.0} (B)	122.5	4.07
Ni _{35.6} Co _{49.1} P _{15.3} (C)	121.2	4.12
Ni _{27.0} Co _{58.0} P _{15.0} (D)	120.0	4.16
Ni _{15.3} Co _{70.0} P _{14.7} (E)	120.4	4.15

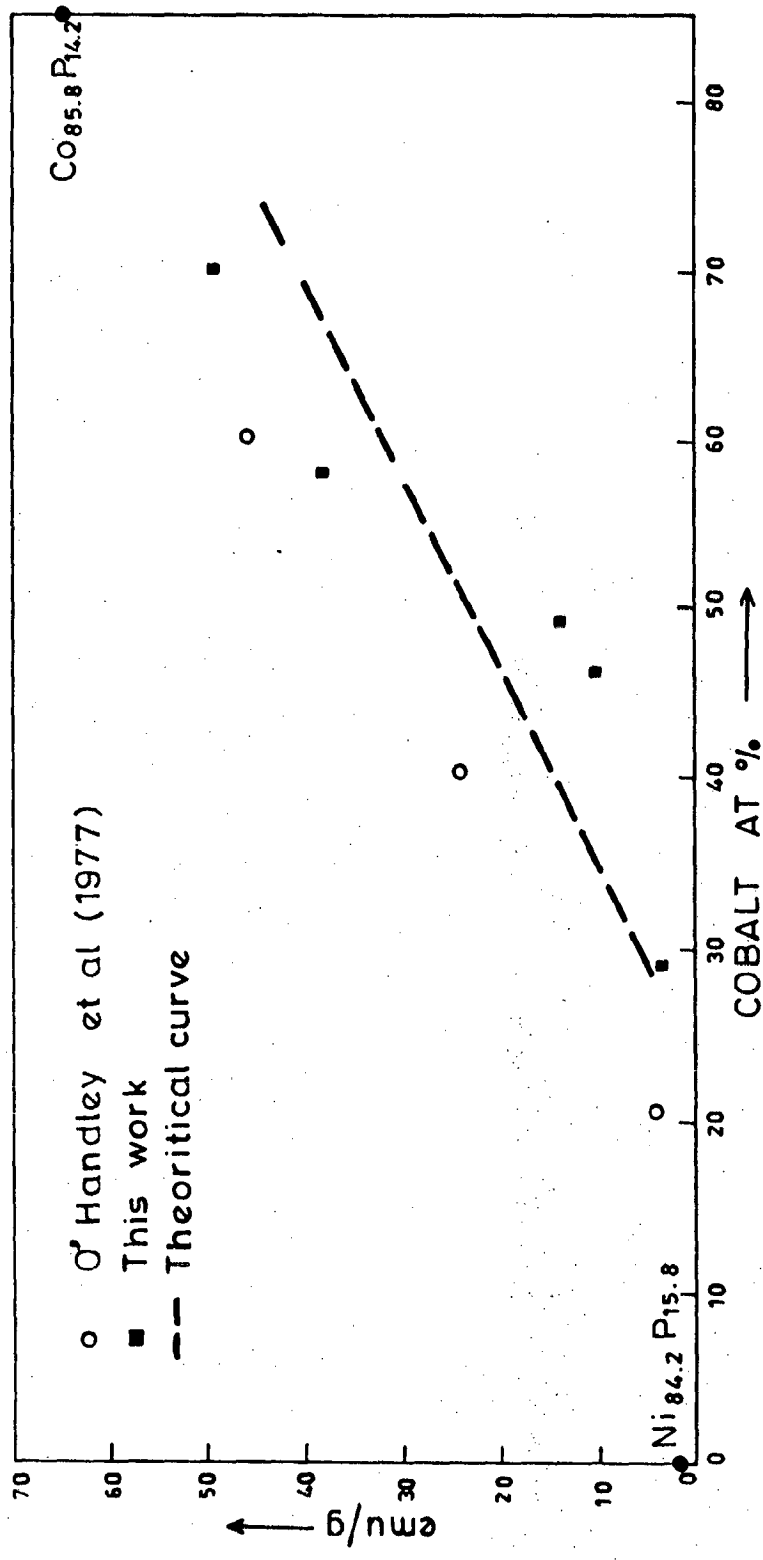


FIG. 6.1 THE VARIATION OF THE 'AS-DEPOSITED' MAGNETIC MOMENT WITH COBALT CONTENT.

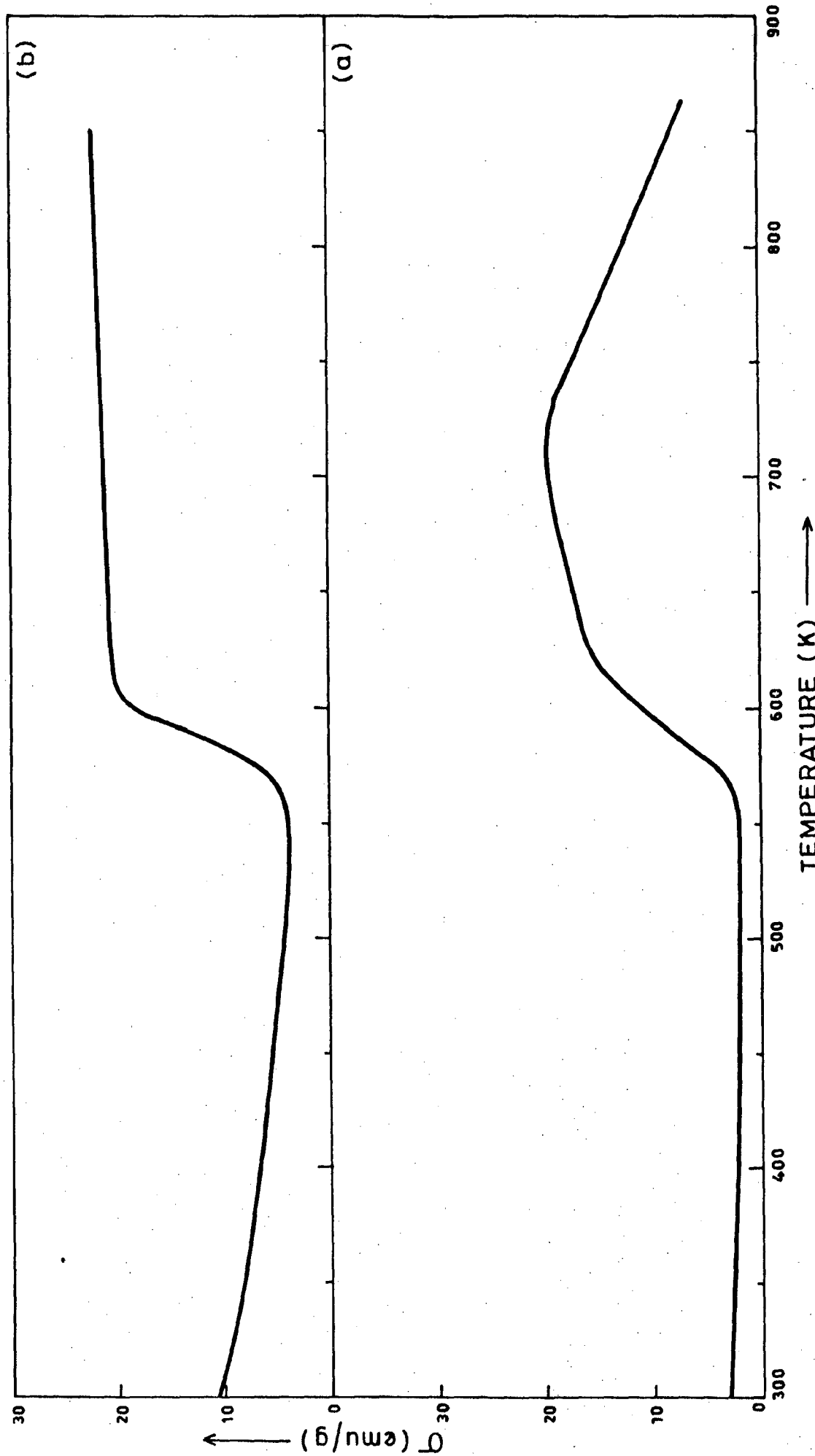


FIG. 6.2 THE VARIATION OF MAGNETIZATION WITH TEMPERATURE FOR, (a) $\text{Ni}_{55.5}\text{Co}_{29.0}\text{P}_{15.5}$ (SAMPLE A)
 (b) $\text{Ni}_{39.0}\text{Co}_{46.0}\text{P}_{15.0}$ (SAMPLE B).

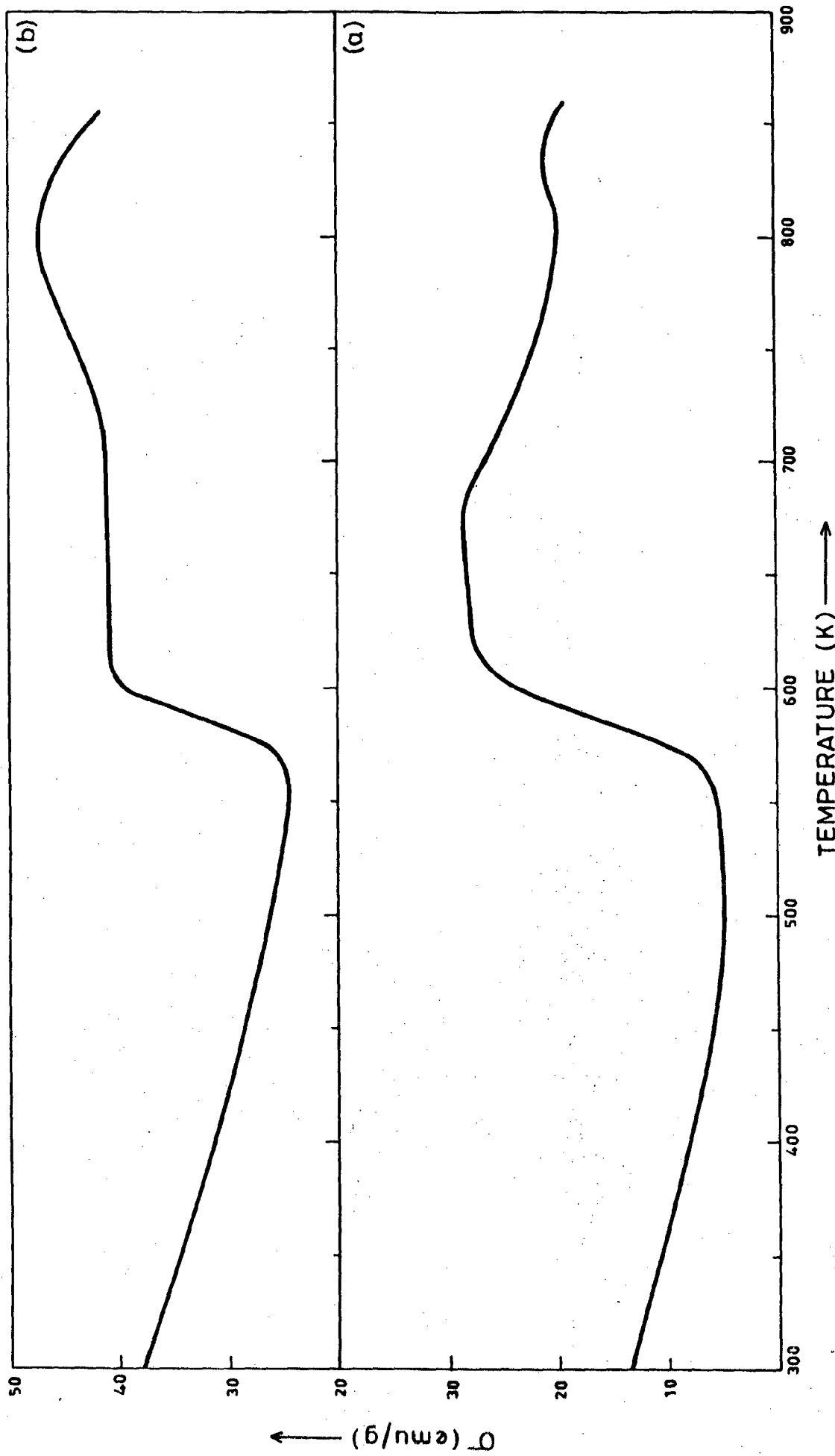


FIG. 6.3 THE VARIATION OF MAGNETIZATION WITH TEMPERATURE FOR, (a) $\text{Ni}_{35.6}\text{Co}_{49.1}\text{P}_{15.3}$ (SAMPLE C), (b) $\text{Ni}_{27.0}\text{Co}_{58.0}\text{P}_{15.0}$ (SAMPLE D).

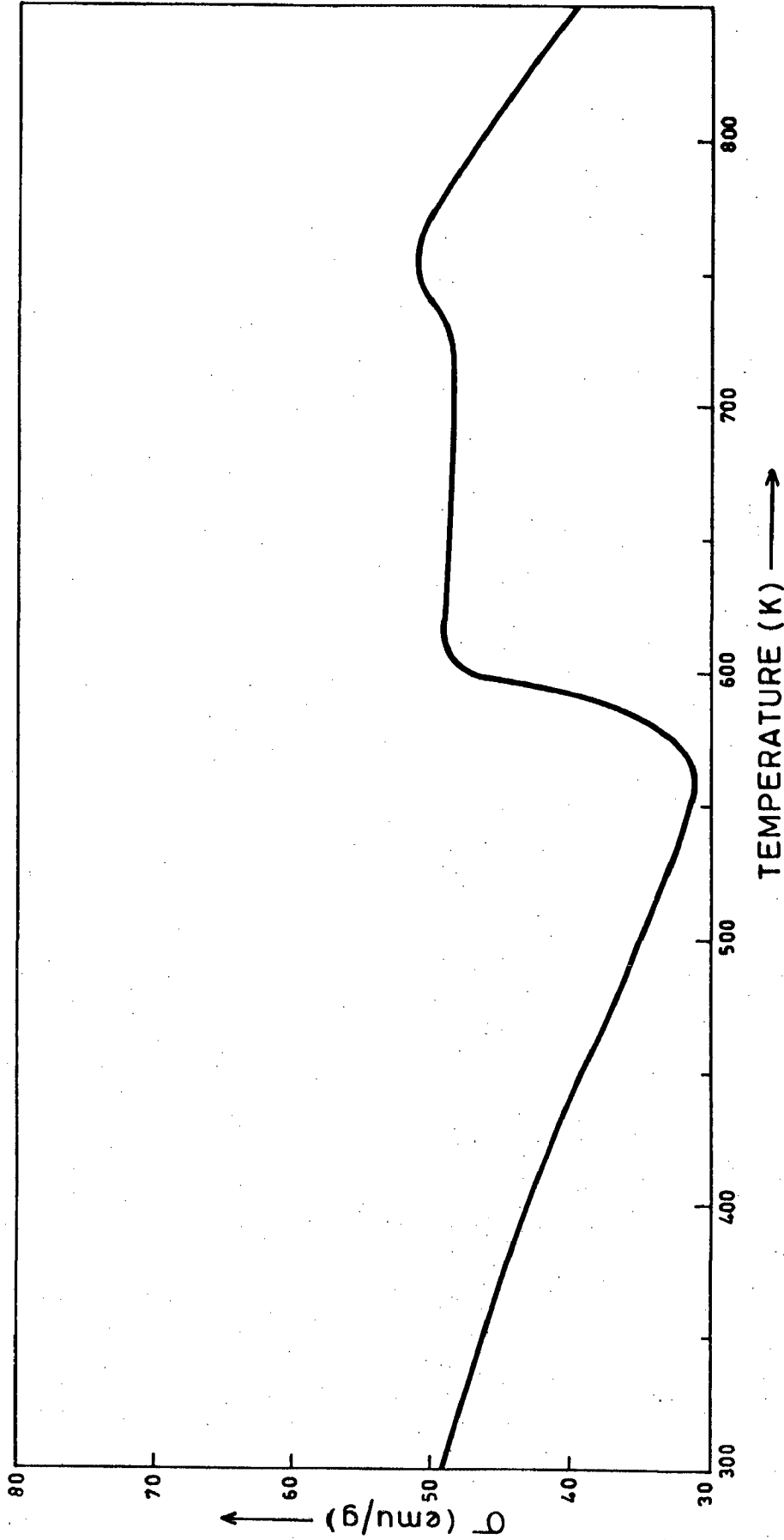


FIG. 6.4 THE VARIATION OF MAGNETIZATION WITH TEMPERATURE FOR $\text{Ni}_{15.0}\text{Co}_{70.0}\text{P}_{15.0}$ (SAMPLE E).

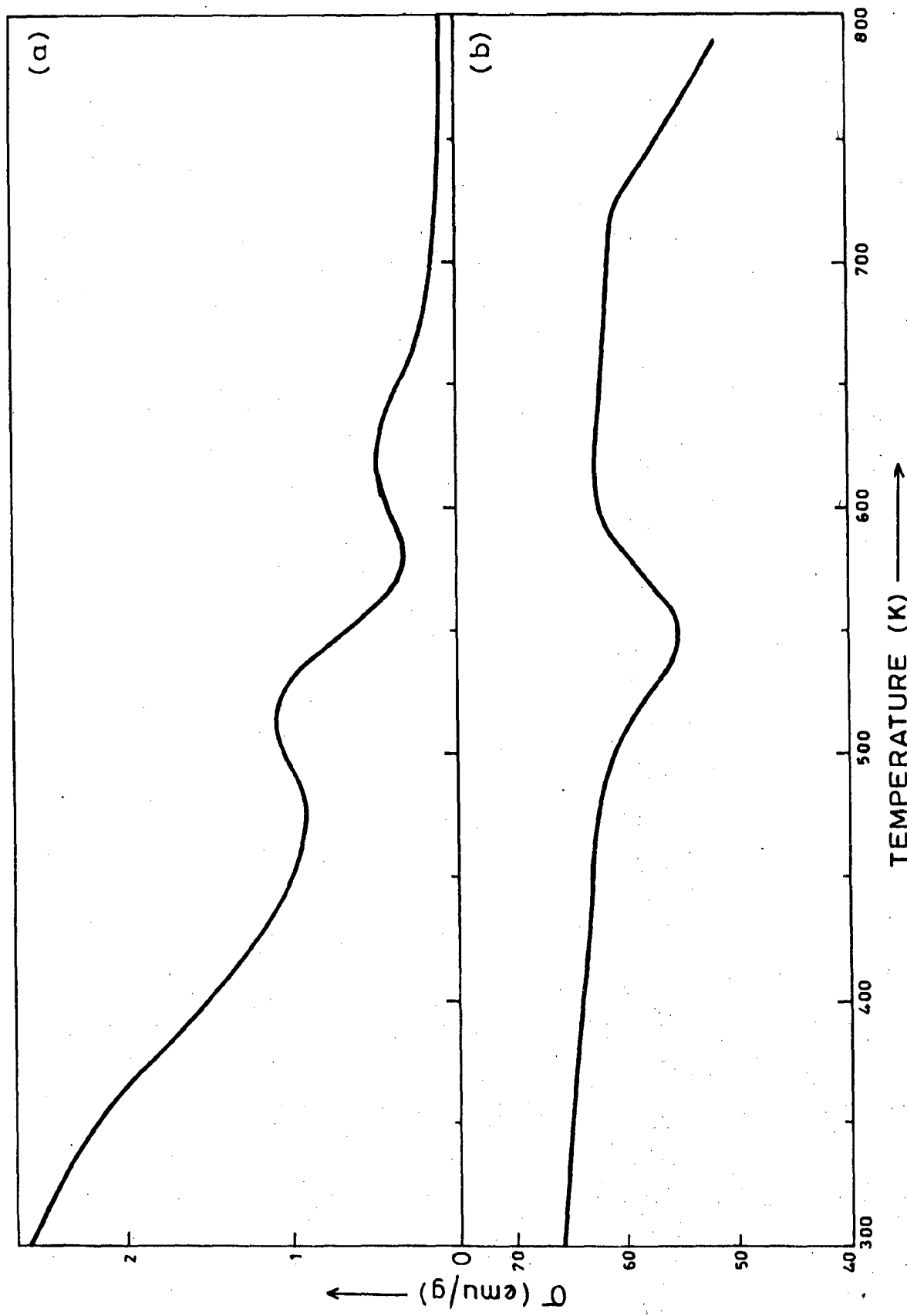


FIG. 6.5 THE VARIATION OF MAGNETIZATION WITH TEMPERATURE FOR
 (a) $\text{Ni}_{84.2}\text{P}_{15.8}$, (b) $\text{Co}_{85.8}\text{P}_{14.2}$

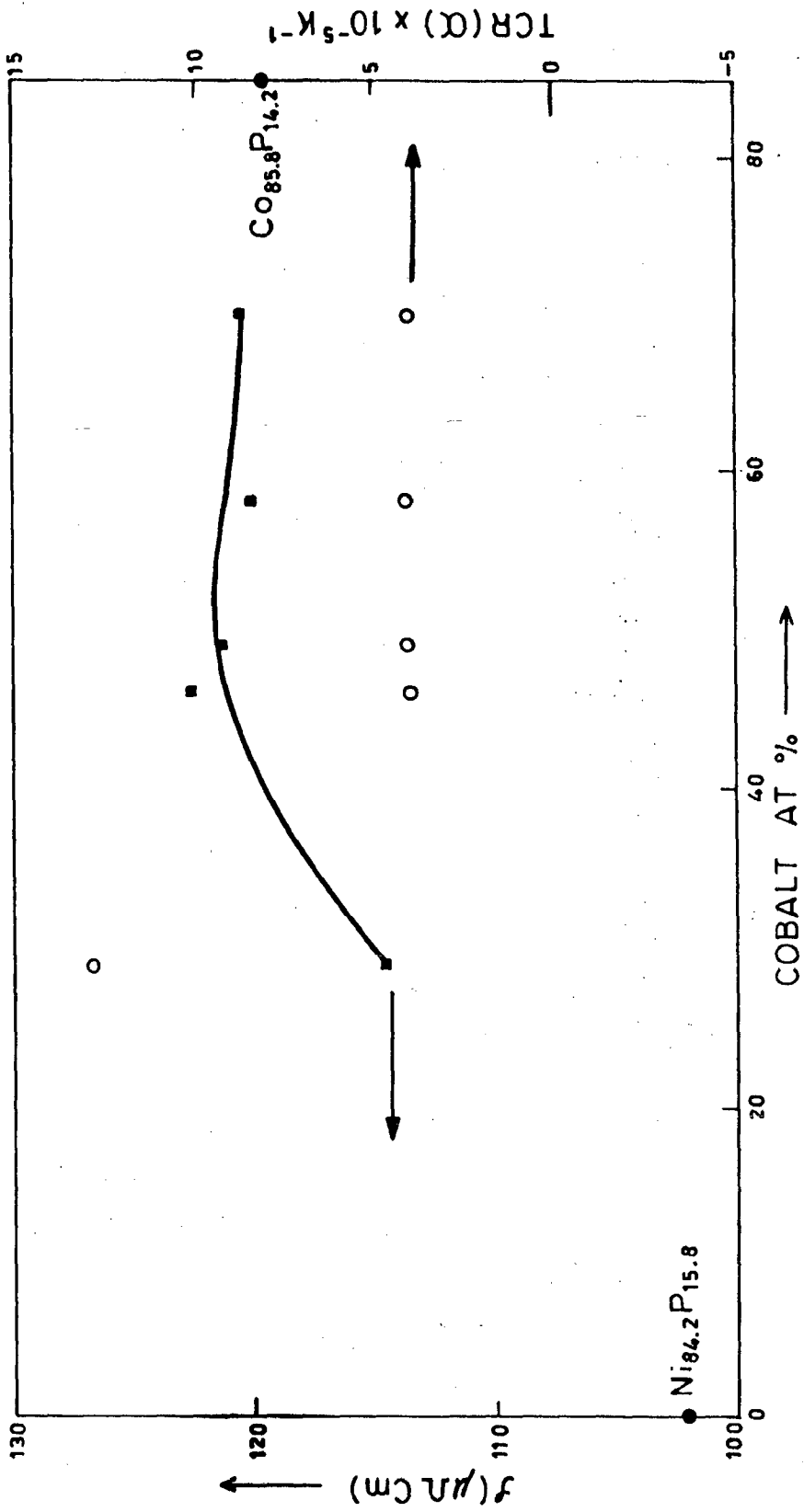


FIG. 6.6 VARIATION OF RESISTIVITY (ρ) AND TEMPERATURE COEFFICIENT OF RESISTIVITY (α) AT 300 K WITH COBALT CONTENT.

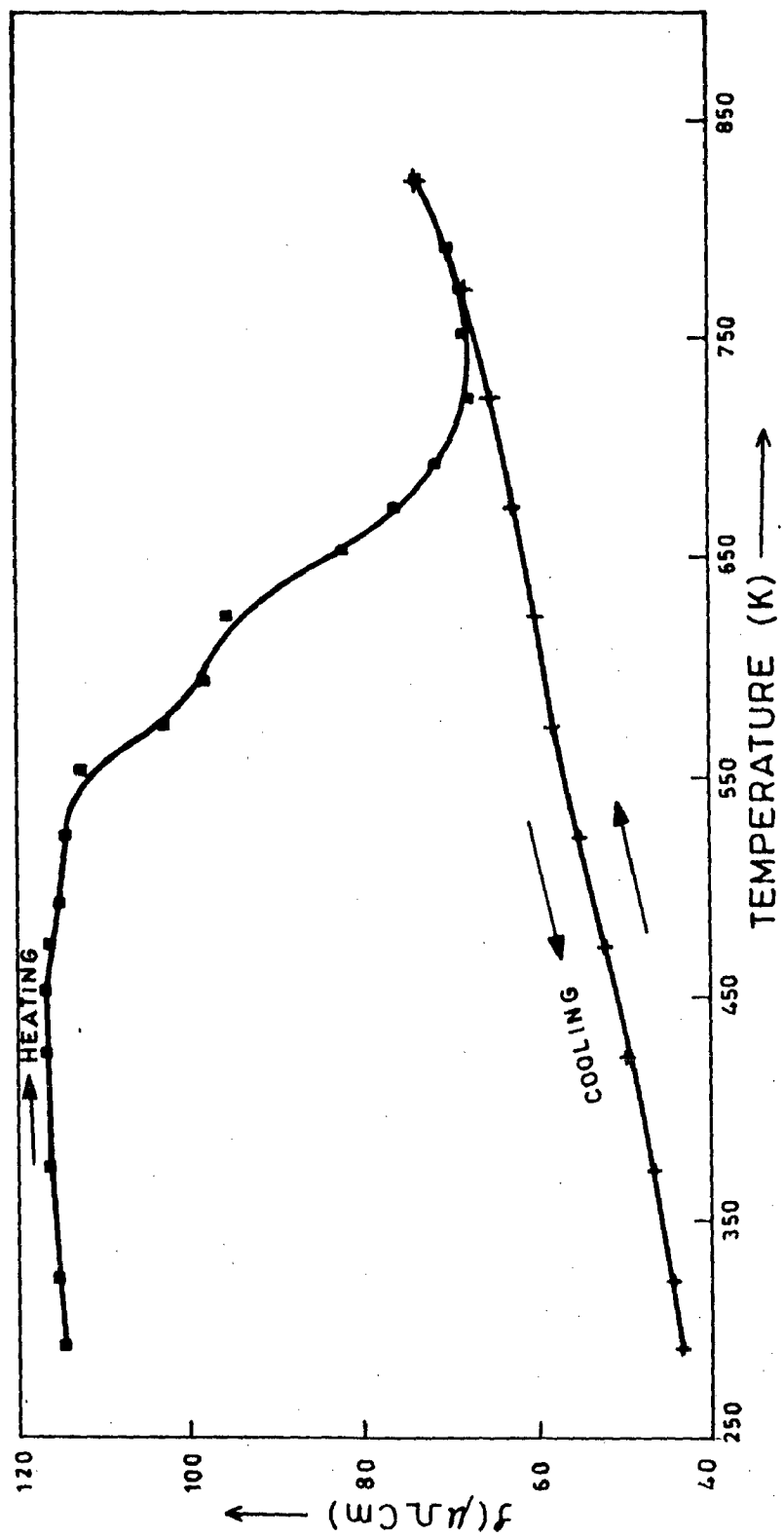


FIG. 6.7 THE VARIATION OF RESISTIVITY (ρ) WITH TEMPERATURE FOR $\text{Ni}_{55.5}\text{Co}_{29.0}\text{P}_{15.5}$ (SAMPLE A).

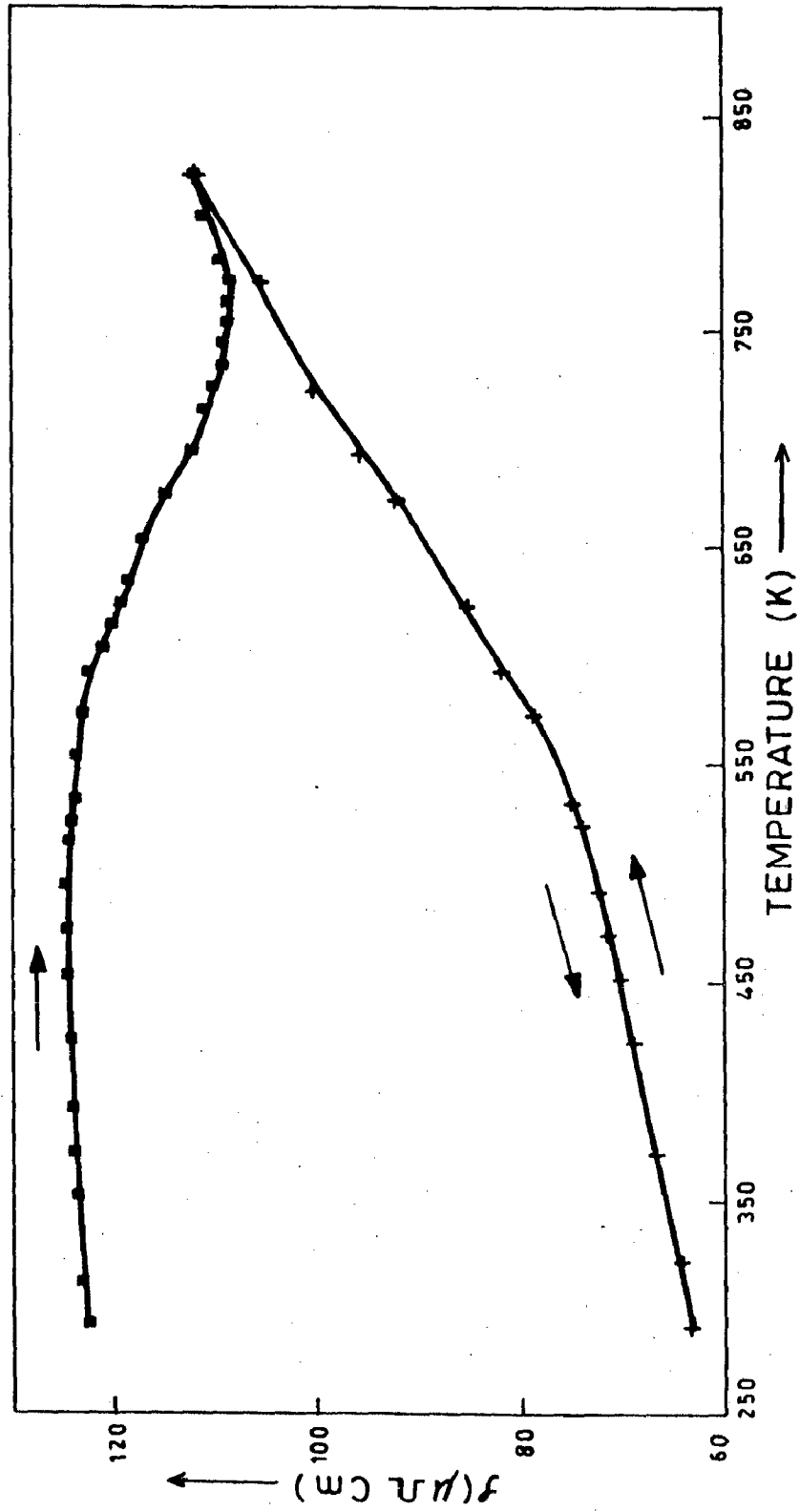


FIG. 6.8 THE VARIATION OF RESISTIVITY (ρ) WITH TEMPERATURE FOR $\text{Ni}_{39.0}\text{Co}_{46.0}\text{P}_{15.0}$ (SAMPLE B).

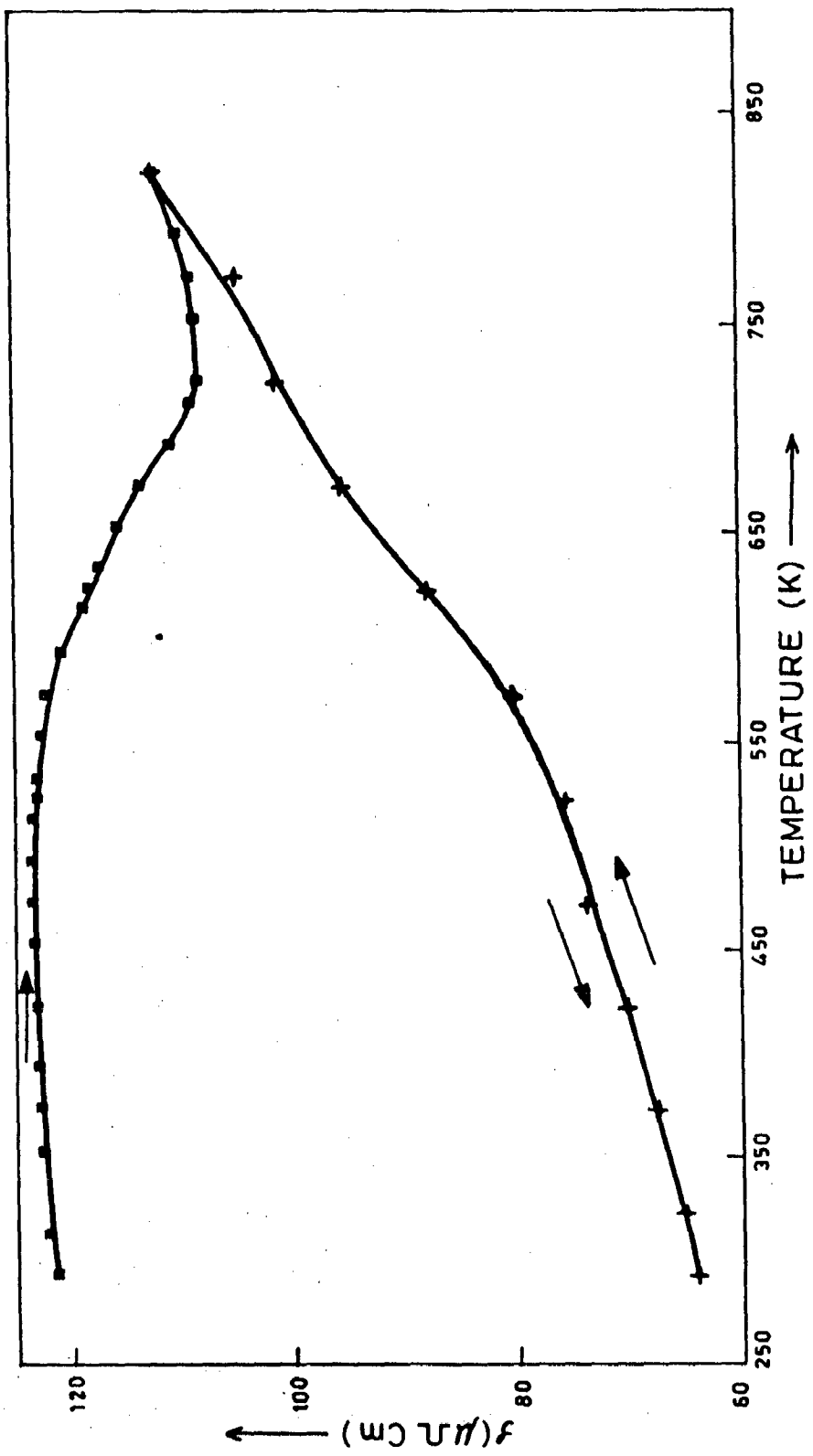


FIG. 6.9 THE VARIATION OF RESISTIVITY (ρ) WITH TEMPERATURE FOR Ni_{35.6}Co_{49.1}P_{15.3} (SAMPLE C) .

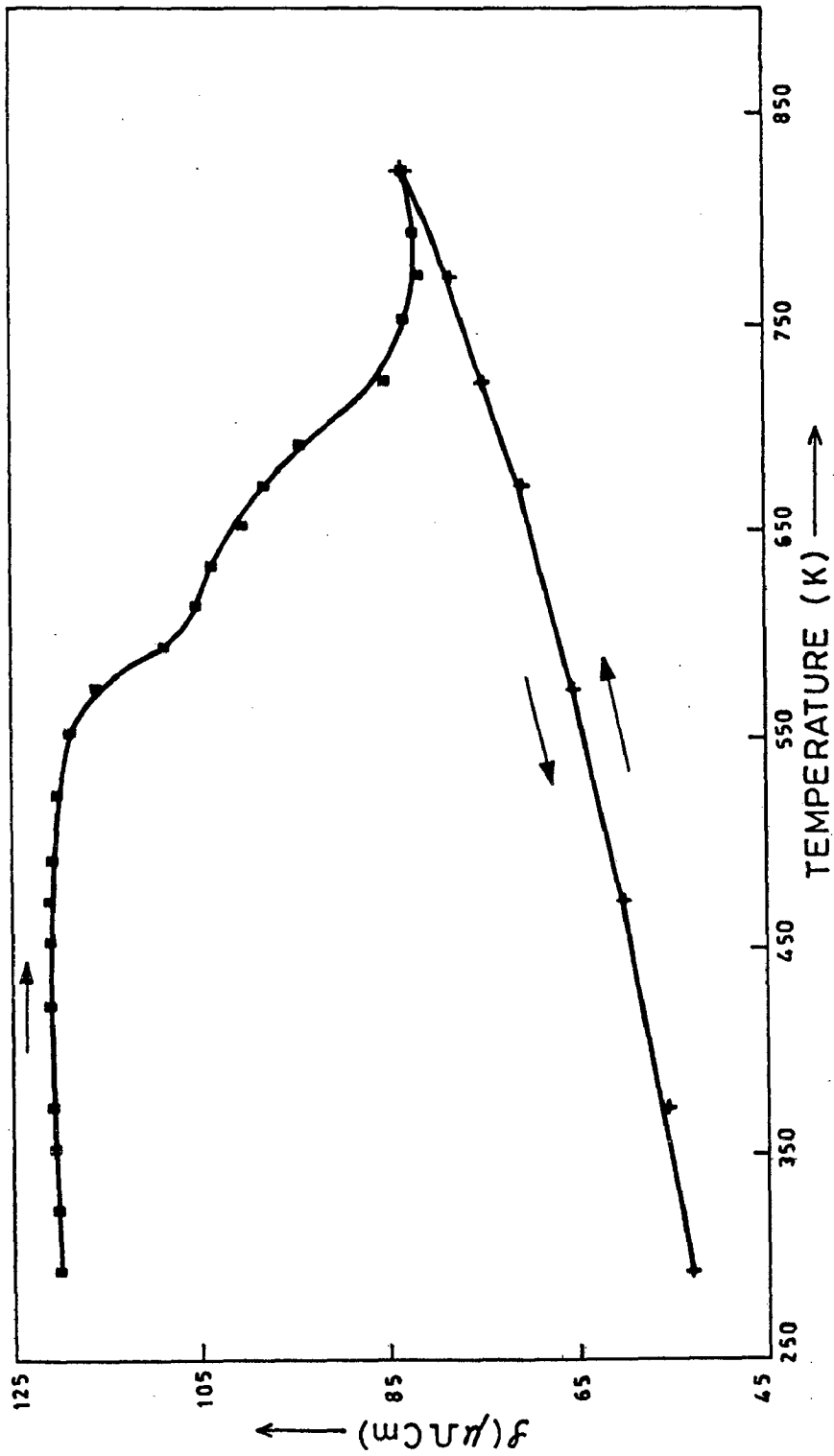


FIG. 6.10 THE VARIATION OF RESISTIVITY (ρ) WITH TEMPERATURE FOR $\text{Ni}_{27.0}\text{Co}_{58.0}\text{P}_{15.0}$ (SAMPLE D).

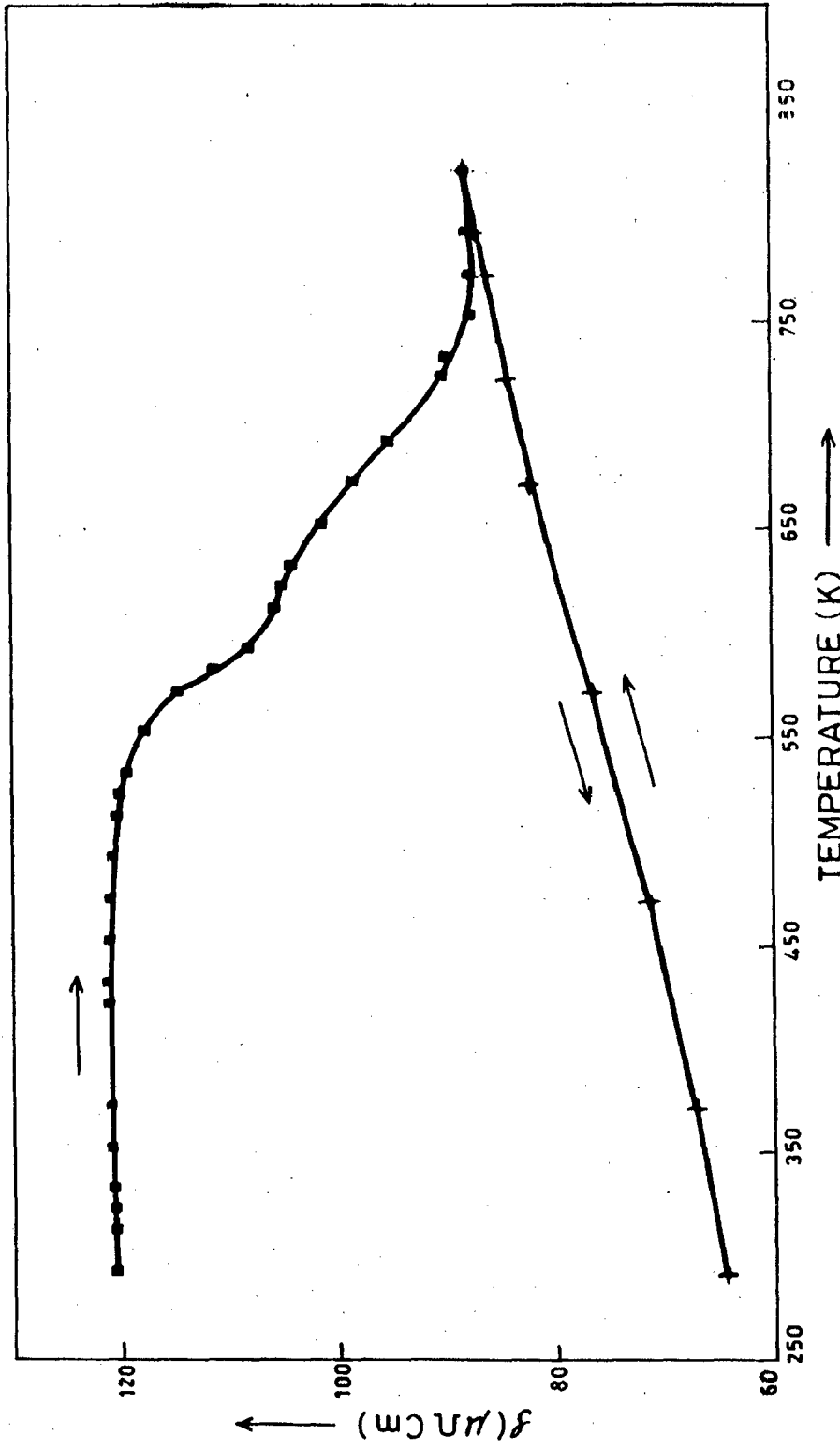


FIG. 6.11 THE VARIATION OF RESISTIVITY (ρ) WITH TEMPERATURE FOR
 $\text{Ni}_{15.3}\text{Co}_{70.0}\text{P}_{14.7}$ (SAMPLE E).

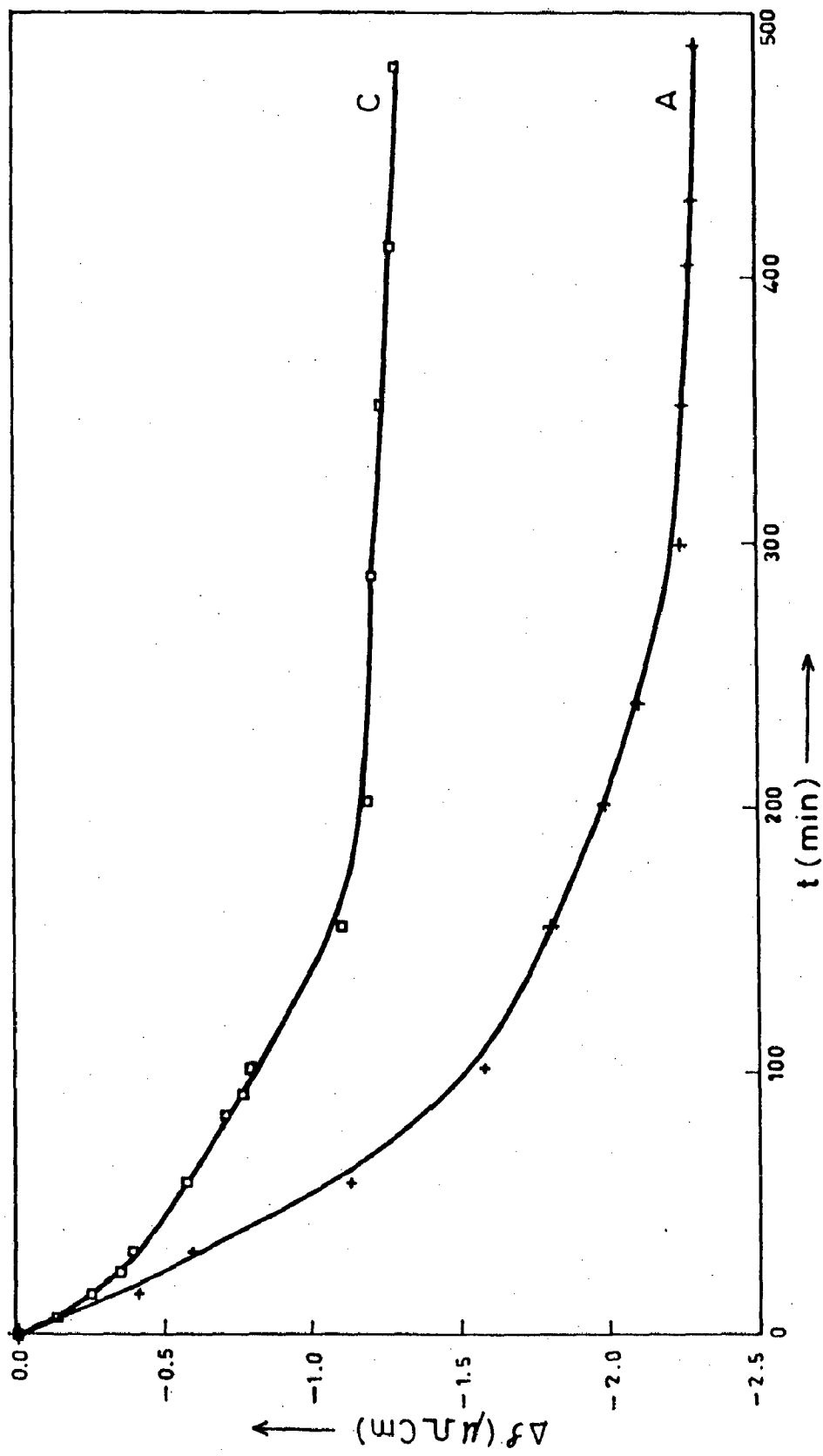


FIG. 6.12 RESISTIVITY CHANGE ($\Delta\rho$) DURING STRUCTURAL RELAXATION WITH RESPECT TO TIME ($t_a = 533 \pm 2K$)

CHAPTER 7

CONCLUSIONS

This thesis has been an attempt to study an amorphous TM-M system. The aspect emphasized is the manner in which amorphous structure transforms to the crystalline one with the increasing input of thermal energy which open up the possibility to move to atomic configurations and equilibrium and non-equilibrium phases not accessible earlier. The experimental probes used for this purpose has been many. In particular, we chose a ternary system for the reason that enough is already known about binary Ni-P and Co-P system that meaningful comparison as well as conclusions will be possible about the effect of ternary addition.

Thus, the present investigation on ternary amorphous Ni-Co-P system at a given pseudo-binary composition of Ni-Co-P is obviously intended to study the effect of addition of another transition element on the TM-M binary system. The compositions under investigation do not cover the dilute limits of ternary addition but extend over intermediate ranges from $\text{Ni}_{55.5}\text{Co}_{29.0}\text{P}_{15.5}$ to $\text{Ni}_{15.3}\text{Co}_{70.0}\text{P}_{14.7}$. There has been some variation in phosphorous content from 14.7 to 15.5 at% due to our inability to control the composition more closely. The films deposited by electroless method for this investigation have been fairly uniform due to effective pH control and are amorphous. In spite of some contrary reports $\text{Ni}_{84.2}\text{P}_{15.8}$ deposited in our laboratory by electroless method

has always been in mixed state containing both crystalline and amorphous regions. But $\text{Co}_{85.8}\text{P}_{14.2}$ has always been completely amorphous. Thus, the same level of phosphorous addition in Cobalt creates more strain in its lattice compared to that in Nickel. Also, the addition of Cobalt in Nickel lattice and Nickel in Cobalt lattice alongwith phosphorous should produce additional strain resulting the increase in 'amorphousness' of the system.

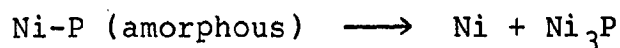
A ternary addition to a binary TM-M system will always create additional strain in the TM lattice and thus, transition metal lattice is expected to become amorphous at a lower level of metalloid content in presence of ternary addition. This may explain amorphous $\text{Ni}_{55.5}\text{Co}_{29.0}\text{P}_{15.5}$ while $\text{Ni}_{84.2}\text{P}_{15.8}$ is not completely amorphous. It will be interesting to study in future the minimum Cobalt content necessary in Ni-Co-P to make it completely amorphous and also the variation of this minimum with a change in Phosphorous content.

In order to characterise and understand 'amorphousness' an investigation of the thermal stability of the films were undertaken. The question of thermal stability is also important from practical point of view because it decides the limits of applicability under thermally active situations.

The crystallization of an amorphous film requires diffusion of constituting atoms and their partitioning into

different crystalline phases forming. The activation energy for the process of crystallization reflects the slowest kinetic step involved. In binary Co-P alloys it has been conjectured that the activation energy for crystallization is similar to that of diffusion of phosphorous. To verify the validity of this conjecture it is necessary to make diffusion measurements in amorphous matrices. If this conjecture is true it appears that the same process of diffusion of phosphorous remains the slowest step in the crystallization of ternary Ni-Co-P amorphous alloys. The change in activation energy with Cobalt addition may be related with the difficulty of diffusion of phosphorous in a matrix alloyed additionally with a ternary element.

Study of mode of crystallization indicate consistently that crystallization in the ternary Ni-Co-P takes place in two distinct steps. The first step involves separation of primary phases of Nickel and Cobalt containing some amounts of the other in solid solution. In the second step there is formation of phosphides. The changes in magnetization accompanying the second step leads us to believe that there is also a simultaneous separation of primary phases as:



in other words the crystallization takes place by eutectic reactions.

It is interesting to note that if one cools Ni-P or Co-P alloys containing about 15 at% phosphorous there are two reactions in sequence; (a) separation of pre-eutectic primary phases, and (b) eutectic reaction to a mixture of primary phase and phosphide. Thus, there is a similarity in the ways a metastable liquid transforms and a supercooled glass of the same alloy crystallizes. There is not much of difference in the activation energies of these two distinct steps probably because phosphorous diffusion is the slowest kinetic step for both the processes.

The Ni-Co-P alloys of intermediate composition (around Nickel: Cobalt atomic ratio of 50:50) there is formation of non-equilibrium phosphides along with equilibrium phosphides observed under TEM. The present study is inclusive about the exact mode of formation of non-equilibrium phosphides. Do these phosphides form through a metastable eutectic reactions and then transform to equilibrium phosphides? The answer to this question will have to await further investigations.

The activation energy for crystallization increases in Ni-Co-P amorphous alloys with increase in ternary addition both from Ni-P or Co-P binary ends. Thus, the stability of the film increases with ternary addition to binary films. However, the values of shape index 'n' for primary phase separation indicate that the first stage of crystallization has taken place almost without nucleation. Does it mean that the films were not completely amorphous and did contain trace

amounts of crystalline phases ? The present investigation can only claim that the films were completely amorphous as observed under TEM and XRD. Now, if the films were completely amorphous what were the heterogeneous nucleants ? The present investigation did not aim to answer this question also, However, in the stage of eutectic crystallization the separated primary phases could act as nucleant for primary phases formed during eutectic crystallization.

The changes in magnetization with composition in the 'as-deposited' ternary films show that within the framework of rigid band model the metalloid phosphorous atoms are transferring on an average 4.5 electrons and this value is just intermediate between the numbers of electrons transferred from phosphorous atoms to TM atoms in Ni-P and Co-P systems. In the present study phosphorous concentration was not changed and it is also expected to show a variation in the average number of electrons transferred from Metalloid to Transition Metal atoms. Future studies should reveal these trends and look into these results in the context of chemical affinities of different participating atoms.

The resistivities of the 'as-deposited' Ni-Co-P alloy films show the expected trend of having a maximum when Nickel and Cobalt are in equal atomic ratios. However, the Temperature Coefficient of Resistivity (TCR) in these alloys have become low but did not attain negative values.

The present investigation apart from characterizing ternary amorphous Ni-Co-P system, has lead to a systematic understanding of crystallization behaviour along a pseudo-binary line represented by Ni-Co-P. The changes in amorphous films as investigated by DSC, TEM, XRD, Magnetization and Resistivity techniques have yielded consistent results and the understanding provided by these results are significant.

REFERENCES

1. Agarwala R.C. and Ray S., (1989);
'TEM Investigation of the Transformation During Annealing in Electroless Ni-P Films', Z. Metallkunde, 80, p.556.
2. Albert P.A., Kovac Z., Lilienthal H.R., Meguire T.R. and Nakumura Y., (1967);
'The Effect of Phosphorous on the Magnetization of Nickel', J. Appl. Phys., 38, p.1258.
3. Azhdari K., Barthwal S.K., Tandon V.K. and Ray S., (1990);
'Kinetics of Phase Separation and Matrix Crystallization in Electroless Ni-Co-15 At% P Amorphous Alloy', J. Non-Cryst. Solids, 117/118, p. 535.
4. Bagley B.G. and Turnbull P., (1965);
'Formation and Magnetic Behaviour of Amorphous Co-P and Ni-P Alloys', Bull. Am. Phys. Soc., 10, p. 1101.
5. Bagley B.G. and Turnbull D., (1970);
'The Preparation and Crystallization Behaviour of Amorphous Nickel Phosphorous Thin Films', Acta Metall., 18, p. 859.
6. Bakonyi I., Cziraki A., Nagy I. and Hosso M., (1986);
'Crystallization Characteristics of Electro-deposited Amorphous Ni-P Alloys', Z. Metallkunde, 77, p. 425.
7. Becker J.J., Luborsky F.E., Walter J.L., (1977);
'Magnetic Moments and Curie Temperatures of $(\text{Fe,Ni})_{80}(\text{P,B})_{20}$ Amorphous Alloys', IEEE, MAG-13, p. 988.

8. Bestgen H. (1985);
'Microstructures of Amorphous and Microcrystalline Electrodeposited Co-P, Ni-P and Fe-P', 'Rapidly Quenched Metals', Vol. I, (Eds.) Steeb S. and Warlimont H., Elsevier Science Publishers, B.V., p. 443.
9. Brenner A. and Riddell G., (1946);
'Nickel Plating on Steel By Chemical Reduction', Res. Nat. U.S. Bur. Stand., 37, p. 31.
10. Buschow K.H.J. and Beckmans N.M., (1979);
'Thermal Stability and Electronic Properties of Amorphous Zr-Co and Zr-Ni Alloys', Phys. Rev., B 19, p. 3843.
11. Buschow K.H.J. and Dirks A.G., (1980);
'On the Crystallization* Behaviour of Amorphous Alloys of Rare-Earth and 3d Transition Metals', J. Appl. Phys., 13, p. 251.
12. Baschow K.H.J., (1985);
'Formation, Thermal Stability and Magnetic Properties of Amorphous Ni-based Alloys', 'Rapidly Quenched Metals', Vol.I, (eds.) Steeb S. and Warlimont H., Elsevier Science Publishers, B.V., p. 163.
13. Calka A. and Radlinski A.P., (1987);
'DSC Study of Surface Induced Crystallization in Pd-Si Metallic Glasses', Acta Metall., 35, p. 1823.

14. Cargill III G.S. and Cochrane R.W., (1974);
'Amorphous Co-P Alloy, Atomic Arrangements and Magnetic Properties', J. de Physique, C4 Supplement au n°5 Tome 35, C4-269.
15. Chen H.S. and Park B.K., (1973);
'Role of Chemical Bonding in Metallic Glasses', Acta Metall., 21, p.395.
16. Chen H.S., (1974);
'Thermodynamic Consideration on the Formation and Stability of Metallic Glasses', Acta Metall., 22, p.1505.
17. Chen H.S. and Sherwood R.C., (1976a);
'The Effect of Structural Relaxation on the Curie Temperature of Fe Based Metallic Glasses', IEEE, MAG-12, p. 933
18. Chen H.S., (1976b);
'Glass Temperature and Stability of Fe, Co, Ni and Pd Based Glasses: Effect of Configurational Entropy and Crystalline Symmetry', Acta Metall., 24, p. 153.
19. Chen H.S., (1977);
'Thermal and Mechanical Stability of Metallic Glass Ferromagnets', Scripta Metall., 11, p. 367.
20. Clements W.G. and Cantor B., (1976);
'Crystallization of Amorphous Alloys Prepared by Electroless Deposition', 'Rapidly Quenched Metals', (eds.) Grant N.J. and Giessen B.C., MIT, USA, p.267.

21. Cohen M.H. and Turnbull D., (1961);
Nature, 189, p. 131.
22. Cote P.J., (1976);
'Electrical Resistivity of Amorphous Ni-P Alloys', Solid State Commun., 18, p. 1311.
23. Criado J.M. and Ortega A., (1987);
'Non-isothermal Crystallization Kinetics of Metal Glasses: Simultaneous Determination of Both the Activation Energy and the Exponent n of the JMA Kinetic Law, Acta Metall., 35, No.7, p. 1715.
24. Cziraky A., Fogarassy B., Bakonyi I., Tompa K., Bagi T. and Hegedus Z., (1980);
'Investigation of Chemically Deposited and Electrodeposited Amorphous Ni-P Alloys', J. De Physique, C8-141.
25. Duwez P. and Willens R.H., (1963);
'Rapid Quenching of Liquid Alloys', Trans. TMS-AIME, 227, p. 362.
26. Duwez P., (1978);
'Metallic Glasses', American Society for Metals, U.S.A.
27. Fogarassy B., Cziraki A., Bakonyi I., Wetzig K., Ziess G. and Szabo I., (1985);
'Amorphous-Crystalline Transition in Ni-P-B Metallic Glasses', Vol.I 'Rapidly Quenched Metals' (eds.) Steeb S. and Warlimont H., Elsevier Science Publishers, B.V., p.389.

28. Fouquet F., Allemand J.P. and Perez J., (1985);
'Structural Evolution of a Fe-B-Si-C Metallic Glass',
'Rapidly Quenched Metals', Vol.I, (eds.) Steeb S. and
Warlimont H., Elsevier Science Publishers, B.V., p. 319.
29. Geoffroy G., Buflos F. and Lasalmonie A., (1983);
'Crystallization of Amorphous Ni-based Alloys', MRS
Meeting on 'Rapidly Solidified Metastable Materials',
Boston, 15-17, November, 1983.
30. Graham A.H., Lindsay R.W. and Read J., (1965);
'The Structure and Mechanical Properties of Electroless
Nickel', J. Electrochem. Soc., 112, p. 401.
31. Greer A.L., (1982);
'Crystallization Kinetics of Fe₈₀ B₂₀ Glass', Acta
Metall., 30, p. 171.
32. Gubanov A.L., (1960);
'Quasi-classical Theory of Amorphous Ferromagnetics',
F₁₂. Tverd. Tela, 2, p. 502.
33. Guntherodt H.J. and Kunzi H.U., (1978);
'Electronic Properties of Metallic Glasses and Melts',
Metallic Glasses, Duwez P., p. 247.
34. Heimendahl M.V., Maussner G., (1978);
'Proceedings of the 3rd International Conference on
Rapidly Quenched Metals, (ed.) Cantor B, Brighton,
(Metals Society, London), Vol.I, p. 424.

35. Henderson D.W., (1979);
'Thermal Analysis of Non-isothermal Crystallization Kinetics in Glass Forming Liquids', J. Non. Cryst. Solids, 30, p. 301.
36. Huller K. and Dietz G. (1985);
'The Temperature Dependence of the Magnetization of Fe-P, Co-P and Ni-P alloys', J. Magn. Magn. Materials, 50, p. 250.
37. Huller K., Dietz G., Hausmann R. and Kolpin K. (1985);
'The Composition Dependence of Magnetization and Curie Temperature of Fe-P, Co-P and Ni-P', J. Magn. Magn. Mater., 53, p. 103.
38. Jackle J., (1986);
'Models of Glass Transition', Rep. Prog. Phys., 49, p. 171.
39. Khan Y., Kruller E. and Sostarich M., (1981);
'Stability and Crystallization of Amorphous Iron-Boron Alloys Obtained by Quenching from the Melt', Z. Metallkde, 72, p. 553.
40. Kissinger H.E., (1957);
'Reaction Kinetics in Differential Thermal Analysis', Anal. Chem. 29, 11, p. 1702.

41. Koster U. and Herold U., (1981);
'Glassy Metals I', (eds.) Guntherodt H.J. and Beck H.,
Springer Verlag, Berlin, p. 225.
42. Kuhnast F.A., Machizaud F., Flechon J., Gunat C. and
Hertz J., (1984);
'Amorphous Metals and Non - Equilibrium Processing',
Edited by M. Von Allmen, p. 199.
43. Luborsky F.E. and Walter J.L., (1977);
'Magnetic Anneal Anisotropy in Amorphous Alloys', IEEE,
MAG-13, p. 953.
44. Luborsky F.E., (1983);
'Amorphous Metallic Alloys', Butterworths, London.
45. Makhsoos E.V., Thomas E.L. and Louis E.T., (1978);
'Electron Microscopy of Crystalline and Amorphous Ni-P
Electrodeposited Films: in Situ Crystallization of an
Amorphous Solid', Met. Trans., 9A, p. 1449.
46. Malmhall R., Bhagat M., Rao K.V., Backstrom G., (1979);
'Transport Properties of Amorphous Ferromagnets', Phys.
Stat. Sol. (a), 53, p. 641.
47. Malozemoff A.P., Williams A.R. and Moruzzi V.L., (1984);
'Band-Gap Theory of Strong Ferromagnetism: Application
to Concentrated Crystalline and Amorphous Fe- and Co-
Metalloid Alloys', Phys. Rev. B, 29, p. 1620.

48. Masui K., Maruno S. and Miyoshi N., (1985);
'Crystallization Kinetics of Electrodeposited Amorphous Co-P Alloys', J. Non-Cryst. Solids, 70, p. 263.
49. Meisel L.V. and Cote P.J., (1983);
'Non-isothermal Transformation Kinetics: Application to Metastable Phases', Acta Metall., 31, No.7, p. 1053.
50. Miyazaki T., Yang X., Takashashi M., (1986);
'Crystallization of Amorphous $Fe_{100-x}P_x$ ($13 < x < 24$) Alloys', J. Magn. Magn. Mater., 60, p. 204.
51. Mooij J.H., (1973);
'Electrical Conduction in Concentrated Transition Metal Alloy', Phys. Status Solidi a), 17, p. 521.
52. Nagel S.R. and Tauc J., (1975);
'Nearly-Free-Electron Approach to the Theory of Metallic Glass Alloys', Phys. Rev. Lett., 35, p. 380.
53. Naka M., Tomizawa S., Watanabe T., Masumoto T., (1976);
'Rapidly Quenched Metals', Section 1 (eds. N.J. Grant and B.C. Giessen) MIT Press, Cambridge, Mass.) p. 273.
54. O'Handley R.C., Hasegawa R., Ray R. and Chow C.P., (1977);
'Magnetic Properties to $TM_{80}P_{20}$ Glasses', J. Appl. Phys. Vol. 48, No.5, p. 2095.
55. Orehotsky J. and Rowlands C. (1982);
'Crystallization of $(Fe_{1-x}Ni_x)_{80}B_{20}$ Amorphous Alloys', J. Appl. Phys., 53(11), p. 7783.

56. Pai S.T. and Marton J.P., (1972);
'Annealing Effects on the Structure and Resistivity of Ni-P Films', J. Appl. Phys., 43, p. 282.
57. Pan D. and Turnbull D., (1974);
'Magnetic Properties of Amorphous Alloys', Res. Rep. No.1, Division of Engg. and Applied Physics, Harvard University.
58. Panek T., Bergmann H.W., Luft U., Langford I., (1985);
'Rapidly Quenched Metals', Vol.I (eds.) Steeb S. and Warlimont H., Elsevier Science Publishers, B.V., p. 537.
59. Pilz O. and Ryder P.L., (1985);
'Crystallization of Amorphous $\text{Ni}_{78}\text{B}_{14}\text{Si}_8$ ', 'Rapidly Quenched Metals', (eds.) Steeb S. and Warlimont H., Elsevier Science Publishers, B.V., p. 377.
60. Pond R. Jr. and Maddin R. (1969);
'A Method of Producing Rapidly Solidified Filamentary Castings', TMS-AIME, 245, p. 2475.
61. Quivy A., Rzepski J., Chevalier J.P. and Calvayrac Y., (1985);
'A Comparative Study of Initial Stage Crystallization Structures and Morphologies For Some Iron and Nickel Based Glassy Alloys', 'Rapidly Quenched Metals', Vol.I (eds.) Steeb S. and Warlimont H., Elsevier Science Publishers, B.V., p. 315.

62. Riveiro J.M., Sanchez-Trujillo M.C., Rivero G., (1986);
'Electrical and Magnetic Properties in Co-P Amorphous Alloys'. J. Magn. Magn. Mater., 60, p. 195.
63. Rivory J., Bouchet B., (1979);
'Electrical and Optical Properties of Co-P Metallic Glasses', J. Phys. F: Metal Phys., Vol.9, No.2, p. 327.
64. Russew K., Budurov S. and Anestiev L., (1985);
'Crystallization Kinetics of $Fe_{40}Ni_{40}P_{14}B_6$ Glassy Alloy under Isothermal and Non-isothermal Conditions',
'Rapidly Quenched Metals, Vol.I, (eds.) steeb S. and Warlimont H., Elsevier Science Publishers, B.V., p. 283.
65. Sharp J.H., (1972);
'Differential Thermal Analysis', (edited by R.C. Mackenzi), Vol.2, Academic Press, New York.
66. Simpson A.W. and Brambley D.R., (1971);
'The Magnetic and Structural Properties of Bulk Amorphous and Crystalline Co-P Alloys', Phys. Stat. Sol. b) 43, p. 291.
67. Simpson A.W. and Brambley D.R., (1972);
'The Temperature Variation of Magnetization Bulk Amorphous $Ni_{85}P_{15}$: An Amorphous Ferrimagnet?', Phys. Stat. Sol. b), 49, p. 685.
68. Simpson A.W. and Clements W.G., (1975);
'Magnetostriction in Some Amorphous Fe-Co-Ni-P Alloys', IEEE, MAG-11, No.5, p. 1338.

69. Sonnberger R. and Dietz G., (1985);
'Electrical Resistance and Structural Relaxation of Amorphous and Microcrystalline $\text{Co}_{1-x}\text{P}_x$ Alloys', 'Rapidly Quenched Metals, Vol.I (eds.) Steeb S. and Warlimont H., Elsevier Science Publishers, B.V., p. 703.
70. Tyagi, S.V.S., Tandon V.K., Ray S. (1985);
'Study of the Crystallization Behaviour of Electroless Ni-P Films by Electron and X-Ray Diffraction', Z. Metallkunde, 76, p. 492.
71. Tyagi S.V.S., (1986);
'The Annealing Studies on the Structure and Properties of Electroless Amorphous Transition Metal-Metalloid System $\text{Ni}_{100-x}\text{P}_x$ ', Ph.D. Thesis, University of Roorkee, Roorkee, India.
72. Tyagi S.V.S., Barthwal S.K., Tandon V.K. and Ray S., (1989);
'The Annealing Behaviour of Electroless Non-Crystalline Nickel Phosphorous Films', Thin Solid Films, 169, p.229.
73. Warlimont H., Gordelik P. (1985);
'On Structures in the Amorphous State in the Fe-Ni-B System', 'Rapidly Quenched Metals', Vol.I (eds.) Steeb S. and Warlimont H., Elsevier Science Publishers, B.V., p. 619.

74. Watanabe T. and Tanabe Y., (1985);
'Preparation and Physical Properties of Fe-W and Co-W Amorphous Alloys by Electroplating Method', 'Rapidly Quenched Metals', Vol.I, (eds.) Steeb S. and Warlimont H., Elsevier Science Publishers, B.V., p. 127.
75. Wendlant W.W., (1974);
'Thermal Methods of Analysis', 2nd edn. Wiley, New York.
76. Yamauchi K. and Mizoquchi T., (1975);
'The Magnetic Moments of Amorphous Metal-metalloid Alloys', J. Phys. Soc., Japan, 39, p. 541.